Directed differentiation of pluripotent stem cells induced by single genes

Dissertation zur Erlangung des

naturwissenschaftlichen Doktorgrades

der Julius-Maximilians-Universität Würzburg

vorgelegt von

Eva Christina Thoma

aus

Memmingen

Würzburg 2011

Eingereicht am: ....

Mitglieder der Promotionskommission:

Vorsitzender: ....

Gutachter : Prof. Dr. Dr. Manfred Schartl

Gutachter: Prof. Dr. Albrecht Müller

Tag des Promotionskolloquiums: ....

Doktorurkunde ausgehändigt am: ....

~ Pectus est enim quod disertos facit et vis mentis. ~

~ Quintilian ~

Inhaltsverzeichnis

Zusammenfassung

Pluripotenz bezeichnet die Fähigkeit einer Stammzelle, jede Zelle des Körpers zu bilden. Zu den pluripotenten Stammzellen gehören embryonale Stammzellen (ESZ), aber auch so genannte induzierte pluripotente Stammzellen (IPS Zellen), die durch Rückprogrammierung ausdifferenzierter Körperzellen in einen pluripotenten Status gewonnen werden. Außerdem wurde gezeigt, dass adulte Spermatogonien (SG) in Maus und Mensch pluripotent sind. Pluripotente Stammzellen sind von großer Wichtigkeit für Forschung und regenerative Medizin. Für letztere bieten diese Zellen aufgrund ihrer Fähigkeit, jede Körperzellen zu bilden, eine vielversprechende Möglichkeit, zerstörte Gewebe oder Organe zu ersetzen. In der Forschung stellen sie ein nützliches System dar, um Entwicklungs- und Differenzierungsprozesse zu untersuchen, die in der physiologischen Situation z.B. der Embryonalentwicklung – schwer zugänglich sind. Eine wichtige Grundlage für diese Anwendungen sind jedoch Methoden, die die effiziente und gerichtete Differenzierung von Stammzellen in einen bestimmten Zelltyp erlauben.

In dieser Arbeit wird zunächst das Differenzierungspotential von SG der Fischspezies Medaka (*Oryzias latipes*) untersucht, um festzustellen, ob Pluripotenz von SG, die bisher nur in Maus und Mensch gezeigt wurde, auch in anderen Wirbeltieren außerhalb der Säuger erhalten ist. Meine Ergebnisse zeigen, dass Medaka-SG fähig sind verschiedene somatische Zelltypen zu bilden, und zwar Fettzellen, Pigmentzellen, Knochenzellen und Nervenzellen und daher ein breites Differenzierungspotential besitzen.

Das zweite Ziel dieser Studie ist die Entwicklung einer Differenzierungsmethode, die nur auf der Expression einzelner so genannter Masterregulatoren (MR) beruht – Gene, die als essentiell für die Entwicklung bestimmter Zelltypen bekannt sind. Meine Ergebnisse zeigen, dass der Pigmentzell-spezifische Transkriptionsfaktor Mitf-M, von dem gezeigt wurde, dass er die Differenzierung von Medaka-ESZ in Pigmentzellen induzieren kann, die Bildung desselben Zelltyps in Medaka-SG induziert. Dieser Ansatz ermöglichte auch die Bildung anderer somatischer Zelltypen. So führte Überexpression der MR *cbfa1* und *mash1* in Medaka SG zur Differenzierung in Osteoblasten bzw. Neuronen. Interessanterweise wurde bei diesen Differenzierungsprozessen die Aktivierung von Genen beobachtet, die während der Embryonalentwicklung vor dem Differenzierung-auslösenden MR aktiviert werden.

Weiterhin zeigen meine Ergebnisse, dass der Ansatz einer gerichteten Differenzierung, ausgelöst durch einzelne MR, auch auf Säuger-Stammzellen übertragen werden kann. So wurde durch Überexpression des neuronalen Genes *ngn2* in murinen ESZ die effiziente und schnelle Bildung von Nervenzellen induziert, wobei auch hier die Aktivierung von Genen beobachtet wurde, deren Expression in der Embryogenese der von *ngn2* vorangeht. Die

Herstellung einer transgenen Zelllinie, in der die Überexpression von *ngn2* aktiviert werden kann, erlaubte die Entstehung einer Kultur mit einem großen Anteil funktionaler Neuronen. Der durch *ngn2* ausgelöste Differenzierungsprozess war unabhängig von zusätzlichen Faktoren und lief sogar unter Bedingungen ab, die normalerweise den pluripotenten Zustand unterstützen. Außerdem führte Überexpression von *ngn2* auch in IPS Zellen zur Bildung von Zellen mit neuronalem Phenotyp. Weiterhin konnte auch durch Transduktion des Ngn2-Proteins in murine ESZ neuronale Differenzierung ausgelöst werden, und zwar die Bildung neuronaler Vorläuferzellen. Zuletzt wird bewiesen, dass gerichtete Differenzierung von murinen ESZ durch einzelne MR Gene neben neuronalen Zelltypen auch die Bildung anderer somatischer Zellen erlaubt: Überexpression der Gene *myoD* oder *cebpa* induzierte die Differenzierung in Muskelzellen bzw. Makrophagen-ähnliche Zellen. Unter Verwendung transgener Zelllinien, die die Aktivierung jeweils eines MRs erlauben, war es möglich, gemischte Kulturen zu erhalten, in denen zwei verschiedene Differenzierungsprozesse parallel abliefen.

Diese Studie zeigt, dass die Überexpression einzelner Gene ausreichend ist, um gerichtete Differenzierungsprozesse in einen bestimmten Zelltyp auszulösen. Die erfolgreiche Durchführung dieses Ansatzes wird nicht nur mit verschiedenen Genen und somit verschiedenen resultierenden Zelltypen nachgewiesen, sondern auch in unterschiedlichen Stammzelltypen aus Fisch und Maus. Dies erlaubt die Schlussfolgerung, dass bestimmte Gene in vitro das Schicksal von Stammzellen festlegen können und dass diese Fähigkeit eine konservierte Eigenschaft in Wirbeltieren zu sein scheint. Somit präsentiert diese Arbeit neue Erkenntnisse über die Rolle von MR bei der Festlegung von Zellidentitäten und in Differenzierungsprozessen. Weiterhin wird eine neue Methode zur Induktion gerichteter Differenzierung in Stammzellen aufgezeigt, die mehrere Vorteile in Bezug auf Effizienz, Geschwindigkeit und Reproduzierbarkeit hat. Auslösung von Differenzierung durch MR Gene bietet somit einen neuen vielversprechenden Ansatz mit potentieller Anwendung sowohl in Stammzellforschung als auch in regenerativer Medizin.

Summary

Pluripotency describes the ability of stem cells to form every cell type of the body. Pluripotent stem cells are e.g. embryonic stem cells (ESCs), but also the so-called induced pluripotent stem cells (IPS cells), that are generated by reprogramming differentiated somatic cells into a pluripotent state. Furthermore, it has been shown that spermatogonia (SG) derived from adult testes of mouse or human are pluripotent. Because of their ability to differentiate into every somatic cell type, pluripotent stem cells have a unique status in research and regenerative medicine. For the latter, they offer a valuable opportunity to replace destroyed tissues or organs. For basic research, stem cells represent a useful system to study differentiation or developmental processes that are difficult to access in the physiological situation e.g. during embryogenesis. Both applications, however, require methods that allow efficient and directed differentiation of stem cells into defined specialized cell types.

This study first aims to investigate the differentiation potential of SG derived from the teleost fish medaka (*Oryzias latipes*). My results demonstrate that medaka SG are able to form different somatic cell types, namely adipocytes, melanocytes, osteoblasts, and neurons. This indicates that medake SG have retained a broad differentiation potential suggesting that pluripotency is not restricted to mouse and human SG but might be conserved among vertebrates.

Next, I wanted to establish a differentiation method that is solely based on ectopic expression of genes known to be essential for the formation of certain somatic cell types – so called master regulators (MRs). My findings show that ectopic expression of the melanocyte-specific transcription factor *mitf-m* that has previously been shown to induce differentiation of medaka ESCs into pigment cells resulted in the formation of the same cell type in medaka SG. This approach could be used to generate other somatic cell types. Thus, ectopic expression of the MRs *cbfa1* and *mash1* in MF-SG was sufficient to induce differentiation into osteoblasts and neurons, respectively. Interestingly, these differentiation processes included the activation of genes that are expressed earlier during embryogenesis than the differentiation-inducing MR.

Furthermore, my findings show that the approach of MR-induced differentiation can be transferred to mammalian stem cell systems. Ectopic expression of the neural transcription factor *ngn2* was sufficient to induce efficient and rapid differentiation of neurons in mouse ESCs. This differentiation process also included the induction of genes that in vivo are activated at earlier stages than *ngn2*. By generating a transgenic cell line allowing induction of ectopic *ngn2* expression, it was possible to obtain a culture containing a large fraction of functional neurons. *Ngn2*-induced differentiation did not require any additional signals and occurred even under pluripotency promoting conditions. Moreover, ectopic expression of *ngn2* did also induce the formation of cells

with neuronal morphology in IPS cells indicating that MR-induced differentiation is operative in different stem cell types. Furthermore, protein transduction of Ngn2 into mouse ESCs also resulted in a neuronal differentiation process up to the appearance of neural precursor cells. Last, my results show that MR-induced differentiation can also be used to generate other cell types than neurons from mouse ESCs. Myoblasts and macrophage-like cells were generated by ectopic expression of the MRs *myoD* and *cebpa*, respectively. Using transgenic cell lines enabling induction of MR expression it was possible to obtain mixed cultures with two different differentiation processes occurring in parallel.

Altogether this study shows that ectopic expression of single genes is sufficient to induce directed differentiation of stem cells into defined cell types. The feasibility of this approach was demonstrated for different MRs and consequently different somatic cell types. Furthermore, MR induced differentiation was operative in various stem cell types from fish and mouse. Thus, one can conclude that certain genes are able to define cell fates of stem cell in vitro and that this cell fate defining potential appears to be a conserved feature in vertebrates. These findings therefore provide new insights in the role of MRs in cell commitment and differentiation processes. Furthermore, this study presents a new method to induce directed differentiation of stem cells that offers several advantages regarding efficiency, rapidness, and reproducibility. MR-induced differentiation therefore represents a promising tool for both stem cell research and regenerative medicine.

Introduction

Pluripotent stem cells are characterized by their ability to form every cell type of the body. The first pluripotent stem cells were embryonic carcinoma cells that were isolated from a certain germ line tumor, a so-called teratocarcinoma [1]. Shortly thereafter, researchers succeeded in isolating pluripotent stem cells from the inner cell mass of normal mouse embryos resulting in so-called embryonic stem cells (ESCs) [2]. These cells have the potential for unlimited self-renewal in culture and contribute to embryogenesis when injected in mouse embryos. The next break-through in stem cell research was marked by the establishment of embryonic stem cell lines from primates [3] and humans [4].

On the molecular level, the state of pluripotency of ESCs is regulated by a complex network of interacting factors. Especially the transcription factors *nanog*, *oct4*, and *sox2* have been identified as key regulators of pluripotency in both human and mouse ESCs [5,6]. Maintaining the state of pluripotency requires the activation of defined signalling pathways. Initially, propagation of undifferentiated ESCs was found to depend on the presence of serum and mitotically inactivated feeder cells. Later, bone morphogenic protein (BMP) and leukemia inhibitory factor (LIF) were identified as important mediators to maintain pluripotency in murine ESCs (mESCs). The BMP signalling pathway includes the activation of so-called *inhibitor of differentiation* genes (*Ids*) and BMP treatment can substitute serum in mESC culture [7]. Similarly, LIF was shown to replace the requirement for feeder cells and to support the maintenance of pluripotency [8,9] by activation of the STAT3 signalling pathway [10]. Interestingly, neither human [11,12] nor medakafish ESCs [13] depend on STAT3 activation to retain pluripotency indicating that LIF signalling might not be an essential regulator of pluripotency. This is also supported by recent findings demonstrating that mESCs can be propagated in an undifferentiated state by small molecule-mediated inhibition of two protein kinases [14]. These results suggest that pluripotency of ESCs is mediated by an intrinsic program that does not depend on extrinsic stimuli.

Despite some difference on the molecular level, all ESCs share the capability to differentiate in numerous somatic cell types in vitro. This feature gives them a unique status in regenerative medicine as they offer a potential approach to replace destroyed tissues or organs. Furthermore, stem cells provide a valuable system to gain insights in differentiation processes as the corresponding in vivo situation is often difficult to access thus impeding detailed analyses. However, there are two important prerequisites that have to be met for application of stem cells both in research and in clinical medicine. First, it is necessary to find valuable sources to obtain pluripotent and patient-specific stem cells in an easy and ethically unproblematic way. Secondly, successful use

of stem cells as clinical therapy or differentiation model requires the establishment of methods that allow homogenous and directed formation of defined cell types.

Regarding the problem of stem cell sources, tremendous progress has been made during the last decade as several recent studies describe methods for derivation of pluripotent stem cells without involving the use of early embryonic stages. One such approach is the directed reprogramming of fibroblasts into pluripotent stem cells (IPS) through introduction of pluripotency-associated transcription factors [15-17]. An alternative source for cells with a broad differentiation potential are spermatogonial cells derived from adult testes of mice and also humans [18,19]. Both, the reprogramming and the spermatogonial stem cell approaches offer the possibility to circumvent ethical as well as immunological limitations linked with ESCs. However, differentiatable spermatogonia (SG) are thus far restricted to the mouse and human system, while cultures were also successfully established from rat [20] and medakafish (*Oryzias latipes*) [21]. Furthermore, recent data challenge pluripotency of human SG as these cells appear to resemble fibroblasts rather than ESCs regarding certain molecular features [22]. Thus, it is not clear if pluripotency of SG is restricted to certain species or a more conserved feature among vertebrates.

The second challenge of stem cell applications is the establishment of differentiation methods allowing the formation of defined cell types from stem cells. Although there are a large number of differentiation protocols available, major problems remain. A large part of commonly proposed differentiation strategies are based on induction of random differentiation e.g. by formation of cellular aggregates (embryoid bodies). Subsequently, differentiation is directed towards a specific lineage by successive changes of culture conditions e.g. addition of growth factors or co-culture with other cell lines [23]. Some of these changes mimic the in vivo situation during embryogenesis, but in general they have to be determined empirically in a time-consuming process.

Furthermore, as most of these protocols depend on several defined parameters, they are rather susceptible to variability as each parameter may have different side-effects. For example, it has been shown that various growth factors promote several differentiation pathways in parallel [24]. This plasticity often leads to slow and inefficient differentiation processes; and therefore only a small proportion of stem cells actually form the desired cell type. However, the efficient generation of pure cultures of defined cell types is one of the most important requirements for potential application of stem cells for tissue regeneration. To enrich for the desired cell type, strategies often include selection mechanisms, e.g. targeted insertion of a fluorescent protein into a lineage-specific locus thus allowing subsequent cell sorting [25]. These approaches, however, include the stable integration of transgenes that may have undesirable effects in later applications.

An alternative approach to enhance fate determination of stem cells towards a defined cell lineage is to mimic the corresponding in vivo development by ectopic expression of genes specific for this lineage. For example, it has been reported that forced expression of the neural transcription factors *sox1* or *sox2* in ESCs promotes the differentiation towards the neuroectodermal lineage upon induction of differentiation [26]. Similarly, the formation of hepatocyte-like cells out of ESCs is enhanced by ectopic expression of the hepatocyte-specific gene *hnf3β* [27]. These findings indicate that the expression of lineage-specific genes can influence the fate determination of stem cells, albeit in these studies differentiation itself still had to be induced and promoted through external signals like e.g. embryoid body formation. In contrast, Bejar et al. demonstrate that ectopic expression of the melanocyte-specific transcription factor *mitf-M* alone is sufficient to induce differentiation of medakafish ESCs (MF-ESCs) into pigment cells [28]. These data indicate the certain key developmental genes – so called master regulators (MRs) - have the potential to induce differentiation of stem cells without the need for any additional signals.

Based on this hypothesis, I wanted to establish a differentiation method that is solely based on ectopic expression of single MRs without the need for additional differentiation-inducing or lineage-promoting signals. I show that certain genes are sufficient to induce directed differentiation of stem cells into defined cell types. The feasibility of this approach is demonstrated in fish and mouse cells indicating that the cell fate defining feature of such MRs might be conserved in different vertebrate species.

Furthermore, this study aims to get more information about the differentiation potential of adult spermatogonia. Thus, I investigated the ability of spermatogonial cell line from the small teleost fish medaka (*Oryzias latipes*) as a representative of non-mammalian vertebrates. My results show that medaka spermatogonia (MF-SG) have the potential to form cells from different somatic germ layers thus indicating that a wide differentiation potential of male germ cells is not restricted to human and mouse.

Results and discussion

Differentiation of adult stem cells: medakafish spermatogonia (MF-SG)

Characterization of medakafish spermatogonia

To analyze the differentiation potential of male germ cells in lower vertebrates I used a medaka spermatogonial cell line (MF-SG) that has been derived from testes of adult medakafish and is stable in culture without immortalization [21]. Furthermore, MF-SG have been shown to express spermatogonial marker genes and to be able to undergo spermatogenesis in vitro indicating that they have retained their spermatogonial character. To verify that this is still the case after long term culture, I performed a detailed analysis of MF-SG regarding spermatogonial markers (see manuscript 1). Furthermore, MF-SG were analysed with respect to stem cell characteristics and compared to MF-ESCs. Both MF-SG and MF-ESCs show alkaline phosphatase activity which is a characteristic for self-renewing cells. Moreover, my results show that MF-SG still exhibit several typical spermatogonial features like e.g. activation of germ cell-specific promoters which are inactive in MF-ESCs. These results confirm that MF-SG have retained their spermatogonial identity after long term culture. Furthermore, they allow discrimination between MF-SG and MF-ESCs in later experiments. Moreover, gene expression analyses showed no expression of the Sertoli marker *dmrt1bY* [29,30] thus excluding MF-SG cultures being contaminated with Sertoli cells.

Altogether, these findings demonstrate that MF-SG have retained numerous spermatogonial characteristics even after long-term culture allowing a clear discrimination between MF-SG and MF-ESC cultures. Furthermore, MF-SG cultures are devoid of Sertoli cell contamination and show features of self-renewing stem cells, like high alkaline phosphatase activity and continuous proliferation in culture without the need for any immortalization procedures.

Retinoic acid induced differentiation of MF-SG

Having verified the spermatogonial and stem cell characteristics of MF-SG I next wanted to analyse if these cells are able to respond to differentiation inducing signals by the formation of other cell types than sperm. First, retinoic acid (RA) was used as signal to induce differentiation (see manuscript 1). RA is known to play a crucial role during physiological development and has been shown to induce differentiation of mESCs into various cell types [31], among others into adipocytes [32]. MF-SG were treated with various RA concentrations and analysed with respect to morphological changes. At RA concentration of 10µM, the formation of adipocytes was observed. Adipocytes were also detected at RA concentration of 1µM albeit with lower efficiency indicating a dose-dependency of RA effects. Adipocytic identity was confirmed by morphology using light and electron-

microscopy, gene expression, and biochemical analyses. Furthermore, by transient transfection with spermatogonia-specific promoters and subsequent RA treatment it was possible to verify that adipocytes arose from cells with former spermatogonial identity. Last, it was tested if RA treatment results in the same effects in MF-SG and MF-ESCs. Thus, same RA concentrations were tested on MF-ESCs. None of these concentrations resulted in the formation of adipocytes. Thus, one can assume that effects of RA treatment depend on the original cell line.

In summary, these findings demonstrate that MF-SG can develop into adipocytes upon RA treatment. Thus, one can conclude that they have a certain differentiation potential as they are able to form at least one cell type from a somatic germ layer. Furthermore, these results show that effects of RA treatment on MF-SG are dose-dependent which is in agreement with numerous other studies reporting RA-induced differentiation of mESCs. Dependent on concentration and time point, RA treatment results in the formation of various cell types, e.g. neuronal cells, cardiomyocytes, smooth muscle cells, and also adipocytes [31]. This underlines that RA represents a highly effective cytokine that induces numerous differentiation pathways dependent on the environmental context. This context also seems to include the stem cell line used for RA-induced differentiation as it has been demonstrated that different mESC lines exposed to the same RA treatment display considerable differences in morphology and number of differentiated cells [33]. This is again in agreement with my results that demonstrate different effects of RA in different cell lines, namely MF-SG and MF-ESCs. Although both cell lines show stem cell characteristics and obviously have a certain differentiation potential, similar treatment resulted in different outcomes.

Interestingly, none of the RA concentrations tested on MF-SG led to the formation of sperm although RA is known play an important role in mammalian spermatogenesis [34]. Thus, one can hypothesize that the stem cell features of MF-SG predominate over their germ cell characteristics as they response to RA by differentiation into somatic cells. Alternatively, the induction of spermatogenesis by RA requires different conditions of the RA treatment or sperm were produced at a number below the detection level. Another possibility is that spermatogenesis in medaka does not require RA at all which is supported by the results of a study demonstrating that spermatogenesis in the closely related zebrafish does not depend on RA [35].

Mitf-M-induced differentiation of MF-SG into melanocytes

Hitherto, my results reveal that MF-SG are able to form other cell types than sperm. Next, I aimed to establish a method to induce differentiation of MF-SG in a more controllable way by introduction of so called master regulators (MRs). MRs are key developmental genes that play an essential role during in vivo formation of

defined cell types. It has previously been shown that Microphtalmia-Associated-Transcription-Factor (Mitf-M) is sufficient to induce terminal differentiation of MF-ESCs into melanocytes suggesting that such genes have the potential to induce in vitro differentiation [28].

Thus, to test if Mitf-M is also sufficient to induce melanocyte formation of MF-SG, MF-SG were transiently transfected with *mitf-M*. Eight days post transfection, pigmented cells were detected in *mitf-M*-transfected cultures. Melanocyte identity was confirmed by morphology, gene expression pattern, and functional features like the absorbtion of a broad spectrum of light. Beside the expression of melanoyte-specific marker genes, the gene expression pattern revealed an interesting phenomenon, namely the upregulation of the neural crest markers *snail2* [36] and *sox10*. In vivo, both genes are expressed earlier than *mitf-M* and *sox10* has been shown to regulate *mitf-M* in vivo [37]. These findings might indicate that *mitf-M*-transfected cells recapitulate typical stages of melanocyte differentiation, including neural-crest-like stages. The molecular mechanism enabling Mitf-M, a downstream transcription factor in the genetic cascade of the neural crest lineage, to initiate early steps of differentiation remains elusive.

These results show that Mitf-M is sufficient to induce terminal differentiation of MF-SG into melanocytes. This again indicates that MF-SG have a wide differentiation potential as they are able to form other cell types than sperm. Furthermore, one can conclude that the cell fate defining potential of *mitf-M* is operative not only in MF-ESCs but also in other cell lineages that have a certain differentiation ability.

Cbfa1-induced differentiation of MF-SG into osteoblasts

Mitf-M was already known to be sufficient to induce differentiation of stem cells. Next, I wanted to investigate if also other key developmental factors have the potential to determine cell fate of spermatogonial cells. Thus, several other potential MRs were tested in MF-SG, namely *cbfa1*[38-40], *mash1*[41,42], *runx1* [43], *scl* [44], *sox10* [45]. Ectopic expression of *runx1*, *scl*, and *sox10* did not result in any morphological changes that suggested the formation of a specific cell type. Thus, for further analyses, I focused on *cbfa1* and *mash1* as ectopic expression of these genes led to more promising phenotypic changes indicating the induction of a directed differentiation process.

Core-binding factor alpha 1 subunit (cbfa1, often referred to as *runx2*) was chosen to induce differentiation into osteoblasts as this factor was previously shown to be essential for osteoblastogenesis [38-40]. Transient transfection of MF-SG with *cbfa1* resulted in the formation of cells expressing numerous marker genes for terminally differentiated osteoblasts indicating that cells differentiated into osteoblasts. Interestingly, gene expression analyses also revealed upregulation of *dlx5* upon *cbfa1* transfection. *Dlx5* is known to regulate *cbfa1*

expression, while its own expression was thus far not shown to be directly controlled by *cbfa1* [46]. Thus, *cbfa1*-mediated differentiation into osteoblasts included a similar phenomenon like *mitf-M*-induced differentiation namely the activation of a gene located upstream of the transfected factor in the corresponding genetic cascade in vivo.

To check whether *cbfa1*-transfected MF-SG also adopted functional features of osteoblasts, Van Kossa staining and calcein staining were performed to visualize calcified matrix depositions. Calcium depositions could only be detected in *cbfa1*-transfected MF-SG cultures. Neither mock-transfected MF-SG nor *cbfa1*-transfected fibroblasts showed positive calcein staining. Together with the results of the gene expression analyses these data indicate that Cbfa1 is sufficient to induce and promote differentiation of MF-SG into functional osteoblasts. This strong cell fate defining potential in vitro is in line with the role of *cbfa1* during in vivo development where this gene is expressed in the developing skeleton and is essential for bone formation. *Cbfa1* null mutant mice die immediately after birth due to the lack of mature osteoblasts [39,40]. The medaka homolog of *cbfa1* displays high similarity with the mammalian *cbfa1* regarding amino acid sequence and embryonic expression pattern [47] thus suggesting a conserved important role of Cbfa1 during physiological osteoblast development.

In vitro, ectopic expression of *cbfa1* promotes differentiation of primary bone marrow stromal cells [48] and adipose tissue derived stem cells [49] into mineral depositing osteoblasts. While the cell lines used in these studies are already committed to the mesodermal lineage, my results additionally show that *cbfa1* is also able to induce and promote osteoblastic differentiation of cells with germ line origin. Albeit these findings indicate that the cell fate defining potential of *cbfa1* is strong enough to allow differentiation across germ layer borders, one cannot conclusively assume that *cbfa1* can induce osteoblast formation in every cell type. Although previous studies show that ectopic expression of *cbfa1* induces the expression of principle osteoblast markers in nonosteoblastic fibroblasts [38], my findings reveal that *cbfa1*-transfected fibroblasts do not adopt functional features of osteoblasts. Thus, one can assume that the potential of *cbfa1* to induce the formation of mature, functional osteoblasts is not operative in every cell type but might require commitment to the mesodermal lineage and/or a certain differentiation potential.

Mash1-induced differentiation of MF-SG into neurons

Having now verified *mitf-M* and *cbfa1* as effective MRs to induce in vitro differentiation I next wanted to investigate if single gene-induced differentiation is also feasible for the generation of neuronal cell types. Thus, *mash1* (*mammalian achaete-scute homolog 1*) was chosen as potential MR for neuronal differentiation. Mash1

belongs to the family of basic-helix-loop-helix transcription factors and plays an essential role during neurogenesis [41,42].

Transient transfection of MF-SG with *mash1* resulted in the appearance of cells displaying typical neuronal morphology including long axon-like protrusions. The number of cells with neuronal morphology was significantly higher in *mash1*-transfected MF-SG compared to mock-transfected MF-SG excluding the possibility of cells arising due to random differentiation. Furthermore, transfection of MF-ESCs also resulted in the formation of neuron-like cells, albeit with slightly lower efficiency.

On the molecular level, *mash1*-transfected MF-SG activated numerous neuron-specific genes supporting the assumption of neuronal differentiation. Interestingly, the neuronal markers activated during *mash1*-induced differentiation also included *foxD3*, *sox1,* and *pax6*. *FoxD3* is an early neural crest marker and is expressed at earlier stages than *mash1* during embryonic development [50,51]. *Sox1* and *pax6* are also known to belong to the earliest marker genes for neuroectodermal lineage and at least the expression of *sox1* precedes that of *mash1* [52]. Thus, *mash1* induced differentiation of MF-SG included the activation of genes activated before *mash1* during embryogenesis. These results are in perfect analogy to the observations described for MR induced differentiation of spermatogonial stem cells into osteoblasts and melanocytes.

To test whether the cells formed upon *mash1* transfection displayed functional characteristics of neuronal cells, calcium imaging was performed. These experiments revealed that *mash1*-transfected cells were able to respond to KCl stimulation by an increase of the intracellular calcium concentration. Although this feature is not restricted to neuronal cell types, it strongly supports the expression data and leads to the conclusion that *mash1* transfection induced differentiation into neuron-like cells.

In conclusion, these findings indicate that Mash1 is able to induce differentiation of MF-SG into neuron-like cells, which was confirmed by morphology, gene expression pattern, and functional features. Moreover, *mash1* induced differentiation also appears to occur in MF-ESCs. These data identify *mash1* as another suitable MR that is sufficient to determine cell fate decisions of cells harbouring a certain differentiation potential. Like for *cbfa1*, the findings showing the cell fate defining potential of *mash1* in vitro are in agreement with the data describing the role of this gene during physiological neurogenesis. Here, *mash1* is expressed in progenitors of the central and peripheral nervous system [41,53]. *Mash1-/-* mice die at birth due to severe defects in several neuronal structures, e.g. the olfactory epithelium and sympathetic, parasympathetic, and enteric ganglia [42]. Furthermore, it has been shown that ectopic expression of *mash1* can enhance survival of neural precursor cells [54]. Another study reports that ectopic expression of a shorter version of *mash1* in mESCs results in the formation of neurons

[55]. In addition to these findings my results demonstrate that *mash1* is sufficient to induce and promote neuronal differentiation of two different medaka cell lines with a certain differentiation potential. Together with existing data, these results reveal that the potential of *mash1* to define a neuronal cell fate is operative in different stem cell types and might also be conserved among vertebrate species.

Loss of spermatogonial features during single gene induced differentiation

Until now, my data reveal that single MRs have the potential to induce the formation of defined somatic cell types of MF-SG. Next, I wanted to test whether this MR-induced differentiation process also included the loss of spermatogonial features. Therefore, MF-SG were co-transfected with the fluorescent protein mOrange, a reporter construct containing GFP under the control of the germ cell-specific *olvas* promoter, and CMV promoter-driven *mitf-M*, *cbfa1*, and *mash1*, respectively. Analyses of GFP fluorescence revealed a significant decrease in *olvas* promoter activity in MR-transfected cultures compared to mock-transfected cultures. This suggests that MR transfected MF-SG not only adopted the features of defined somatic cell types but also lost their germ cell properties.

Transcriptional changes of MF-SG induced by *dmrt1* genes

Dmrt1bY function and transcriptional regulation

Having now demonstrated that MRs specific for certain somatic cell types are able to induce differentiation of MF-SG, I next wanted to analyze the effects of ectopic expression of *dmrt1a* and *dmrt1bY* which are involved in sex differentiation and determination. In medaka, *dmrt1a* is the ancestral, autosomal version of the *dmrt1* gene whereas *dmrt1bY* represents the duplicated copy of this gene located on the Y chromosome. *Dmrt1* (*Doublesex and mab-3 related transcription factor 1*) is conserved among various vertebrates and is involved in sex determination and Sertoli cell function [56]. Its duplicated copy *dmrt1bY* has adopted the function of master regulator of male development in medaka [29,30]. A loss-of-function mutation in *dmrt1bY* results in XY male to female sex reversal [30]. Furthermore, XX sex reversal to a male phenotype can be achieved by ectopic expression of *dmrt1bY* in medaka embryos [57]. These data demonstrate that *dmrt1bY* acts as dominant male determiner in medaka and has thus adopted a position at the top of the sex determining cascade. In our laboratory, it could be shown that this new hierarchy has developed by the insertion of a transposable element in the regulatory region of the *dmrt1bY* gene (see manuscript 2). This transposable element contains a Dmrt1 binding site suggesting that *dmrt1bY* expression is regulated by Dmrt1 proteins. To verify that this transcriptional regulation is active we analysed the effects of Dmrt1a and Dmrt1bY on *dmrt1bY* promoter activity in MF-ESCs and MF-SG. In both cell lines, neither expression of *dmrt1bY* nor of *dmrt1a* can be detected (data not shown). Cells were cotransfected with a luciferase reporter construct containing the part of the *dmrt1bY*

promoter harbouring the Dmrt1 binding site and different amounts of plasmids encoding *dmrt1bY* or *dmrt1a*. The results show that *dmrt1bY* promoter activity is remarkably reduced in the presence of both Dmrt1a and Dmrt1bY (see manuscript 2). This effect is not detectable when a mutant promoter with a modified Dmrt1 binding site is used. Thus, one can conclude the regulating effect of Dmrt1 proteins on *dmrt1bY* promoter is the results of an interaction with the putative Dmrt1 binding site. Furthermore, these findings demonstrate the machinery regulating *dmrt1bY* expression can be activated in two different medaka cell lines with stem cell characteristics, namely MF-ESCs and MF-SG.

Ectopic expression of dmrt1bY and dmrt1a in MF-SG

Next, I wanted to investigate the effects of ectopic expression of *dmrt1bY* and *dmrt1a* in MF-SG. As mentioned previously, MF-SG do not express *dmrt1bY* nor *dmrt1a* according to RT-PCR. This is in agreement with in vivo expression analyses demonstrating that in testes of adult medaka both *dmrt1* genes are exclusively expressed in Sertoli cells [29,30] with *dmrt1a* expression being 50 fold higher than that of *dmrt1bY* [58]. However, in mammals, *dmrt1* is expressed both in Sertoli cells and germ cells [59] and is required in both cell types for correct testis differentiation [60]. Furthermore, *dmrt1* has been shown to regulate proliferation and pluripotency in fetal germ cells [61]. Thus, in mammals, *dmrt1* obviously fulfils several important functions in differentiation and maintenance of germ cells. Therefore, it is interesting to investigate the effects of the medaka orthologues of *dmrt1* in MF-SG. Moreover, the effects mediated by *dmrt1* in SG represent a physiological situation where MR genes influence the fate of cells with a wide differentiation potential. Thus, the analyses of effects of ectopic expression of *dmrt1* genes in MF-SG could give insights in the physiological mechanism activated by MR genes.

MF-SG were transiently transfected with *dmrt1bY* and *dmrt1a* expression constructs and expression levels of potential target genes were analysed using quantitative RT-PCR. Potential target genes were chosen according to the results of a binding site search for theoretical Dmrt1 binding sites and according to the literature regarding sex determination. Figure 1A shows the expression levels of genes displaying a remarkable up- or downregulation upon ectopic expression of *dmrt1bY* compared to untreated MF-SG. Upregulated genes included *spata7*, *aromatase*, *follistatin*, and *dmrt1a*, whereas *Rspo1* was downregulated. Analyses of the expression levels of the same genes upon transient transfection with *dmrt1a* (Figure 1B) revealed a similar regulation of *follistatin*, *aromatase*, and *Rspo1*. *Spata7* expression levels were largely unchanged and expression of *dmrt1bY*, which was analyzed instead of *dmrt1a*, was downregulated. The latter is in agreement with previous results demonstrating that *dmrt1bY* expression is repressed by Dmrt1a (see manuscript 2). One has to keep in mind that *dmrt1bY* expression was not detected in MF-SG by RT-PCR. Using quantitative RT-PCR, however, a downregulation of *dmrt1bY* was observed in *dmrt1a*-transfected MF-SG compared to untreated MF-SG. Thus, one can assume that

dmrt1bY is transcribed in MF-SG, but at levels below the detection level of RT-PCR. Obviously, this basal expression is further repressed by Dmrt1a.

Furthermore, ectopic expression of *dmrt1a* resulted in remarkable increase in *aromatase* and *follistatin* expression. Both genes have been shown to be expressed in the developing and mature female gonad [62-64] suggesting that ectopic expression of *dmrt1a* induced a kind of feminization process in MF-SG. This is interesting as vertebrate *dmrt1* is generally considered as an effector of male sex determination and has been shown to repress *aromatase* transcription [65]. Furthermore, *dmrt1a*, the autosomal version of *dmrt1* in medaka, is specifically expressed in testes of adult males. However, in female medaka, low levels of *dmrt1a* expression were also detected in the ovary [58]. Similarly, in zebrafish, *dmrt1* transcripts were detected in developing germ cells of both testes and ovary indicating that - additionally to its role in male development - *dmrt1* might also be involved in ovary differentiation in fish [66]. Although this hypothesis explains the upregulation of *follistatin* and *aromatase* in *dmrt1a*-transfected MF-SG, it is not in agreement with the downregulation of *Rspo1* (*R-spondin*). *Rspo1* expression has been shown to be specifically upregulated during ovary development in different vertebrates [67] and to regulate differentiation of the mammalian ovary [68]. Thus, downregulation of *Rspo1* in *dmrt1a*-transfected MF-SG is contradictory to the assumption of a feminization process. One can hypothesize that either Dmrt1a is not sufficient to induce complete conversion of MF-SG to an ovarian cell type or that overexpressed *dmrt1a* exerted a dual function in MF-SG resulting in both the activation and repression of different ovary-specific genes. Another possibility is that conversion of MF-SG to an ovarian cell type requires not only Dmrt1a but additional co-factors that are not present in MF-SG.
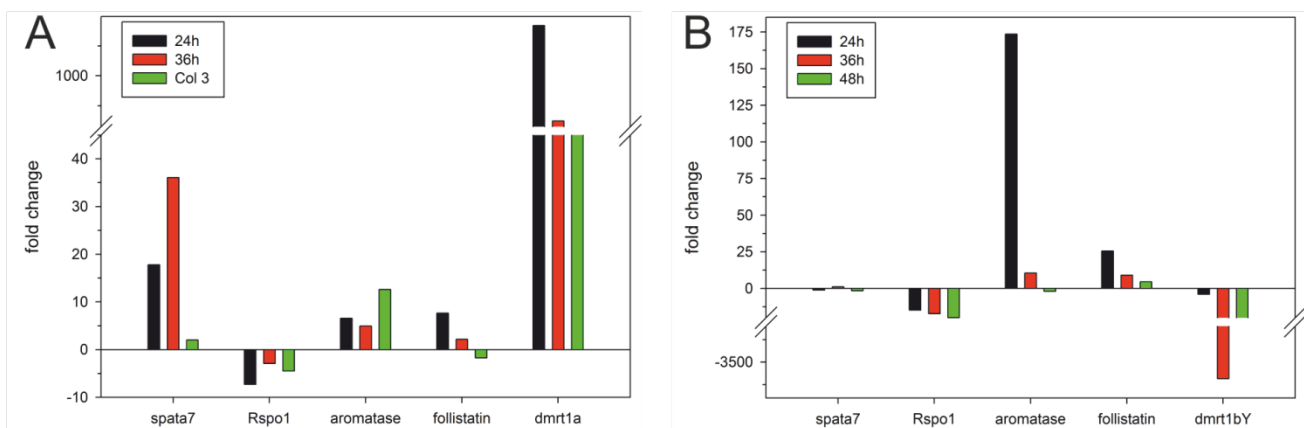

Figure 1: Regulation of potential target genes upon transient transfection of MF-SG with *dmrt1bY* (A) or *dmrt1a* (B) 24, 36, and 48 hours post transfection. Expression levels of untreated MF-SG were set as 1. qRT-PCR were experiments were performed by Maria Hinzmann.

Ectopic expression of *dmrt1bY* in MF-SG resulted in similar changes in expression levels of *follistatin*, *aromatase*, and *Rspo1*. Furthermore, *dmrt1a* was remarkably upregulated. Possibly, *dmrt1bY*-mediated

activation of *dmrt1a* led to similar process observed upon direct overexpression of *dmrt1a*. Interestingly, no Dmrt1 binding site was found in the *dmrt1a* promoter region (see manuscript 2) indicating that activation of *dmrt1a* by *dmrtbY* requires unknown additional factors. Another possible explanation for the induction of ovary marker genes upon *dmrt1bY* transfection can be found in the results of studies analysing *dmrt1bY* expression in estrogen-treated XY reversed female medaka. These studies show that in XY females, *dmrt1bY* is expressed in the ovary at levels even higher than in testes of normal males [58] suggesting that *dmrt1bY* might support ovarian development, possibly redundant to *dmrt1a*.

Dmrt1bY-transfected cells also displayed upregulation of *spata7* (*spermatogenesis-associated 7*), a gene that, in rats, is exclusively expressed in meiotic male germ cells [69]. This indicates that *dmrt1bY* might be able to induce meiosis in MF-SG which is in contrast to previous findings demonstrating that in mouse *dmrt1* prevents meiosis [70]. Additionally, it is not clear why ectopic expression of the dominant male determining gene *dmrt1bY* induces the activation of both ovary-specific and testes-specific genes. A possible explanation can be found in the experimental setup. Transfection efficiencies were only between 15 and 30 percent and thus transient transfection resulted in a mixed culture of non-transfected cells and cells containing different copy numbers of the transgene. Thus, activation of different genes might depend on the level of Dmrt1bY and furthermore it cannot be excluded that transfected cells influenced non-transfected cells by secreted factors etc [71]. As quantitative RT-PCR does not allow gene expression level analysis on cellular resolution, it cannot be determined whether *dmrt1bY* transfection of MF-SG resulted in the formation of cells expressing male and female marker genes or in a mixed population of "male" and "female" cells. To analyze the effects of Dmrt1a and Dmrt1bY in detail, it is necessary to establish transgenic cell lines with stably integrated *dmrt1* genes allowing homogenous induction of *dmrt1a*/*dmrt1bY* expression in all cells.

Nevertheless, these results show that both Dmrt1a and Dmrt1bY can induce remarkable changes in the gene expression pattern of MF-SG. However, these changes indicated that ectopic expression of both genes did not induce the formation of a distinct cell type but led to the appearance of a dual phenotype showing features of both male and female gonad cells. It has to be investigated whether prolonged culture of *dmrt1a*/*dmrt1bY*-transfected cells would result in preferential choice towards only one cell type. However, until now, it cannot be conclusively determined if medaka *dmrt1* genes are suitable for MR-induced differentiation.

Conclusion: Differentiation potential and directed differentiation of MF-SG

In summary, my results reveal that adult MF-SG still are able to differentiate across germ-layer boarders into four different somatic cell types of mesodermal and ectodermal origin. Although these findings do not allow a

definite conclusion whether MF-SG are pluripotent one can assume that also in lower vertebrate like medakafish spermatogonia have retained at least a broad differentiation potential. Together with the data describing pluripotency of mouse and human spermatogonia, these results strongly indicate that a wide differentiation potential might be conserved among vertebrates albeit the degree of differentiation potential might be different in different species.

Moreover, these experiments show that MRs are able to induce and promote differentiation into defined cell types. It has already been known that Mitf-m is sufficient to induce differentiation of medaka ESCs into melanocytes. My results demonstrate the feasibility of this approach for MF-SG and furthermore expand the number of in vitro effective MRs with *cbfa1* for osteoblast and *mash1* for neuronal differentiation. However, ectopic expression of *dmrt1a* and *dmrt1bY* did apparently not induce the formation of one defined cell type. Although it has not been tested if *dmrt1* genes can induce differentiation into only one cell type under different culture conditions, these data indicate that not every key developmental gene can act as differentiation inducing MR in vitro. Nevertheless, my findings suggest that - if the correct MRs can be identified - single gene induced differentiation can be used to generate different somatic lineages. Furthermore, this approach is operative in MF-SG and MF-ESCs but not in fibroblasts – at least for *mitf-m* and *cbfa1* - suggesting that a certain differentiation potential is a prerequisite for MR-induced differentiation.

Interestingly, the process of differentiation of MF-SG included the activation of marker genes that in vivo are expressed earlier than the transfected MR. This phenomenon was observed in all three cases of MR induced differentiation and also described for *mitf-m*-induced differentiation of MF ESCs. Hence, this early marker activation seems to be part of MR induced differentiation and not an experimental side-effect.

Differentiation of embryonic stem cells: Master regulator-induced differentiation of mouse embryonic stem cells (mESCs)

Hitherto, my results demonstrate that key developmental genes are sufficient to determine the cell fate of medaka stem cells. This raises the question if this approach can be transferred to a mammalian system. Thus, I wanted to test whether MRs can induce directed differentiation of murine pluripotent stem cells without the need for additional signals. I focused on the formation of neuronal cell types as this differentiation pathway is of great importance for many applications. Neuronal differentiation offers a valuable system for in vitro studies of neurogenesis or drug testing as the corresponding in vivo situation is often difficult to access. Moreover, the generation of neuronal cell types out of stem cells represents a promising therapeutic approach to replace destroyed or injured neuronal tissues.

In order to establish a neuronal differentiation method that is based on only one factor, I attempted to investigate whether ectopic expression of a neuronal transcription factor in mESCs can induce formation of mature neurons without any other differentiation-inducing or promoting signals. As potential master regulator *neurogenin2 (ngn2)* was chosen which is known to play a crucial role during in vivo neurogenesis [72,73] (see manuscript 3).

Neuronal differentiation of mESCs induced by *neurogenin2* (*ngn2*)

To test if *ngn2* is sufficient to direct neuronal differentiation of mouse stem cells, mESCs were transiently transfected with *ngn2*. Subsequently, LIF, which is a potent factor to keep ESCs pluripotent, was withdrawn from the medium. Five days post transfection (dpt), *ngn2*-transfected cells displayed clear neuronal morphology and stained positive for neuronal marker genes like beta III tubulin (Tuj1) and microtubule associated protein 2ab (Map2ab) indicating the formation of neurons upon *ngn2* transfection. Quantification of Tuj1 positive cells in *ngn2* and mock-transfected cultures resulted in a significant higher number of neuronal cells in *ngn2*-transfected cells. This excludes the possibility of neurons arising by random differentiation due to LIF withdrawal.

On the molecular level, *ngn2*-transfected cells expressed numerous neuronal marker genes that either are not expressed or only at background levels in mock-transfected cells. This again confirms that Ngn2 induced directed neuronal differentiation of mESCs. Interestingly, activated marker genes included *olig2*, *sox1*, and *pax6*. *Sox1* and *pax6* were also detected in MF-SG transfected with *mash1*. As mentioned before, they belong to the earliest markers for the neuroectodermal lineage and *pax6* has been shown to regulate *ngn2* expression in vivo [74,75]. Similarly, *olig2* regulates *ngn2* expression during in vivo neurogenesis in defined neuronal cell types [76]. Thus, *ngn2*-induced differentiation includes the activation of markers located upstream of *ngn2* in the corresponding genetic cascade in vivo. This phenomenon was also observed in different MR-induced differentiation processes in MF-SG strongly supporting the hypothesis that it might represent a part of in vitro differentiation.

Next, I wanted to test if ectopic expression of *ngn2* does not only lead to the appearance of neuronal features but also induces the loss of stem cell markers. Thus, *ngn2* and mock-transfected cells were stained for the stem cell marker Nanog 3dpt. The results clearly demonstrate that *ngn2* transfection results in the loss of Nanog expression.

Ngn2-induced differentiation in the presence of pluripotency-promoting factors

As a next step, I wanted to investigate the strength of the signal mediated by *ngn2*. Therefore, mESCs were transfected with *ngn2* and propagated in complete stem cell growth medium containing LIF. Medium was

changed every day to foreclose the effects of factors potentially secreted by the cells. Furthermore, immunofluorescence staining for STAT3, a downstream effector of LIF signalling [10], was performed in mESCs treated with conditioned medium from *ngn2*-transfected cells. The results reveal clear activation of STAT3 thus confirming the presence of active LIF in the medium.

Surprisingly, in the presence of LIF, *ngn2*-transfected cells displayed similar phenotypical changes like in the absence of LIF within five days. Cells showed neuronal morphology and expressed Tuj1 and Map2ab indicating the formation of neurons. Gene expression analyses revealed expression of neuronal marker genes. Compared to gene expression pattern of *ngn2*-transfected cells cultured without LIF the only detectable difference was a slight retardation of activation of some marker genes. However, numbers of Tuj1 positive cells were comparable to those observed in the absence of LIF. These data indicate that Ngn2 is sufficient to induce neuronal differentiation of mESCs even in the presence of LIF with only a slight retardation on maker gene mRNA levels compared to *ngn2*-induced differentiation under LIF-free conditions. Furthermore, immunofluorescence staining revealed that *ngn2* transfection resulted in the loss of Nanog protein expression even in the presence of LIF.

Ngn2 inducible system

To avoid the disadvantages linked to transient transfection systems I generated two clonal cell lines containing inducible versions of *ngn2*. The cell line E14-P2Angn2 allows induction of *ngn2* by addition of Cre recombinase as transducible protein [77]. The cell line E14-CreP2Angn2 is transgenic for a similar induction construct that additionally contains a tamoxifen inducible version of the Cre recombinase [78]. Thus, induction of *ngn2* expression is achieved solely by addition of 4OHT (4-hydroxytestosterone) and resulting activation of Cre. Both cell lines allow selection of *ngn2*-expressing cells with puromycin.

Having verified that induction of a transgenic version of *ngn2* also results in neuronal differentiation in a similar time course like in transient transfection experiments, I next wanted to evaluate the efficiency of *ngn2*-mediated differentiation. As the inducible cell lines allow efficient selection of *ngn2*-expressing cells, it is possible to determine the percentage of cells forming neurons upon *ngn2* expression. Quantification of Tuj1 positive cells in E14-CreP2Angn2 cells 7 days after induction of *ngn2* revealed that in the absence of LIF about 40 percent of *ngn2* expressing cells differentiated into neurons. In the presence of LIF, Tuj1 positive cells were about 16 percent. The lower percentage observed in the presence of LIF resulted from a higher total cell number whereas the number of Tuj1 positive cells showed no remarkable difference from that detected in the absence of LIF. Possibly, LIF did not influence the number of cells undergoing neuronal differentiation upon *ngn2* expression but did promote continued proliferation of the cells that did not respond to the signal mediated by *ngn2*.

Next, I wanted to analyze the effects of *ngn2* expression in mESCs with regard to stem cell features. Thus, immunofluorescence staining for the stem cell marker Nanog was performed. Similar to the results observed in transient transfection experiments, induction of *ngn2* in E14-CreP2Angn2 cells led to a significant decrease in Nanog positive cells both in the presence and absence of LIF.

The gene expression pattern of E14-CreP2Angn2 cells upon *ngn2* induction was also comparable to the pattern described for transient transfection experiments. Early and late neuronal marker genes were upregulated, among others *pax6* and *olig2*. As mentioned before, these genes are expressed at earlier stages than *ngn2* during embryogenesis. Thus, neuronal differentiation upon *ngn2* induction in E14-CreP2Angn2 cell line showed high similarities to the process induced by transient transfection with *ngn2* including the activation of upstream marker genes. Interestingly, quantitative real time PCR revealed that expression levels of ectopic *ngn2* were similar in transient transfection assays and in E14-CreP2Angn2 cell line at day 3 of neuronal differentiation. At day 7, however, ectopic *ngn2* levels were largely unchanged in transgenic cell line, but had decreased remarkably in transient transfection experiments. This decrease is possible due to stem cell characteristic silencing of the CMV promoter in the *ngn2* expression construct that was used for transient transfection [79]. In contrast, the *ngn2* induction construct CreP2Angn2 contains the promoter of the housekeeping gene *ef1a1* that remains active in pluripotent stem cells [80]. Obviously, the differences of *ngn2* expression levels did not influence the neuronal differentiation process at least with regard to the aspects analysed in this study.

Next, I wanted to analyse if *ngn2*-derived cells form a specific neuronal subtype. RT-PCR revealed activation of the vesicular glutamate transporters vGLUT 1 and 2. These genes are known to be expressed in glutamatergic neurons [81,82] thus indicating the formation of glutamatergic neurons in *ngn2*-expressing mESCs. To confirm this hypothesis, protein expression of vGLUT1 and the glutamate receptor NMDA receptor 1 (NR1) [83] was analysed by immunofluorescence staining. The results show a clear expression of vGLUT1 and NR1 protein in E14-CreP2Angn2 cultures supporting the conclusion that *ngn2*-induced differentiation led to the formation of glutamatergic neurons.

Next, functional analyses of *ngn2*-induced neurons were performed. Patch clamp analyses of neurons at day 10 after *ngn2* induction showed currents typical for terminally differentiated neurons. Furthermore, cells were able to respond to depolarisation by generation of action potentials. Next, *ngn2*-derived neurons were co-cultured with primary hippocampal embryonic neurons and subsequently stained for synaptic markers. Analyses of co-cultures show that E14-CreP2Angn2 cells express the presynaptic marker Synapsin1 and form tight contacts

with hippocampal neurons thus demonstrating that these cells are able to integrate into pre-existing neuronal networks.

In summary, these findings show that Ngn2 is sufficient to induce directed differentiation of mESCs into mature neurons without the need for additional factors and even in the presence of pluripotency-promoting signals. These results prove that the approach of MR-induced differentiation can be transferred from fish to mouse stem cells and furthermore identify *ngn2* as additional suitable MR. This conclusion is supported by other studies reporting that *ngn2* can greatly influence cell fate choice. Thus, *ngn2* has been shown to enhance the survival and differentiation of neural precursor cells [54] and to induce the formation of neurons in embryonic carcinoma cells [84]. However, in these studies, the cell fate defining potential of *ngn2* was either demonstrated in cells already committed to a neural cell fate [54] or in the presence of a specific dimerization factor of *ngn2* [84]. The results presented in my study expand previous findings by revealing that ectopic expression of *ngn2* is sufficient to determine a neuronal cell fate in pluripotent stem cells independent of any additional signals.

Ngn2-mediated differentiation in induced pluripotent stem cells

Hitherto, my findings point out a new method to induce directed differentiation of ESCs. However, the question arises whether this approach is feasible for other stem cells types as the use of ESCs is linked to several problems. Especially, their application in regenerative medicine is hampered by ethical and immunological constraints. Induced pluripotent stem cells (IPS cells) appear to offer a possible solution to this problem as they represent patient-specific stem cells that can be derived without the use of embryonic stages. Thus, I wanted to test if ectopic expression of *ngn2* in IPS cells leads to a similar effect like in ESCs. Mouse IPS cells were transiently transfected with a construct encoding for *ngn2* and mCherryZeo, a fusion protein of the mCherry fluorescent protein and the zeocin resistance gene allowing both selection and visualization of transfected cells. To promote differentiation, LIF was withdrawn from the medium. Beside zeocin selection and LIF removal no other changes to culture conditions were made. Seven days post transfection, *ngn2*-transfected cells could still be visualized by mCherry fluorescence (Figure 2B, D). Several *ngn2*-transfected cells displayed clear neuronal morphology like long axon-like protrusions (Figure 2A, C). This indicates the induction of neuronal differentiation upon *ngn2* transfection.
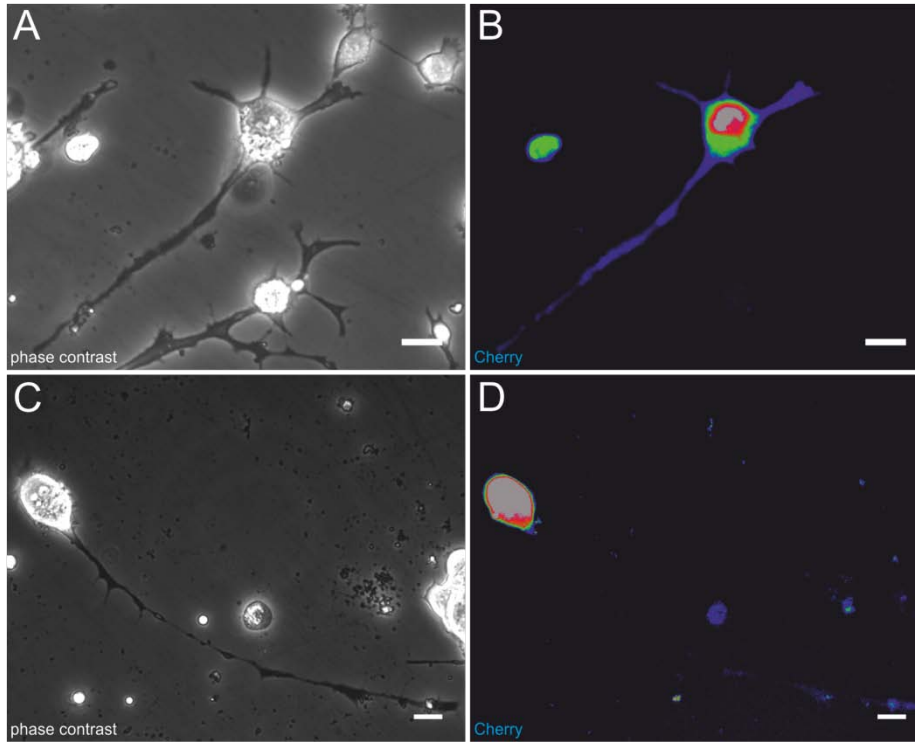
Figure 2: Neuronal differentiation of IPS cells induced by ectopic expression of *ngn2*. Examples of ngn2-2A-CherryZeo transfected IPS cells displaying neuronal morphology 7 days post transfection. (A, C) Phase contrast images. (B, D) Cherry fluorescence verifying expression of transfected construct. Fluorescence intensity is depicted in pseudocolours (rainbow RGB) ranging from black (lowest) to white (strongest). All scale bars represent 20µm.

These findings reveal that ectopic expression of *ngn2* in IPS cells leads to the formation of cells with clear neuronal characteristics suggesting the induction of neuronal differentiation. Although further experiments are necessary to confirm this conclusion, these results strongly indicate that the cell fate defining potential of *ngn2* is also operative in IPS cells. Thus, it is possible that the approach of MR-induced differentiation is feasible for various stem cell lines.

Ngn2-induced differentiation using protein transduction

Differentiation protocols including genetic manipulation of stem cells have the disadvantage that unexpected or late effects of integrated transgenes can impede applications of the generated cell types. Especially, potential use of stem cells in regenerative medicine requires differentiation methods that do not include genetic alterations of the original cells. To address this requirement, I wanted to improve the approach of *ngn2*-induced differentiation by replacing the introduction of *ngn2* coding DNA by introduction of a transducible version of Ngn2 protein. Recombinant, transducible versions of proteins have been successfully generated by fusing the proteins to so-called protein transductions domains. Here, I used the HIV protein transduction domain TAT [85] together with a His-Tag and a nuclear localisation signal linked to the N-terminus of the *ngn2* coding sequence. Additionally, a Flag-Tag was linked to the C-terminal end of *ngn2* resulting in the recombinant protein HTNngn2F (Figure 3A). HTNngn2F expression construct was transfected into HEK293 cells. Cells were harvested and HTNngn2F protein was isolated using Flag-Antibody gel matrix. Expression of HTNngn2F in HEK293 cells as well as effective purification was confirmed using western blot analysis (Figure 3B).
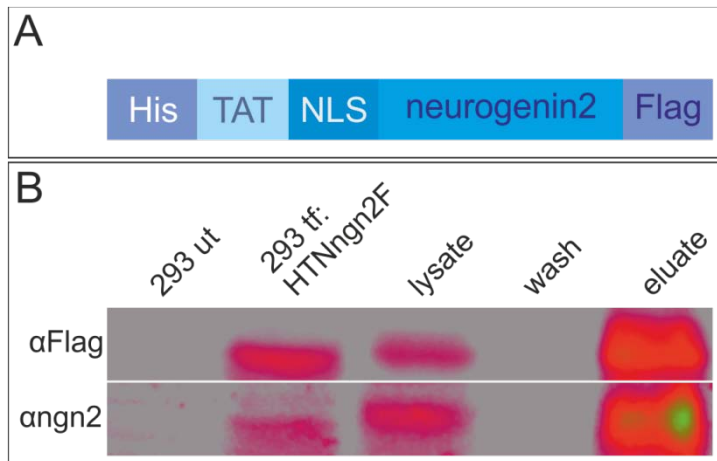
Figure 3: Purification of HTNngn2F protein. (A) Scheme of HTNngn2F construct containing His-tag, protein transduction domain TAT, nuclear localization signal (NLS), and Flag-tag. (B) Western blot analysis showing HTNngn2F expression in HEK293 cells (lane 1+2) and lysate, wash1, and eluate fraction of HTNngn2F purification. Band intensities are depicted in pseudocolours.

Next, protein was transduced in mESCs. Four hours after protein transduction cells were stained using antiFlag antibody to verify successful introduction of HTNngn2F into the cells. HTNngn2F-treated cells displayed a positive staining signal located in or near the nucleus (Figure 4). This suggests that HTNngn2F protein was successfully taken up by the cells and subsequently translocated into the nucleus.
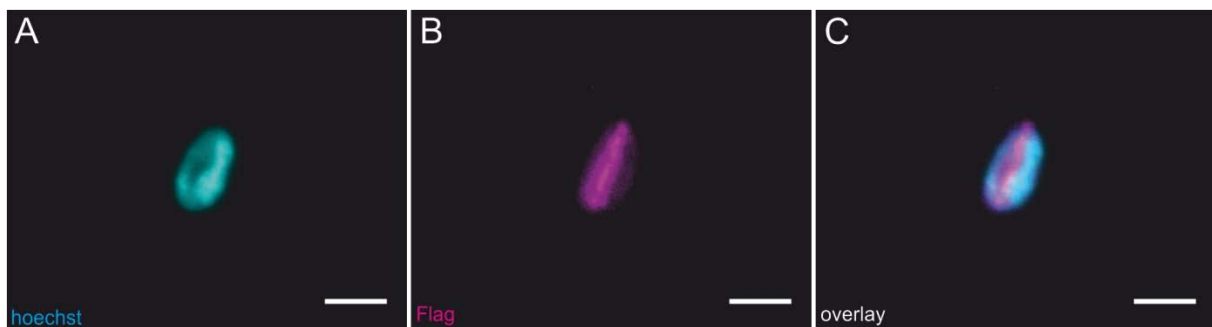

Figure 4: Immunofluorescence staining of HTNngn2F-treated mESCs. (A) Nucleus visualized by Hoechst staining. (B) HTNngn2F protein visualized using anti-Flag antibody. (C) Overlay showing nuclear localization of HTNngn2F protein. All scale bars represent 10µm.

Having verified that HTNngn2F protein can be transduced into mESCs, the next step was to analyze whether the transduced protein HTNngn2F is able to induce a differentiation process like *ngn2* coding DNA. Thus, cells were treated with HTNngn2F protein for 7 days and subsequently analysed for expression of neuronal marker genes. The neuronal marker genes *dcx*, *math3*, *olig2*, *pax6*, and *NeuroD* were activated in HTNngn2F-treated cells compared to mock-treated cells albeit expression levels of *dcx*, *math3*, and *olig2* were very low (Figure 5A). *Pax6* is known to be a marker gene for neuronal progenitor cells [86]. Thus, immunofluorescence staining of nestin at day 14 of HTNngn2F treatment was performed as expression of Nestin is also known to be a characteristic feature of neural progenitor cells [87]. Nestin expression was detected in almost all HTNngn2F-treated cells while mock-treated cells showed only background staining (Figure 5B-F). Thus, one can conclude that transduction of HTNngn2F protein is able to induce neuronal differentiation of mESCs albeit obviously only until the appearance of neural progenitors. It cannot be excluded that a minor part of HTNngn2F-treated cells

differentiated into mature neurons as I observed low activation of *dcx* expression that is transiently expressed in early postmitotic neurons [88,89]. However, expression of *neuN* that is considered a marker for terminally differentiated neurons could not be detected (data not shown) [90]. Possibly, HTNngn2F-treated cultures contained a fraction of postmitotic, but not fully differentiated neurons or the fraction of *neuN*-expressing cells was below the detection level of the RT-PCR method. To conclusively determine if HTNngn2F protein treatment also led to the appearance of mature neurons it is necessary to perform immunofluorescence staining for terminal neuronal marker.

Nevertheless, one can conclude that differentiation induced by HTNngn2F treatment mostly resulted in the formation of neural progenitors. However, protein transduction protocols include numerous unpredictable parameters like efficiency of transduction or half-life time and activity of the recombinant protein. These factors make it difficult to compare the effects of protein transduction to observations made after introduction of DNA encoding for the same protein. For example, it is possible that levels of active HTNngn2F protein were too low or varying too much to promote neuronal differentiation until the appearance of mature neurons. Nevertheless, these results show that the idea of inducing directed differentiation by MRs can be in principle be realised without the introduction of DNA into the original stem cells. As there is a lot of room for technical improvement, this approach potentially represents a new useful method to obtain defined cell types of stem cells without the need for genetic modification.
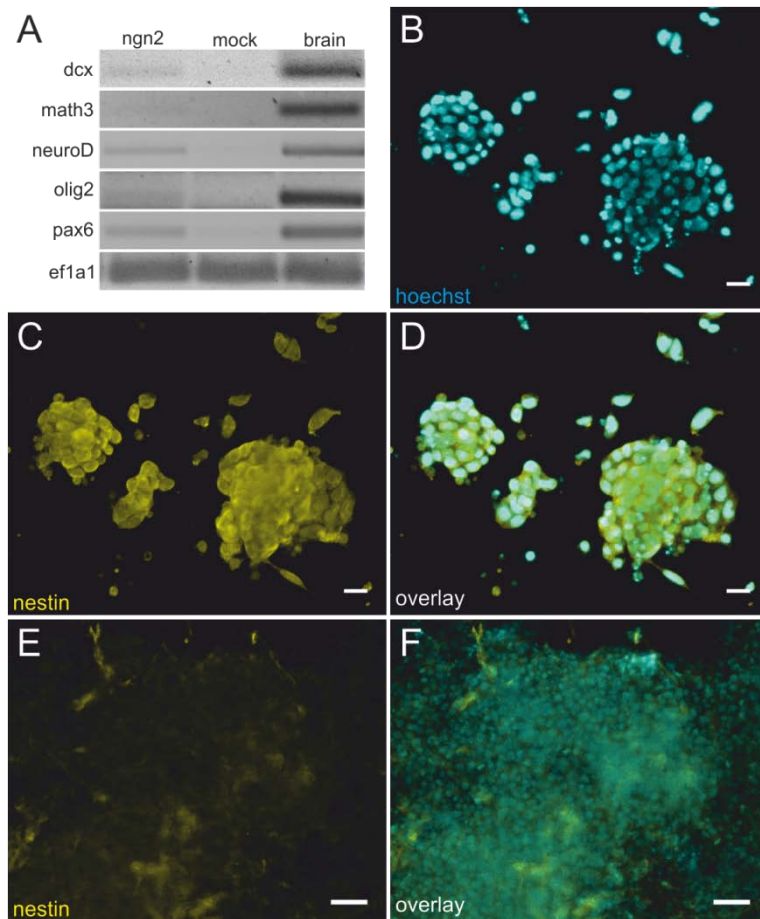
Figure 5: Neuronal differentiation of mESCs induced by treatment with HTNngn2F protein. (A) Gene expression analyses revealing upregulation of neural markers in protein-treated cells compared to mock-treated cells. (B-F) Immunofluorescence staining showing Nestin expression in HTNngn2F-treated cells (B-D), but not in mock-treated cells (E, F). Scale bars represent 20µm (B-D) and 50µm (E, F), respectively.

Master regulator-induced differentiation of mESCs into other lineages

My previous results demonstrate that it is possible to induce and promote neuronal differentiation of mouse pluripotent stem cells solely by ectopic expression of a neural specific transcription factor without any additional signals. Now, the question arises whether this approach can be transferred to generate other cell types. Thus, I replaced the coding sequence of *ngn2* in the CreP2Angn2 construct by other potential MRs and generated mESC lines transgenic for these inducible constructs (Figure 6). As MR candidates I chose *myoD* and *cebpa* resulting in the transgenic cell lines E14-CreP2AmyoD and E14-CreP2Acebpa, respectively. *MyoD* is expressed in developing skeletal muscle during embryogenesis [91] and has already been shown to be able to induce the appearance of myoblastic features when overexpressed in various cell types [92-94]. *Cebpa* (CCAAT/enhancer binding protein alpha) is a transcription factor involved in the development specific hematopoetic lineages [95] and ectopic expression of *cebpa* has been shown to convert B-cells and T-cells into macrophages [96,97].
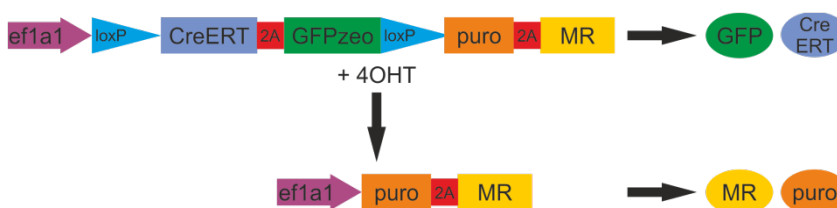

Figure 6: Scheme of CreP2A-MR constructs allowing induction of MR expression by 4OHT treatment.

As a first step I tested the functionality of the induction construct in the cell lines E14-CreP2AmyoD and E14-CreP2Angn2. After treatment with 4OHT GFP fluorescence was analysed. In both cell lines, a large part of 4OHT-treated cells showed a loss of GFP signal indicating successful recombination (Figure 7A, B, D, E and Figure 8A, B, D, E).

Ten days post recombination, E14-CreP2Acebpa cells displayed morphological alterations very similar to a macrophage phenotype. Macrophage-like cells could be detected at high frequency in 4OHT-treated cells and only occasionally in mock-treated cells thus suggesting induction of directed differentiation into macrophages by ectopic expression of cebpa (Figure 7C, F).
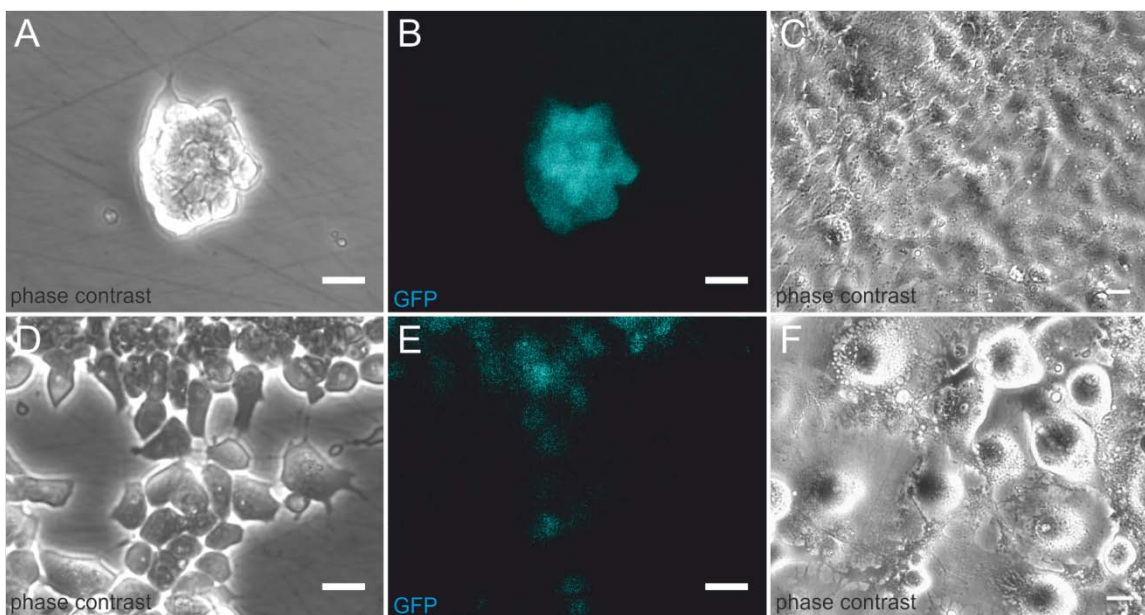

Figure 7: Directed differentiation of E14-CreP2A-cebpa cell line into macrophage –like cells. (A-C) Mock treatedcells. (D-F) 4OHT-treated cells. (A, B, D, E) Day1 post recombination. Loss of GFP signal in 4OHT-treated cells (D, E) indicates Cre-mediated recombination and induction of *cebpa* expression. Mock-treated cells (A, B) show clear GFP signal. (C, F) Day 10 post recombination.4OHT-treated cells (F) showed clear macrophage morphology not detectable in mock-treated cells (C). All scale bars represent 20µm.

Analyses of E14-CreP2AmyoD cells revealed that nine days post recombination cells showed an elongated cell shape characteristic for myoblastic cells (Figure 8F). Cells stained positive for the myoblast marker myosin and, moreover, several multinuclear cells could be detected (Figure 9). Hence, one can conclude that ectopic expression of *myoD* in mESCs induced directed differentiation into myoblastic cells.
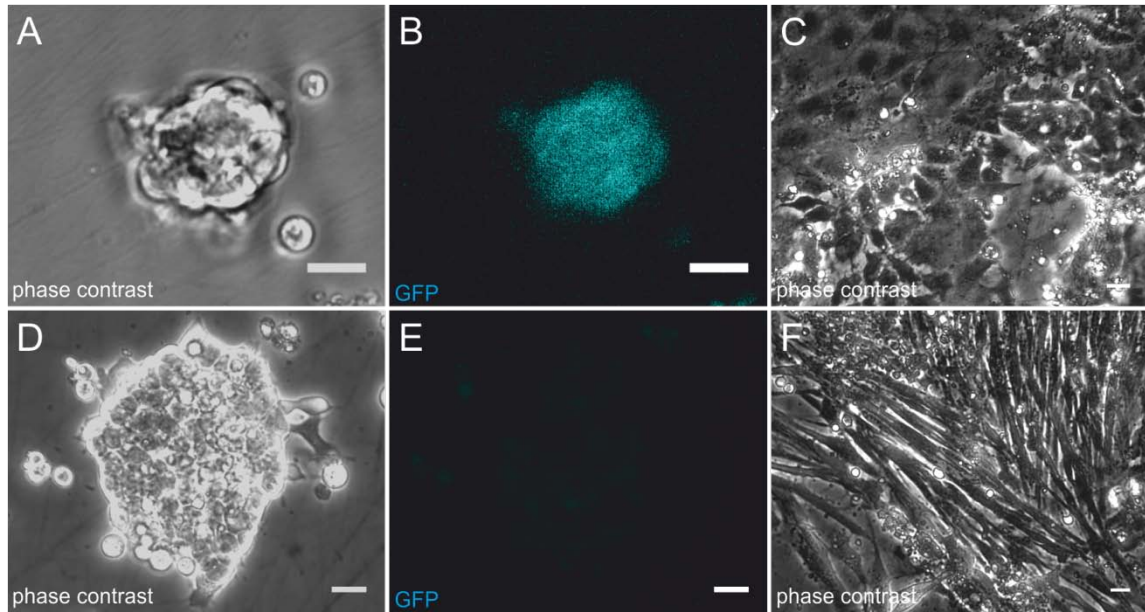
Figure 8: Directed differentiation of E14-CreP2A-myoD cell line into myoblasts. (A-C) Mock treated cells. (D-F) 4OHT-treated cells. (A, B, D, E) Day1 post recombination. Loss of GFP signal in 4OHT-treated cells (D, E) indicates Cre-mediated recombination and induction of *myoD* expression. Mock-treated-cells (A, B) show clear GFP signal. (C, F) Day 9 post recombination. Myoblasts detectable in 4OHT-treated cells (F) but not in mock-treatedcells (C). All scale bars represent 20μm.
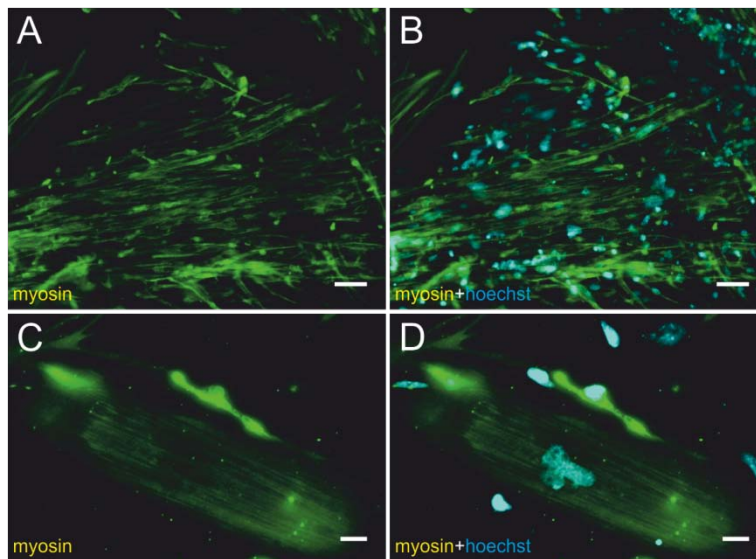
Figure 9: Immunofluorescence staining of E14-CreP2A-myoD cells 10 days post recombination showing myosin expression and multinuclear cells (D). Scale bars represent 50μm (A, B) and 20μm (C, D), respectively.

Having now verified that the CreP2A-MR constructs allow induction of MR expression and subsequent directed differentiation with different MR genes I wanted to investigate whether this system allows the generation of two different cell types in parallel. Thus, a mixed culture of E14-CreP2Angn2 and E14-CreP2AmyoD cells was treated with 4OHT. Nine days post recombination, immunofluorescence staining revealed that cells had developed into a mixed culture of myosin positive myoblasts and Tuj1 positive neurons (Figure 10).

Figure 10: Parallel differentiation into myoblasts and neurons using mixed culture of E14-CreP2Angn2 and E14-CreP2AmyoD cells. 10 days post recombination myosin and Tuj1 positive cells can be detected. Scale bars represent 20µm.

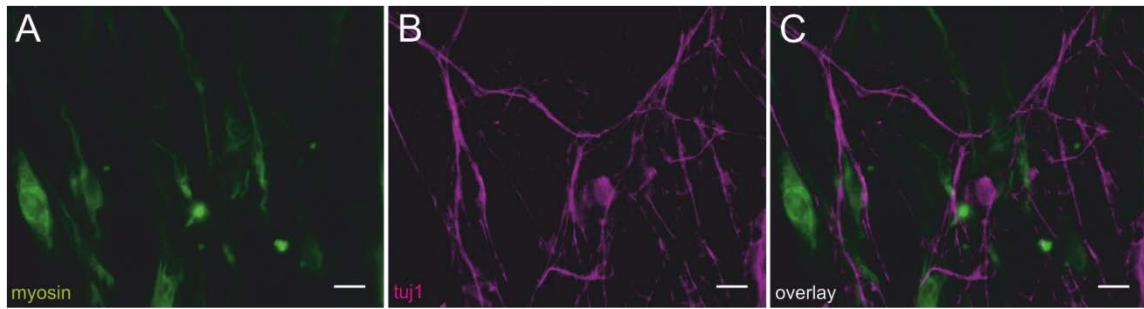Altogether, these data reveal that ectopic expression of both *cebpa* and *myoD* in mESCs results in directed differentiation into defined cell types proving that MR-induced differentiation of mESCs can in principle be used to generate different cell lineages. As myoblasts and macrophages are mesodermal representatives whereas neurons are of ectodermal origin, one can assume that this approach is not restricted to the generation of derivatives of one germ layer. Furthermore, MR-induced differentiation apparently allows the simultaneous formation of two unrelated cell types –myoblasts and neurons – in one culture thus representing a useful tool to obtain mixed cultures of defined cell types.

Conclusion: Cell fate defining potential of master regulator genes

During embryogenesis, various stem cell types have to pass through numerous steps of lineage commitment. Key developmental genes often play a crucial role in these processes of cell fate determination by regulating the specific gene expression program of the various stages or triggering the transition to the next stage. The results presented in this study demonstrate that such master regulator genes are also able to influence cell identity in a non-physiological context. Ectopic expression of MR genes is obviously sufficient to induce direct differentiation into defined cell types. My findings prove that this process does not require any additional differentiation-inducing or promoting signals and is operative in different stem cell types from fish and mouse. This underlines the strength of the cell fate defining potential of MRs and suggests that this function of MR genes is conserved among vertebrates.

So far, the cell fate defining potential of MRs has not been addressed extensively. Only few other studies exist that demonstrate the capability of certain genes to alter a cell's identity. It has been shown that ectopic expression of stem cell specific genes can reprogram somatic cells into a pluripotent state [15-17]. While this represents cell conversion from a differentiated to an unspecialized cell state, there are also several studies indicating that this approach can be inverted in the physiological direction, namely the differentiation of stem cells into specialized cells. For example, ectopic expression of *nurr1*, a transcription factor expressed in the substantia nigra, in mESCs promotes the formation of dopaminergic neurons in a conventional neuronal

differentiation protocol [98]. Similarly, the myoblast-specific gene *myoD* enhances myoblast formation of differentiating ESCs under certain environmental conditions [99]. These findings indicate that MR genes are able to influence cell fate decisions of pluripotent stem cells. However, as in all these studies ectopic expression of MRs was always accompanied by changes of culture conditions - like the addition of a specific differentiation medium or embryoid body formation - it is difficult to evaluate the cell fate defining potential of MRs in these experiments. In contrast, my study shows that the ability of certain MRs to induce differentiation of stem cells does not require additional environmental signals.

Reprogramming and differentiation induced by ectopic gene expression both represent processes from differentiated cells into stem cells or from stem cells into differentiated cells. Here, ectopic expression of single genes induces a change in the status of pluripotency. However, there are also reports of approaches using the cell fate defining potential of key developmental genes to directly convert one somatic cell type into another. For example, ectopic expression of a combination of neuron-specific genes induces the formation of neurons from fibroblasts [100]. Similarly, ß-cells were generated from exocrine pancreatic cells using three pancreas-specific transcription factors [101]. These studies also underline the ability of certain genes to change a cell's identity. However, cell conversion required a set of genes and was either performed in neural differentiation medium [100] or in vivo [101], where it is difficult to evaluate the influence of environmental signals. Thus, it cannot be determined whether the cell fate defining potential of MRs is only operative in a defined environmental context.

Interestingly, already 20 years ago, it has been shown that *myoD* can convert various somatic cell types to myoblastic cells without any medium changes [94]. Thus, cell conversion of somatic cells can be induced solely by ectopic expression of one MR. However, there are also several data that are contradictory to this assumption. For example ectopic expression of *mitf-M* in mouse fibroblasts resulted in the appearance of some features of melanocytes, but was not sufficient to induce melanin production [102]. Similarly, Mitf-M was able to induce formation of melanocytes in medaka ESCs and SG, but not in medaka fibroblasts [28]. Likewise, my results show that the osteoblast MR *cbfa1* can induce the formation of functional osteoblasts in MF-SG, but not in fibroblasts.

In an attempt to put all these data in context one can hypothesize that MR genes have the potential to define a cell's identity, but this cell fate defining potential varies for different MRs. While *myoD* obviously is able to alter the cell fate of pluripotent stem cells as well as differentiated cells, *mitf-M* or *cbfa1* can only define the fate of cells harboring a certain differentiation potential like ESCs or SG and only induce an incomplete cell conversion in terminally differentiated cells like fibroblasts. However, one has to keep in mind that studies investigating the effects of MRs various cell types in vitro might differ in several issues like medium composition, cell line origin

etc. that might influence experimental results. Thus, to exactly compare the cell fate defining potential of MR genes it is necessary to investigate their effects under exactly similar conditions.

Interestingly, in my study and in a previous study using medaka ESCs [28], MR-induced differentiation processes included the activation of genes expressed before the differentiation-inducing MR during embryonic development. One possible explanation for this observation would be that a minor part of cells underwent spontaneous differentiation into progenitor cells expressing these genes. However, medaka cells were constantly kept in pluripotency-promoting medium that should prevent random differentiation processes. For several experiments using mouse ESCs, LIF was withdrawn from the medium which could indeed lead to spontaneous differentiation processes. However, the activation of upstream markers was not detected in control treated cells strongly indicating that this phenomenon is a result of ectopic MR expression. This conclusion is also supported by the fact that this phenomenon was observed both in medaka and mouse cells and using different MR genes. This strongly indicates that it is not an experimental artifact but might be part of MR induced differentiation. One could hypothesize that cells differentiating in vitro into a defined cell type recapitulate the stages occurring during the formation of this cell type during embryogenesis. This would include the recapitulation of early developmental stages although the differentiation-inducing MR is not expressed in these progenitors (Figure 11).
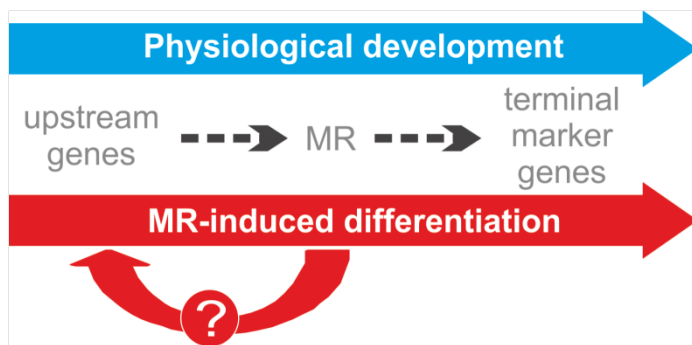

Figure 11: Schematic illustration of early gene activation occurring during MR-induced differentiation

It is not clear whether this upstream marker activation always occurs during MR-induced cell fate changes. Studies reporting cell conversion of differentiated cells by ectopic expression of MR genes describe either no dedifferentiation step at all [101] or the appearance of an intermediate stage of the converting cells [96]. However, it has to be mentioned that in the major part of studies describing induction of cell fate changes by MRs analyses were focused on the identification of the resulting cell type. Thus, it cannot be excluded that recapitulation of early markers might have occurred during MR-induced cell fate determination but below the detection level. A possible approach to address this question would be to compare different MR-induced differentiation processes into various cell types regarding the expression of upstream genes. For this purpose, the cell lines that were created in my study offer a useful tool as they allow the generation of various cell types by homogenous induction of different MR genes. Furthermore, it is an interesting question if the activation of

upstream genes is essential for the formation of mature differentiated cells induced by MR expression. Stem cells with loss-of-function mutations of such early progenitor markers would represent a valuable system to test this hypothesis.

Another interesting aspect of MR-induced differentiation is that obviously single genes are sufficient to break the complex network maintaining pluripotency. Although the mechanisms regulating the status of pluripotency are not fully understood, several recent studies have helped to identify important factors involved in this process. For example, it has been shown that differentiation includes the upregulation of certain microRNAs that are required to shut down the self renewal program [103]. Another important step during differentiation is the remodeling of the epigenetic landscape. The chromatin of differentiated cells is characterized by repressive marks highly organized in foci. In contrast, stem cells display a more dynamic, open chromatin structure that allows rapid activation of differentiation programs [104]. It is not clear if these procedures also occur during MR-induced differentiation. However, as loss of pluripotency is a common step during all differentiation processes it is probable that the mechanisms regulating this step are similar independent of the differentiation protocol used. If this is the case, it would be interesting to analyse how single transcription factors are able to activate this machinery. Analyses of the direct binding sites of MR genes would be a possible approach to address this question. Furthermore, such experiments would reveal if the open chromatin status of pluripotent cells allows the binding of MR genes to additional targets that are not accessible for MRs in the physiological situation.

Altogether, one can conclude that key developmental genes are able to define cell fates outside of their physiological function. Thus, ectopic expression MR genes can be used to generate various cell types from either different stem cell types by induction of differentiation, but also from differentiated cells by induction of cell conversion processes. These approaches represent a promising tool to investigate the mechanisms inducing and regulating the determination of cell identity. Furthermore, MR-induced differentiation or cell conversion offers a valuable opportunity to generate certain somatic cell types for potential use in regenerative medicine.

Materials and Methods (for unpublished experiments from this dissertation)

Cell culture

Culture of MF-SG and MF-ESCs was performed as described in manuscript 1. For *dmrt1a/dmrt1bY* transfections, MF-SG were transfected with 2 ug of *dmrt1a/dmrt1bY* coding plasmids using Fugene HD transfection reagent (Roche) according to the manufacturer's instructions.

Murine IPS cells derived from peritoneal fibroblasts [105] were a kind gift from K. Hochedlinger (Harvard University). IPS cells were grown on mitomycin C-inactivated SNHL feeder cells at 37°C and 5% CO_2 on gelatin-coated wells in DMEM supplemented with 10% FCS, glutamine (4mM), non-essential amino acids (0.1mM), penicillin (1mM), streptomycin (1mM), ß-mercaptoethanol (0.1mM), and LIF (1000U/ml). For transfection experiments, feeder cells were removed by preplating cell suspension of feeder and IPS cells for 30 minutes on gelatin-coated wells. IPS cells were transfected with 2µg pMTE-mCherryZeo2Angn2 plasmid using Fugene HD transfection reagent (Roche) according to the manufacturer's instructions. During differentiation, transfected cells were cultured in complete growth medium without LIF. Selection with zeocin (200µg/ml) was started at day 2 post transfection. Medium was changed every day.

SNHL feeder cells (SNL feeder cells [106] with additional hygromycin resistance) were a kind gift from M. Gessler (University of Wuerzburg). Cells were grown at 37°C and 5% CO_2 in DMEM supplemented with 10% FCS, glutamine (4mM), penicillin (1mM), and streptomycin (1mM). For inactivation, cells were treated with 10µg/ml mitomycin C (Roche) for 3hours at 37°C and 5% CO2, washed three times with PBS, trypsinized and seeded on gelatin-coated wells.

HEK293T cells were grown at 37°C and 5% CO_2 in DMEM supplemented with 10% FCS, glutamine (4mM), penicillin (1mM), and streptomycin (1mM). For small scale protein expression analyses, cells were transfected with 10µg HTNngn2F plasmid using Polyethylenimine (PEI; Roth). PEI was diluted 1:100 in 150mM NaCl and subsequently mixed with plasmid DNA at a ratio of 3µl PEI per 1µg DNA. After incubation of 15min at room temperature, transfection mix was transferred to cells in complete growth medium. 30 hours post transfection, cells were harvested for western blot analysis.

Mouse ESCs were cultured as described in manuscript 3. Generation and culture of cell lines E14-CreP2A-cebpa and E14-CreP2A-myoD was performed as described for E14-CreP2A-ngn2 cell line (manuscript 3).

For transduction of HTNngn2F protein mESCs were seeded at single cell suspension. After attachment of cells, cells were treated with stem cell medium without serum, antibiotics, NEAA, and ß-mercaptoethanol, and LIF

supplemented with 1μM HTNngnF protein or same volume of 50% glycerin/PBS buffer (mock). Cells were incubated at 37°C and 5% CO2 for 4 hours. Subsequently, for mRNA expression analyses, growth medium without LIF was added so that final concentrations of antibiotics, NEAA, and ß-mercaptoethanol, and serum were 0.75x of concentrations in complete stem cell medium. Protein transduction was performed at day 1-3. Subsequently, cells were grown in complete stem cell growth medium without LIF for 4 days and then harvested for RNA isolation. For immunofluorescence staining, protein transduction was performed as described above, however, with modification that after 4 hours incubation medium was supplemented to final concentrations of 1x antibiotics, NEAA, and ß-mercaptoethanol and 0,5x serum. Protein transduction was performed at days 1, 2, 3, 4, and 6 and cells were cultured in Neurobasal medium (Invitrogen) supplemented with 1% penicillin/streptomycin and 2% B27 from day 5 to day 14.

Plasmids

Dmrt1a and *dmrt1bY* expression plasmids were generated by J. Klughammer and contain the coding sequences of *dmrt1a* and *dmrt1bY* respectively with a C-terminal FTH-tag under control of the CMV promoter (J. Klughammer, Bachelorthesis, University of Wuerzburg, 2010).

For *ngn2*-induced differentiation of IPS cells, a construct encoding for *ngn2* and a fusion protein (mCherryZeo) of the fluorescent protein mCherry and the zeocin resistance was generated. Coding sequence of mCherryZeo together with a 2A sequence were amplified by PCR using primers 5'-AGTGGATCCATGGTGAGCAAGGGCG-3' and 5'-GACTCTAGAAGGGCCGGGATTCTCCTCCACGTCACCGCATGTTAGAAGACTTCCTCTGCCCTCGTCCTGCTCCTCGGCCA-3'. PCR product was cloned into pMTE-EGFP-Zeo-P2Angn2 using BamHI and XbaI restriction enzymes resulting pMTE-mCherryZeo2Angn2.

For generation of the construct encoding for HTNngn2F protein *ngn2* coding sequence was amplified by PCR using primers 5'-GCATGAATTCTAAGAAGAAGAGGAAGGTGATGTTCGTCAAATCTG-3' and 5'-TGACCTCGAGCTAGATACAGTCCCTG-3'. PCR product was cloned into HTN-Klf4 vector (kind gift from F. Edenhofer) using EcoRI and XhoI restriction enzymes resulting in HTNngn2 vector. Subsequently, C-terminal region of *ngn2* was amplified by PCR with reverse primer containing the Flag-Tag sequence. Primers were 5'-TCGCCCGCTAGCCCCGGGTC-3' and 5'-TACGCTCGAGCTACTTATCGTCGTCATCCTTGTAATCGATACAGTCCCTGGC-3'. PCR product was cloned into HTNngn2 using NheI and XhoI restriction enzymes resulting in HTNngn2F.

The MR inducible constructs CreP2A-myoD and CreP2A-cebpa were generated like CreP2A-ngn2 (see manuscript 3).

HTNngn2F protein production and purification

Large scale production of HTNngn2F protein in HEK293 cells in suspension culture was performed by Mattia Matasci (Ecole polytechnique fédérale de Lausanne). HTNngn2F-transfected cells were collected by centrifugation 3 days post transfection. For cell lysis, cell pellet was resuspended in TBS (50mM Tris HCl, pH 7.4, 150mM NaCl) supplemented with 1mM EDTA and 1% Triton X-100. After incubation of 20min, protease inhibitor mix (Sigma, 10µl/ml) was added and cell suspension was incubated for additional 10min. Then, cell debris was removed by centrifugation. Purification of HTNngn2F protein from cell lysate was performed by column chromatography using ANTI-FLAG M2 affinity gel (Sigma). Column was prepared according to manufacturer's instructions. Cell lysate was loaded onto the column and unbound proteins were removed by washing the column with 10 column volumes TBS. Subsequently, HTNngn2F protein was eluated by three column volumes TBS containing 100µg/ml FLAG peptide (Sigma). Purified HTNngnF fractions were transferred to storage buffer (50% glycerin, 1M NaCl, 1mM DTT, 1mM EDTA) by dialysis and stored at -20°C.

Western blot

Western blot analyses were performed as previously described [13] using anti-Flag antibody (1:2000; NatuTec, 10-146) and anti-ngn2 antibody (1:1000; Santa Cruz, sc-50402).

RT-PCR

Total RNAs were isolated from cell cultures using the Total RNA Isolation Reagent (AB Gene). Samples were digested with DNAseI (Fermentas) to exclude gDNA contamination followed by cDNA synthesis (Fermentas). Quantitative RT-PCR of *dmrt1a*/*dmrt1bY*-transfected MF-SG were run from 50µg cDNA using a Biorad-iCycler. Primers were as follows: ef1a1 5'-GCCCCTGGACACAGAGACTTCATCA-3', 5'-AAGGGGGCTCGGTGGAGTCCAT-3'; spata7 5'-TAGCCCTGAAGTGAGAGGTCAG-3', 5'-CGTCCATCTTTCCTCTGCTGC-3'; Rspo1 5'-CAATGAGACCATGGAGTGTGTCG-3', 5'-CTCTCCGATTGTGAAGTGCAGG-3'; aromatase 5'-TACCACTGTAGGACTCCCATCC-3', 5'-TCCACACTCGAACAATGTCTCC-3', follistatin 5'-GAAGGAACGGGAGATGTCAGGTC-3', 5'-TGATGTTGGAGCAGTCTGGAGC-3'; dmrt1a 5'-TCCGGCTCCACAGCGGTC-3', 5'-TCCGCAATCAGCTTGCATTTGG-3'; dmrt1bY 5'-CTGGAAAGACTGCCAGTGCTT-3', 5'-

GACTCTCTGGCGGACCATG-3'. Results are average values of three PCR reactions from each RT reaction. Ef1a1 primers were used for template normalization. Relative expression levels were calculated according to the equation $2^{-\Delta CT}$.

For expression analyses upon Ngn2 protein transduction, PCR were run from 25µg cDNA for 32 cycles. For primer sequences of *ef1a1*, *dcx*, *math3*, *olig2*, and *pax6* see manuscript 3. Primers for *NeuroD* were 5'-CAACCTGCGCAAGGTGGTA-3' and 5'-GTCGCTGCAGGGTAGTGCAT-3'.

Immunofluorescence staining

Immunofluorescence staining of Myosin was performed according to staining protocol described in manuscript 3 using anti-myosin antibody (kind gift from R. Hock, University of Wuerzburg). For Nestin staining, cells were washed with PBS, treated with MSP buffer for 30s at room temperature and subsequently fixed in 100% methanol for 3min at -20°C. Then, staining was performed according to the staining protocol described in manuscript 3 using anti-nestin antibody (1: 80; Neuromics, CH23001).

Microscopy

Images were taken at room temperature using a Leica DMI6000B inverted microscope with a Leica DFC350FX camera and the Leica Advanced fluorescence software. Objectives were HCX FL PLAN 10.0x0.25 DRY and HCX PL FLUOTAR L 20.0x0.40 DRY. Imaging medium was phosphate-buffered saline for immunofluorescence staining or standard growth medium for imaging of living cells. All images were analysed and formatted using ImageJ software.

References

[1]   B.L. Hogan, "Changes in the behaviour of teratocarcinoma cells cultivated in vitro.," *Nature*, vol. 263, Sep. 1976, pp. 136-7.

[2]   M.J. Evans and M.H. Kaufman, "Establishment in culture of pluripotential cells from mouse embryos.," *Nature*, vol. 292, Jul. 1981, pp. 154-6.

[3]   J.A. Thomson, J. Kalishman, T.G. Golos, M. Durning, C.P. Harris, R.A. Becker, and J.P. Hearn, "Isolation of a primate embryonic stem cell line.," *Proceedings of the National Academy of Sciences of the United States of America*, vol. 92, Aug. 1995, pp. 7844-8.

[4]   J.A. Thomson, J. Itskovitz-Eldor, S.S. Shapiro, M.A. Waknitz, J.J. Swiergiel, V.S. Marshall, and J.M. Jones, "Embryonic stem cell lines derived from human blastocysts.," *Science (New York, N.Y.)*, vol. 282, Nov. 1998, pp. 1145-7.

[5]   L.A. Boyer, T.I. Lee, M.F. Cole, S.E. Johnstone, S.S. Levine, J.P. Zucker, M.G. Guenther, R.M. Kumar, H.L. Murray, R.G. Jenner, D.K. Gifford, D.A. Melton, R. Jaenisch, and R.A. Young, "Core transcriptional regulatory circuitry in human embryonic stem cells.," *Cell*, vol. 122, Sep. 2005, pp. 947-56.

[6]   Y.-H. Loh, Q. Wu, J.-L. Chew, V.B. Vega, W. Zhang, X. Chen, G. Bourque, J. George, B. Leong, J. Liu, K.-Y. Wong, K.W. Sung, C.W.H. Lee, X.-D. Zhao, K.-P. Chiu, L. Lipovich, V. a Kuznetsov, P. Robson, L.W. Stanton, C.-L. Wei, Y. Ruan, B. Lim, and H.-H. Ng, "The Oct4 and Nanog transcription network regulates pluripotency in mouse embryonic stem cells.," *Nature genetics*, vol. 38, Apr. 2006, pp. 431-40.

[7]   Q.L. Ying, J. Nichols, I. Chambers, and A. Smith, "BMP induction of Id proteins suppresses differentiation and sustains embryonic stem cell self-renewal in collaboration with STAT3.," *Cell*, vol. 115, Oct. 2003, pp. 281-92.

[8]   A.G. Smith, J.K. Heath, D.D. Donaldson, G.G. Wong, J. Moreau, M. Stahl, and D. Rogers, "Inhibition of pluripotential embryonic stem cell differentiation by purified polypeptides.," *Nature*, vol. 336, Dec. 1988, pp. 688-90.

[9]   R.L. Williams, D.J. Hilton, S. Pease, T.A. Willson, C.L. Stewart, D.P. Gearing, E.F. Wagner, D. Metcalf, N.A. Nicola, and N.M. Gough, "Myeloid leukaemia inhibitory factor maintains the developmental potential of embryonic stem cells.," *Nature*, vol. 336, Dec. 1988, pp. 684-7.

[10]   H. Niwa, T. Burdon, I. Chambers, and a Smith, "Self-renewal of pluripotent embryonic stem cells is mediated via activation of STAT3.," *Genes & development*, vol. 12, Jul. 1998, pp. 2048-60.

[11]   R.K. Humphrey, G.M. Beattie, A.D. Lopez, N. Bucay, C.C. King, M.T. Firpo, S. Rose-John, and A. Hayek, "Maintenance of pluripotency in human embryonic stem cells is STAT3 independent.," *Stem cells (Dayton, Ohio)*, vol. 22, Jan. 2004, pp. 522-30.

[12] L. Dahéron, S.L. Opitz, H. Zaehres, M.W. Lensch, W.M. Lensch, P.W. Andrews, J. Itskovitz-Eldor, and G.Q. Daley, "LIF/STAT3 signaling fails to maintain self-renewal of human embryonic stem cells.," *Stem cells (Dayton, Ohio)*, vol. 22, Jan. 2004, pp. 770-8.

[13] T.U. Wagner, M. Kraeussling, L.M. Fedorov, C. Reiss, B. Kneitz, and M. Schartl, "STAT3 and SMAD1 signalling in Medaka embryonic stem-like cells and blastula embryos.," *Stem cells and development*, 2008.

[14] Q.-L. Ying, J. Wray, J. Nichols, L. Batlle-Morera, B. Doble, J. Woodgett, P. Cohen, and A. Smith, "The ground state of embryonic stem cell self-renewal.," *Nature*, vol. 453, May. 2008, pp. 519-23.

[15] K. Takahashi and S. Yamanaka, "Induction of pluripotent stem cells from mouse embryonic and adult fibroblast cultures by defined factors.," *Cell*, vol. 126, Aug. 2006, pp. 663-76.

[16] K. Takahashi, K. Tanabe, M. Ohnuki, M. Narita, T. Ichisaka, K. Tomoda, and S. Yamanaka, "Induction of pluripotent stem cells from adult human fibroblasts by defined factors.," *Cell*, vol. 131, Nov. 2007, pp. 861-72.

[17] M. Wernig, A. Meissner, R. Foreman, T. Brambrink, M. Ku, K. Hochedlinger, B.E. Bernstein, and R. Jaenisch, "In vitro reprogramming of fibroblasts into a pluripotent ES-cell-like state.," *Nature*, vol. 448, Jul. 2007, pp. 318-24.

[18] K. Guan, K. Nayernia, L.S. Maier, S. Wagner, R. Dressel, J.H. Lee, J. Nolte, F. Wolf, M. Li, W. Engel, and G. Hasenfuss, "Pluripotency of spermatogonial stem cells from adult mouse testis.," *Nature*, vol. 440, Apr. 2006, pp. 1199-203.

[19] S. Conrad, M. Renninger, J. Hennenlotter, T. Wiesner, L. Just, M. Bonin, W. Aicher, H.-J. Bühring, U. Mattheus, A. Mack, H.-J. Wagner, S. Minger, M. Matzkies, M. Reppel, J. Hescheler, K.-D. Sievert, A. Stenzl, and T. Skutella, "Generation of pluripotent stem cells from adult human testis.," *Nature*, vol. 456, Nov. 2008, pp. 344-9.

[20] F.K. Hamra, K.M. Chapman, D.M. Nguyen, A.A. Williams-Stephens, R.E. Hammer, and D.L. Garbers, "Self renewal, expansion, and transfection of rat spermatogonial stem cells in culture.," *Proceedings of the National Academy of Sciences of the United States of America*, vol. 102, Nov. 2005, pp. 17430-5.

[21] Y. Hong, T. Liu, H. Zhao, H. Xu, W. Wang, R. Liu, T. Chen, J. Deng, and J. Gui, "Establishment of a normal medakafish spermatogonial cell line capable of sperm production in vitro.," *Proceedings of the National Academy of Sciences of the United States of America*, vol. 101, May. 2004, pp. 8011-6.

[22] K. Ko, M.J. Araúzo-Bravo, N. Tapia, J. Kim, Q. Lin, C. Bernemann, D.W. Han, L. Gentile, P. Reinhardt, B. Greber, R.K. Schneider, S. Kliesch, M. Zenke, and H.R. Schöler, "Human adult germline stem cells in question.," *Nature*, vol. 465, Jun. 2010, p. E1; discussion E3.

[23]   D. a F. Loebel, C.M. Watson, R.A. De Young, and P.P.L. Tam, "Lineage choice and differentiation in mouse embryos and embryonic stem cells," *Developmental Biology*, vol. 264, Dec. 2003, pp. 1-14.

[24]   M. Schuldiner, O. Yanuka, J. Itskovitz-Eldor, D.A. Melton, and N. Benvenisty, "Effects of eight growth factors on the differentiation of cells derived from human embryonic stem cells.," *Proceedings of the National Academy of Sciences of the United States of America*, vol. 97, Oct. 2000, pp. 11307-12.

[25]   M. Wernig, K.L. Tucker, V. Gornik, A. Schneiders, R. Buschwald, O.D. Wiestler, Y.-A. Barde, and O. Brüstle, "Tau EGFP embryonic stem cells: an efficient tool for neuronal lineage selection and transplantation.," *Journal of neuroscience research*, vol. 69, 2002, pp. 918-24.

[26]   S. Zhao, J. Nichols, A.G. Smith, and M. Li, "SoxB transcription factors specify neuroectodermal lineage choice in ES cells.," *Molecular and cellular neurosciences*, vol. 27, 2004, pp. 332-42.

[27]   S. Kanda, A. Shiroi, Y. Ouji, J. Birumachi, S. Ueda, H. Fukui, K. Tatsumi, S. Ishizaka, Y. Takahashi, and M. Yoshikawa, "In vitro differentiation of hepatocyte-like cells from embryonic stem cells promoted by gene transfer of hepatocyte nuclear factor 3 beta.," *Hepatology research : the official journal of the Japan Society of Hepatology*, vol. 26, Jul. 2003, pp. 225-231.

[28]   J. Béjar, Y. Hong, and M. Schartl, "Mitf expression is sufficient to direct differentiation of medaka blastula derived stem cells to melanocytes.," *Development (Cambridge, England)*, vol. 130, Dec. 2003, pp. 6545-53.

[29]   I. Nanda, M. Kondo, U. Hornung, S. Asakawa, C. Winkler, A. Shimizu, Z. Shan, T. Haaf, N. Shimizu, A. Shima, M. Schmid, and M. Schartl, "A duplicated copy of DMRT1 in the sex-determining region of the Y chromosome of the medaka, Oryzias latipes.," *Proceedings of the National Academy of Sciences of the United States of America*, vol. 99, Sep. 2002, pp. 11778-83.

[30]   M. Matsuda, Y. Nagahama, A. Shinomiya, T. Sato, C. Matsuda, T. Kobayashi, C.E. Morrey, N. Shibata, S. Asakawa, N. Shimizu, H. Hori, S. Hamaguchi, and M. Sakaizumi, "DMY is a Y-specific DM-domain gene required for male development in the medaka fish.," *Nature*, vol. 417, May. 2002, pp. 559-63.

[31]   J. Rohwedel, K. Guan, and a M. Wobus, "Induction of cellular differentiation by retinoic acid in vitro.," *Cells, tissues, organs*, vol. 165, Jan. 1999, pp. 190-202.

[32]   C. Dani, A.G. Smith, S. Dessolin, P. Leroy, L. Staccini, P. Villageois, C. Darimont, and G. Ailhaud, "Differentiation of embryonic stem cells into adipocytes in vitro.," *Journal of cell science*, vol. 110 (Pt 1, Jun. 1997, pp. 1279-85.

[33]   C.M. Ward, K.M. Barrow, and P.L. Stern, "Significant variations in differentiation properties between independent mouse ES cell lines cultured under defined conditions," *Experimental Cell Research*, vol. 293, Feb. 2004, pp. 229-238.

[34]   T. Haneji, M. Maekawa, and Y. Nishimune, "Retinoids induce differentiation of type A spermatogonia in vitro: organ culture of mouse cryptorchid testes.," *The Journal of nutrition*, vol. 113, Jun. 1983, pp. 1119-23.

[35]   D. Alsop, J. Matsumoto, S. Brown, and G. Van Der Kraak, "Retinoid requirements in the reproduction of zebrafish.," *General and comparative endocrinology*, vol. 156, Mar. 2008, pp. 51-62.

[36]   C. Thisse, B. Thisse, and J.H. Postlethwait, "Expression of snail2, a second member of the zebrafish snail family, in cephalic mesendoderm and presumptive neural crest of wild-type and spadetail mutant embryos.," *Developmental biology*, vol. 172, Nov. 1995, pp. 86-99.

[37]   S. Elworthy, J.A. Lister, T.J. Carney, D.W. Raible, and R.N. Kelsh, "Transcriptional regulation of mitfa accounts for the sox10 requirement in zebrafish melanophore development.," *Development (Cambridge, England)*, vol. 130, Jun. 2003, pp. 2809-18.

[38]   P. Ducy, R. Zhang, V. Geoffroy, a L. Ridall, and G. Karsenty, "Osf2/Cbfa1: a transcriptional activator of osteoblast differentiation.," *Cell*, vol. 89, May. 1997, pp. 747-54.

[39]   T. Komori, H. Yagi, S. Nomura, A. Yamaguchi, K. Sasaki, K. Deguchi, Y. Shimizu, R.T. Bronson, Y.H. Gao, M. Inada, M. Sato, R. Okamoto, Y. Kitamura, S. Yoshiki, and T. Kishimoto, "Targeted disruption of Cbfa1 results in a complete lack of bone formation owing to maturational arrest of osteoblasts.," *Cell*, vol. 89, May. 1997, pp. 755-64.

[40]   F. Otto, A.P. Thornell, T. Crompton, A. Denzel, K.C. Gilmour, I.R. Rosewell, G.W. Stamp, R.S. Beddington, S. Mundlos, B.R. Olsen, P.B. Selby, and M.J. Owen, "Cbfa1, a candidate gene for cleidocranial dysplasia syndrome, is essential for osteoblast differentiation and bone development.," *Cell*, vol. 89, May. 1997, pp. 765-71.

[41]   L.C. Lo, J.E. Johnson, C.W. Wuenschell, T. Saito, and D.J. Anderson, "Mammalian achaete-scute homolog 1 is transiently expressed by spatially restricted subsets of early neuroepithelial and neural crest cells.," *Genes & development*, vol. 5, Sep. 1991, pp. 1524-37.

[42]   F. Guillemot, L.C. Lo, J.E. Johnson, A. Auerbach, D.J. Anderson, and A.L. Joyner, "Mammalian achaete-scute homolog 1 is required for the early development of olfactory and autonomic neurons.," *Cell*, vol. 75, Nov. 1993, pp. 463-76.

[43]   M.L. Kalev-Zylinska, J.A. Horsfield, M.V.C. Flores, J.H. Postlethwait, M.R. Vitas, A.M. Baas, P.S. Crosier, and K.E. Crosier, "Runx1 is required for zebrafish blood and vessel development and expression of a human RUNX1-CBF2T1 transgene advances a model for studies of leukemogenesis.," *Development (Cambridge, England)*, vol. 129, Apr. 2002, pp. 2015-30.

[44]   K.A. Dooley, A.J. Davidson, and L.I. Zon, "Zebrafish scl functions independently in hematopoietic and endothelial development.," *Developmental biology*, vol. 277, Jan. 2005, pp. 522-36.

[45] K.A. Dutton, A. Pauliny, S.S. Lopes, S. Elworthy, T.J. Carney, J. Rauch, R. Geisler, P. Haffter, and R.N. Kelsh, "Zebrafish colourless encodes sox10 and specifies non-ectomesenchymal neural crest fates.," *Development (Cambridge, England)*, vol. 128, Nov. 2001, pp. 4113-25.

[46] K. Shirakabe, K. Terasawa, K. Miyama, H. Shibuya, and E. Nishida, "Regulation of the activity of the transcription factor Runx2 by two homeobox proteins, Msx2 and Dlx5.," *Genes to cells : devoted to molecular & cellular mechanisms*, vol. 6, Oct. 2001, pp. 851-6.

[47] K. Inohaya and A. Kudo, "Temporal and spatial patterns of cbfal expression during embryonic development in the teleost, Oryzias latipes.," *Development genes and evolution*, vol. 210, Nov. 2000, pp. 570-4.

[48] B.A. Byers and A.J. García, "Exogenous Runx2 expression enhances in vitro osteoblastic differentiation and mineralization in primary bone marrow stromal cells.," *Tissue engineering*, vol. 10, pp. 1623-32.

[49] X. Zhang, M. Yang, L. Lin, P. Chen, K.T. Ma, C.Y. Zhou, and Y.F. Ao, "Runx2 overexpression enhances osteoblastic differentiation and mineralization in adipose--derived stem cells in vitro and in vivo.," *Calcified tissue international*, vol. 79, Sep. 2006, pp. 169-78.

[50] M.L. Allende and E.S. Weinberg, "The expression pattern of two zebrafish achaete-scute homolog (ash) genes is altered in the embryonic brain of the cyclops mutant.," *Developmental biology*, vol. 166, Dec. 1994, pp. 509-30.

[51] J. Odenthal and C. Nüsslein-Volhard, "fork head domain genes in zebrafish.," *Development genes and evolution*, vol. 208, Jul. 1998, pp. 245-58.

[52] L.H. Pevny, S. Sockanathan, M. Placzek, and R. Lovell-Badge, "A role for SOX1 in neural determination.," *Development (Cambridge, England)*, vol. 125, May. 1998, pp. 1967-78.

[53] F. Guillemot and A.L. Joyner, "Dynamic expression of the murine Achaete-Scute homologue Mash-1 in the developing nervous system.," *Mechanisms of development*, vol. 42, Aug. 1993, pp. 171-85.

[54] S.-H. Yi, A.-Y. Jo, C.-H. Park, H.-C. Koh, R.-H. Park, H. Suh-Kim, I. Shin, Y.-S. Lee, J. Kim, and S.-H. Lee, "Mash1 and neurogenin 2 enhance survival and differentiation of neural precursor cells after transplantation to rat brains via distinct modes of action.," *Molecular therapy : the journal of the American Society of Gene Therapy*, vol. 16, Nov. 2008, pp. 1873-82.

[55] R. Ikeda, M.S. Kurokawa, S. Chiba, H. Yoshikawa, T. Hashimoto, M. Tadokoro, and N. Suzuki, "Transplantation of motoneurons derived from MASH1-transfected mouse ES cells reconstitutes neural networks and improves motor function in hemiplegic mice.," *Experimental neurology*, vol. 189, Oct. 2004, pp. 280-92.

[56] C.S. Raymond, C.E. Shamu, M.M. Shen, K.J. Seifert, B. Hirsch, J. Hodgkin, and D. Zarkower, "Evidence for evolutionary conservation of sex-determining genes.," *Nature*, vol. 391, Feb. 1998, pp. 691-5.

[57] M. Matsuda, A. Shinomiya, M. Kinoshita, A. Suzuki, T. Kobayashi, B. Paul-Prasanth, E.-lieng Lau, S. Hamaguchi, M. Sakaizumi, and Y. Nagahama, "DMY gene induces male development in genetically female (XX) medaka fish.," *Proceedings of the National Academy of Sciences of the United States of America*, vol. 104, Mar. 2007, pp. 3865-70.

[58] U. Hornung, a Herpin, and M. Schartl, "Expression of the male determining gene dmrt1bY and its autosomal coorthologue dmrt1a in medaka.," *Sexual development : genetics, molecular biology, evolution, endocrinology, embryology, and pathology of sex determination and differentiation*, vol. 1, Jan. 2007, pp. 197-206.

[59] C.S. Raymond, J.R. Kettlewell, B. Hirsch, V.J. Bardwell, and D. Zarkower, "Expression of Dmrt1 in the genital ridge of mouse and chicken embryos suggests a role in vertebrate sexual development.," *Developmental biology*, vol. 215, Nov. 1999, pp. 208-20.

[60] S. Kim, V.J. Bardwell, and D. Zarkower, "Cell type-autonomous and non-autonomous requirements for Dmrt1 in postnatal testis differentiation.," *Developmental biology*, vol. 307, Jul. 2007, pp. 314-27.

[61] A.D. Krentz, M.W. Murphy, S. Kim, M.S. Cook, B. Capel, R. Zhu, A. Matin, A.L. Sarver, K.L. Parker, M.D. Griswold, L.H.J. Looijenga, V.J. Bardwell, and D. Zarkower, "The DM domain protein DMRT1 is a dose-sensitive regulator of fetal germ cell proliferation and pluripotency.," *Proceedings of the National Academy of Sciences of the United States of America*, vol. 106, Dec. 2009, pp. 22323-8.

[62] T. Wu, H. Patel, S. Mukai, C. Melino, R. Garg, X. Ni, J. Chang, and C. Peng, "Activin, inhibin, and follistatin in zebrafish ovary: expression and role in oocyte maturation.," *Biology of reproduction*, vol. 62, Jun. 2000, pp. 1585-92.

[63] Y. Wang and W. Ge, "Developmental profiles of activin betaA, betaB, and follistatin expression in the zebrafish ovary: evidence for their differential roles during sexual maturation and ovulatory cycle.," *Biology of reproduction*, vol. 71, Dec. 2004, pp. 2056-64.

[64] S. Nakamura, H. Kurokawa, S. Asakawa, N. Shimizu, and M. Tanaka, "Two distinct types of theca cells in the medaka gonad: germ cell-dependent maintenance of cyp19a1-expressing theca cells.," *Developmental dynamics : an official publication of the American Association of Anatomists*, vol. 238, Oct. 2009, pp. 2652-7.

[65] D.-S. Wang, L.-Y. Zhou, T. Kobayashi, M. Matsuda, Y. Shibata, F. Sakai, and Y. Nagahama, "Doublesex- and Mab-3-related transcription factor-1 repression of aromatase transcription, a possible mechanism favoring the male pathway in tilapia.," *Endocrinology*, vol. 151, Mar. 2010, pp. 1331-40.

[66] Y. Guo, H. Cheng, X. Huang, S. Gao, H. Yu, and R. Zhou, "Gene structure, multiple alternative splicing, and expression in gonads of zebrafish Dmrt1.," *Biochemical and biophysical research communications*, vol. 330, May. 2005, pp. 950-7.

[67] C.A. Smith, C.M. Shoemaker, K.N. Roeszler, J. Queen, D. Crews, and A.H. Sinclair, "Cloning and expression of R-Spondin1 in different vertebrates suggests a conserved role in ovarian development.," *BMC developmental biology*, vol. 8, Jan. 2008, p. 72.

[68] A.-A. Chassot, F. Ranc, E.P. Gregoire, H.L. Roepers-Gajadien, M.M. Taketo, G. Camerino, D.G. de Rooij, A. Schedl, and M.-C. Chaboissier, "Activation of beta-catenin signaling by Rspo1 controls differentiation of the mammalian ovary.," *Human molecular genetics*, vol. 17, May. 2008, pp. 1264-77.

[69] X. Zhang, H. Liu, Y. Zhang, Y. Qiao, S. Miao, L. Wang, J. Zhang, S. Zong, and S.S. Koide, "A novel gene, RSD-3/HSD-3.1, encodes a meiotic-related protein expressed in rat and human testis.," *Journal of molecular medicine (Berlin, Germany)*, vol. 81, Jun. 2003, pp. 380-7.

[70] C.K. Matson, M.W. Murphy, M.D. Griswold, S. Yoshida, V.J. Bardwell, and D. Zarkower, "The mammalian doublesex homolog DMRT1 is a transcriptional gatekeeper that controls the mitosis versus meiosis decision in male germ cells.," *Developmental cell*, vol. 19, Oct. 2010, pp. 612-24.

[71] A. Herpin, D. Schindler, A. Kraiss, U. Hornung, C. Winkler, and M. Schartl, "Inhibition of primordial germ cell proliferation by the medaka male determining gene Dmrt I bY.," *BMC developmental biology*, vol. 7, Jan. 2007, p. 99.

[72] L. Sommer, Q. Ma, and D.J. Anderson, "neurogenins, a novel family of atonal-related bHLH transcription factors, are putative mammalian neuronal determination genes that reveal progenitor cell heterogeneity in the developing CNS and PNS.," *Molecular and cellular neurosciences*, vol. 8, Jan. 1996, pp. 221-41.

[73] C. Fode, G. Gradwohl, X. Morin, a Dierich, M. LeMeur, C. Goridis, and F. Guillemot, "The bHLH protein NEUROGENIN 2 is a determination factor for epibranchial placode-derived sensory neurons.," *Neuron*, vol. 20, Mar. 1998, pp. 483-94.

[74] R. Scardigli, C. Schuurmans, G. Gradwohl, and F. Guillemot, "Crossregulation between Neurogenin2 and pathways specifying neuronal identity in the spinal cord.," *Neuron*, vol. 31, Aug. 2001, pp. 203-17.

[75] R. Scardigli, "Direct and concentration-dependent regulation of the proneural gene Neurogenin2 by Pax6," *Development*, vol. 130, 2003, pp. 3269-3281.

[76] Q. Zhou and D.J. Anderson, "The bHLH transcription factors OLIG2 and OLIG1 couple neuronal and glial subtype specification.," *Cell*, vol. 109, Apr. 2002, pp. 61-73.

[77] M. Peitz, R. Jäger, C. Patsch, A. Jäger, A. Egert, H. Schorle, and F. Edenhofer, "Enhanced purification of cell-permeant Cre and germline transmission after transduction into mouse embryonic stem cells.," *Genesis (New York, N.Y. : 2000)*, vol. 45, 2007, pp. 508-17.

[78] R. Feil, J. Brocard, B. Mascrez, M. LeMeur, D. Metzger, and P. Chambon, "Ligand-activated site-specific recombination in mice.," *Proceedings of the National Academy of Sciences of the United States of America*, vol. 93, Oct. 1996, pp. 10887-90.

[79] D. Meilinger, K. Fellinger, S. Bultmann, U. Rothbauer, I.M. Bonapace, W.E.F. Klinkert, F. Spada, and H. Leonhardt, "Np95 interacts with de novo DNA methyltransferases, Dnmt3a and Dnmt3b, and mediates epigenetic silencing of the viral CMV promoter in embryonic stem cells.," *EMBO reports*, vol. 10, Nov. 2009, pp. 1259-64.

[80] Y.-P. Liu, O.V. Dovzhenko, M.A. Garthwaite, S.V. Dambaeva, M. Durning, L.M. Pollastrini, and T.G. Golos, "Maintenance of pluripotency in human embryonic stem cells stably over-expressing enhanced green fluorescent protein.," *Stem cells and development*, vol. 13, Dec. 2004, pp. 636-45.

[81] L. Bai, H. Xu, J.F. Collins, and F.K. Ghishan, "Molecular and functional analysis of a novel neuronal vesicular glutamate transporter.," *The Journal of biological chemistry*, vol. 276, Sep. 2001, pp. 36764-9.

[82] A.J. Todd, D.I. Hughes, E. Polgár, G.G. Nagy, M. Mackie, O.P. Ottersen, and D.J. Maxwell, "The expression of vesicular glutamate transporters VGLUT1 and VGLUT2 in neurochemically defined axonal populations in the rat spinal cord with emphasis on the dorsal horn.," *The European journal of neuroscience*, vol. 17, Jan. 2003, pp. 13-27.

[83] K.A. Waters and R. Machaalani, "NMDA receptors in the developing brain and effects of noxious insults.," *Neuro-Signals*, vol. 13, pp. 162-74.

[84] M.H. Farah, J.M. Olson, H.B. Sucic, R.I. Hume, S.J. Tapscott, and D.L. Turner, "Generation of neurons by transient expression of neural bHLH proteins in mammalian cells.," *Development (Cambridge, England)*, vol. 127, Feb. 2000, pp. 693-702.

[85] S. Fawell, J. Seery, Y. Daikh, C. Moore, L.L. Chen, B. Pepinsky, and J. Barsoum, "Tat-mediated delivery of heterologous proteins into cells.," *Proceedings of the National Academy of Sciences of the United States of America*, vol. 91, Jan. 1994, pp. 664-8.

[86] C. Walther and P. Gruss, "Pax-6, a murine paired box gene, is expressed in the developing CNS.," *Development (Cambridge, England)*, vol. 113, Dec. 1991, pp. 1435-49.

[87] U. Lendahl, L.B. Zimmerman, and R.D. McKay, "CNS stem cells express a new class of intermediate filament protein.," *Cell*, vol. 60, Feb. 1990, pp. 585-95.

[88] F. Francis, a Koulakoff, D. Boucher, P. Chafey, B. Schaar, M.C. Vinet, G. Friocourt, N. McDonnell, O. Reiner, a Kahn, S.K. McConnell, Y. Berwald-Netter, P. Denoulet, and J. Chelly, "Doublecortin is a developmentally regulated, microtubule-associated protein expressed in migrating and differentiating neurons.," *Neuron*, vol. 23, Jun. 1999, pp. 247-56.

[89] J.G. Gleeson, P.T. Lin, L. a Flanagan, and C. a Walsh, "Doublecortin is a microtubule-associated protein and is expressed widely by migrating neurons.," *Neuron*, vol. 23, Jun. 1999, pp. 257-71.

[90] R.J. Mullen, C.R. Buck, and a M. Smith, "NeuN, a neuronal specific nuclear protein in vertebrates.," *Development (Cambridge, England)*, vol. 116, Sep. 1992, pp. 201-11.

[91] D. Sassoon, G. Lyons, W.E. Wright, V. Lin, A. Lassar, H. Weintraub, and M. Buckingham, "Expression of two myogenic regulatory factors myogenin and MyoD1 during mouse embryogenesis.," *Nature*, vol. 341, Sep. 1989, pp. 303-7.

[92] R.L. Davis, H. Weintraub, and a B. Lassar, "Expression of a single transfected cDNA converts fibroblasts to myoblasts.," *Cell*, vol. 51, Dec. 1987, pp. 987-1000.

[93] H. Weintraub, S.J. Tapscott, R.L. Davis, M.J. Thayer, M.A. Adam, A.B. Lassar, and A.D. Miller, "fibroblast cell lines by forced expression of MyoD," *Developmental Biology*, vol. 86, 1989, pp. 5434-5438.

[94] J. Choi, "MyoD converts primary dermal fibroblasts , chondroblasts , smooth muscle , and retinal pigmented epithelial cells into striated mononucleated myoblasts and multinucleated myotubes," *Developmental Biology*, vol. 87, 1990, pp. 7988-7992.

[95] D.E. Zhang, P. Zhang, N.D. Wang, C.J. Hetherington, G.J. Darlington, and D.G. Tenen, "Absence of granulocyte colony-stimulating factor signaling and neutrophil development in CCAAT enhancer binding protein alpha-deficient mice.," *Proceedings of the National Academy of Sciences of the United States of America*, vol. 94, Jan. 1997, pp. 569-74.

[96] H. Xie, M. Ye, R. Feng, and T. Graf, "Stepwise reprogramming of B cells into macrophages.," *Cell*, vol. 117, 2004, pp. 663-76.

[97] C.V. Laiosa, M. Stadtfeld, H. Xie, L.D. Andres-aguayo, and T. Graf, "Reprogramming of Committed T Cell Progenitors to Macrophages and Dendritic Cells by C / EBPa and PU . 1 Transcription Factors," *Control*, 2006, pp. 731-744.

[98] S. Chung, K.-C. Sonntag, T. Andersson, L.M. Bjorklund, J.-J. Park, D.-W. Kim, U.J. Kang, O. Isacson, and K.-S. Kim, "Genetic engineering of mouse embryonic stem cells by Nurr1 enhances differentiation and maturation into dopaminergic neurons," *European Journal of Neuroscience*, vol. 16, Nov. 2002, pp. 1829-1838.

[99] M. Shani, A. Faerman, C.P. Emerson, S. Pearson-White, I. Dekel, and Y. Magal, "The consequences of a constitutive expression of MyoD1 in ES cells and mouse embryos.," *Symposia of the Society for Experimental Biology*, vol. 46, Jan. 1992, pp. 19-36.

[100] T. Vierbuchen, A. Ostermeier, Z.P. Pang, Y. Kokubu, T.C. Südhof, and M. Wernig, "Direct conversion of fibroblasts to functional neurons by defined factors.," *Nature*, vol. 463, 2010, pp. 1035-41.

[101] Q. Zhou, J. Brown, A. Kanarek, J. Rajagopal, and D.A. Melton, "In vivo reprogramming of adult pancreatic exocrine cells to beta-cells.," *Nature*, vol. 455, 2008, pp. 627-32.

[102] M. Tachibana, K. Takeda, Y. Nobukuni, K. Urabe, J.E. Long, K.A. Meyers, S.A. Aaronson, and T. Miki, "Ectopic expression of MITF, a gene for Waardenburg syndrome type 2, converts fibroblasts to cells with melanocyte characteristics.," *Nature genetics*, vol. 14, 1996, pp. 50-4.

[103] G. Tiscornia and J.C. Izpisua Belmonte, "MicroRNAs in embryonic stem cell function and fate," *Genes & Development*, vol. 24, Dec. 2010, pp. 2732-2741.

[104] A. Mattout and E. Meshorer, "Chromatin plasticity and genome organization in pluripotent embryonic stem cells.," *Current opinion in cell biology*, vol. 22, Mar. 2010, pp. 334-341.

[105] M. Stadtfeld, N. Maherali, M. Borkent, and K. Hochedlinger, "A reprogrammable mouse strain from gene-targeted embryonic stem cells.," *Nature methods*, vol. 7, Jan. 2010, pp. 53-5.

[106] A.P. McMahon and A. Bradley, "The Wnt-1 (int-1) proto-oncogene is required for development of a large region of the mouse brain.," *Cell*, vol. 62, Sep. 1990, pp. 1073-85.

Original publications

Manuscript 1: Ectopic expression of single transcription factors directs differentiation of a Medaka spermatogonial cell line. Stem Cells Dev 2010

ORIGINAL RESEARCH REPORT

Ectopic Expression of Single Transcription Factors Directs Differentiation of a Medaka Spermatogonial Cell Line

Eva C. Thoma,[1,*] Toni U. Wagner,[1,*] Isabell P. Weber,[1] Amaury Herpin,[1] Andreas Fischer,[2] and Manfred Schartl[1]

The capability to form all cell types of the body is a unique feature of stem cells. However, many questions remain concerning the mechanisms regulating differentiation potential. The derivation of spermatogonial cell lines (SGs) from mouse and human, which can differentiate across germ-layer borders, suggested male germ cells as a potential stem cell source in addition to embryonic stem cells. Here, we present a differentiation system using an SG of the vertebrate model organism *Oryzias latipes* (medaka). We report differentiation of this cell line into 4 different ectodermal and mesodermal somatic cell types. In addition to differentiation into adipocytes by retinoic acid treatment, we demonstrate for the first time that directed differentiation of an SG can be induced by ectopic expression of single transcription factors, completely independent of culture conditions. Transient transfection with *mitf-m*, a transcription factor that has been shown to induce differentiation into melanocytes in medaka embryonic stem cells, resulted in the formation of the same cell type in spermatogonia. Similarly, the formation of neuron-like cells and matrix-depositing osteoblasts was induced by ectopic expression of *mash1* and *cbfa1*, respectively. Interestingly, we found that the expression of all mentioned fate-inducing transcription factors leads to recapitulation of the temporal pattern of marker gene expression known from in vivo studies.

Introduction

SEVERAL RECENT STUDIES describing methods for derivation of pluripotent stem cells without involving the use of early embryonic stages have attracted much attention. One such approach is the directed reprogramming of fibroblasts into germ-line competent embryonic stem cell (ESC)-like (iPS) cells through virus-mediated introduction of pluripotency-associated transcription factors [1–4].

An alternative source for cells with a wide ability for differentiation appears to be spermatogonial cells derived from testes of adult mice and also humans [5,6]. Both the reprogramming and the spermatogonial stem cell approaches offer the possibility to circumvent ethical as well as immunological problems associated with ESC-based therapies. However, differentiable spermatogonia are thus far restricted to the mouse and human systems, and cultures were also successfully established from rat [7] and medaka fish (*Oryzias latipes*) [8]. Further, recent data challenge pluripotency of human spermatogonia as these cells appear to resemble fibroblasts rather than ESCs regarding certain molecular features [9]. Thus, it is not clear if pluripotency of spermatogonia is restricted to certain species or a more conserved feature among vertebrates.

Here, we investigated the differentiation potential of a medaka fish spermatogonial cell line (MF-SG). This cell line was derived from testes of adult medaka fish and was previously shown to be able to undergo meiosis and form motile sperm [8]. However, attempts toward transdifferentiation of the cells into derivatives of different germ layers have thus far not been reported. We demonstrate that MF-SGs are able to form 4 different cell types from different germ layers, thus suggesting that they have a certain in vitro differentiation potential.

Differentiable cells have a unique status in developmental and cell biology as well as in potential clinical therapies as they represent an excellent system to study developmental processes, but also offer a promising tool for tissue regeneration. However, applications in both research and clinical therapy face one major problem, that is, the establishment of protocols allowing directed and homogeneous formation of one defined cell type. Most conventional differentiation protocols use a combination of embryoid body formation and cytokine addition [10–12]. But these changes to culture conditions often have to be determined in an empirical and time-consuming fashion. An alternative approach is to enhance lineage-specific differentiation by ectopic expression of transcription factors [13–16].

In this study, we demonstrate for the first time that spermatogonia can be directly differentiated into various cell types belonging to different germ layers by expression of single genes and without the need for additional signals.

[1]Department of Physiological Chemistry I, University of Wuerzburg, Wuerzburg, Germany.
[2]Joint Research Division Vascular Biology, Medical Faculty Mannheim, Heidelberg University, and German Cancer Research Center Heidelberg (DKFZ-ZMBH Alliance), Mannheim, Germany.
*These two authors contributed equally to this work.

1

Materials and Methods

Cell culture

AU3 ▶ MF-SGs were cultured as previously described (4). Cells were grown at 28°C on gelatin-coated wells in ESM4 medium consisting of Dulbecco's modified Eagle's medium (DMEM) high glucose (4.5 g/L) with HEPES (20 mM, pH 7.8) supplemented with 15% fetal calf serum, glutamine (4 mM), nonessential amino acids (0.1 mM), antibiotics, sodium pyruvate (1 mM), sodium selenite (2 nM), 2-mercaptoethanol (100 μM), basic fibroblast growth factor (10 ng/mL), medaka embryo extract (1 embryo/mL), and 1% trout serum. Culture conditions were similar for medaka ESCs. The cells and protocols for culture were a kind gift of Y. Hong. The cells were cultured for up to 30 passages.

Medaka fibroblast cell line (OLF) was grown at 28°C and 5% CO_2 in DMEM high glucose (4.5 g/L) supplemented with 15% fetal calf serum, glutamine (4 mM), and antibiotics.

For characterization of SGs and MF-ESCs, cells were transfected with 0.75 μg pStra8::EGFP and vasa::GFP, respectively, and 0.25 μg pH2B-Cherry. Transfections were performed using the Fugene HD transfection reagent (Roche). The expression vector pStra8::EGFP was a kind gift of W. Engel and encodes EGFP under the control of the murine Stra8 promoter [6]. The vasa::GFP construct was a kind gift from Minuro Tanaka and encodes EGFP under the control of the medaka *vasa* promoter and followed by the 3′UTR of the medaka vasa gene [17]. pH2B-Cherry encodes a fusion protein of Histone2B and the fluorescent protein mCherry.

For adipocyte differentiation, the cells were incubated in medium containing 10 μM retinoic acid (RA). The medium was changed every 48 h.

All transfections were performed using the Fugene HD transfection reagent (Roche). The following expression vectors were used: Xmitf-M/Tre2Hyg, the *Xiphophorus maculatus* variant cloned by J. Bejar; Mash1-IRES-NLSGFP-pCAGGS, which contains the full coding sequence of murine Mash1 (a kind gift of F. Guillemot [18]); and MFCbfa1A18/pCS2p+ (the gene was identified by screening the Medaka Ensembl Genome Database) [19]. Polymerase chain reaction (PCR) primers for amplification of MF-*cbfa1* from embryonic cDNA were MF-CBFA1-f01 (GGAATTCCTGTCAAGGGTCACC GAAA) and MF-CBFA1-r01 (CCGCTCGAGGCCTTTC CATCCTCTCTCCACCC). Cloning was done using *Eco*RI and *Xho*I restriction sites. As a transfection control, cells were cotransfected with pmOrange(C1)-Zeo, a vector coding for a fusion protein of the fluorescent protein mOrange and the Zeocin resistance. Ratios were 1.5 μg expression vector + 0.5 μg pmOrange(C1)-Zeo. Cells were selected with Zeocin (200 μg/mL) and according to the ratio of transfected and nontransfected cells. The *mash1* transfected cells were in addition selected with G418 (200 μg/mL). During the differentiation process, cells were cultured in ESM4 medium. The medium was changed every 48 h.

Preparation of RNA and PCR

Total RNAs were isolated from cell cultures using the Total RNA Isolation Reagent (AB Gene). Prior to cDNA synthesis, DNA digestion was performed using DNAseI (Fermentas) to exclude gDNA contamination. cDNA was synthesized from 1, 2, or 3 μg of total RNA using the Revertaid Kit (Fermentas) and random hexamer primers. For PCR, cDNAs were diluted according to the amount of total RNA used. PCRs were run for 33 cycles.

Quantitative real-time PCR was performed with a Biorad-iCycler; MF-*ef1a1* (medaka fish elongation factor 1a1) expression was used as reference. Each PCR was performed at least 3 times. Data from 3 independent experiments were evaluated using Student's *t*-test. Primers were designed using the primer3 program and medaka sequence from the Ensembl database. Primer sequences and annealing temperatures are shown in Supplementary Table S1 (Supplementary Data are available online at www.liebertonline .com/scd). ◀ ST1 ◀ AU4

Electron microscopy

Cells were washed with phosphate-buffered saline (PBS) and fixed [2.5% glutaraldehyde, 50 mM cacodylat (pH 7.2), 50 mM KCl, and 2.5 mM $MgCl_2$] on ice for 1 h. Thereafter, cells were washed 5 times with 50 mM cacodyl buffer (pH 7.2) and subsequently postfixed with 2% OsO_4 in 50 mM cacodylat (pH 7.2) buffer. After 5 washing steps with H_2O, the cells were stained with 2% uranylacetate overnight and then washed again with H_2O. After gradual dehydration with ethanol, cells were transferred to propylenoxid and subsequently embedded in Epon 812 (Serva). The sections were analyzed using an EM10 from Zeiss.

Thin-layer chromatography

The cells were lysed with 0.1 × trypsin ethylenediamine-tetraacetic acid for 1 h at room temperature. Then, lipids were isolated by addition of 1.3 volume methanol and 2.6 volume of initial volume of cell lysate and subsequent centrifugation at 1000 rpm for 5 min. The lower phase containing the lipids was transferred to a new glass vial. After evaporation under nitrogen, lipids were resolved in chloroform/methanol (2:1). Thin-layer chromatography was performed on a silica gel 60 in a running buffer of hexane, diethylether, and glacial acetic acid (90 v/10 v/1 v). Subsequently, lipids were visualized by staining with 0.4% anisaldehyde and 2% concentrated sulfuric acid in glacial acetic acid under heating. The analysis was performed using ImageJ. The regions of interest were all of the same size and measured relative to an equally large area directly adjacent, thereby giving the *y*-axis description "integrated density/background."

Calcein staining

For staining of matrix-complexed calcium, a saturated aqueous stock solution of calcein (Sigma) was diluted 1:100 in DMEM-HEPES. Cells were washed twice with PBS, kept in the staining solution at room temperature for 5 min, washed twice with PBS, and covered with fresh medium for imaging. As a control, staining was also performed with mock and *cbfa1*-transfected OLFs.

For imaging, a LEICA DMI6000 microscope was used. Images were analyzed using the ImageJ software. For exact quantification, the experiment was repeated and all pictures were taken using the same camera settings including exposure time and gain. Fluorescence intensities were quantified

by 3-dimensional histograms, which display signal intensity by both color-coding and height of bars.

von Kossa staining

At 14 days posttransfection (dpt), *cbfa1*-transfected MF-SGs were washed with PBS and fixed with 10% formalin in PBS for 1 h at room temperature. After the fixing process, the cells were treated with 5% $AgNO_3$ for 30 min at room temperature under ultraviolet light. Subsequently, unreacted $AgNO_3$ was removed with 2% $Na_2S_2O_3$ for 10 min. The cells were washed twice with distilled water and analyzed using a LEICA DMI6000.

Alkaline phosphatase staining

MF-SG, MF-ESCs, and OLFs were washed with PBS and fixed in 4% PFA in PBS for 1 min at room temperature. After the fixing process, the cells were rinsed in ALP buffer (0.1 M Tris-HCl, 0.01 N NaOH, 0.05 M $MgCl_2$) and subsequently stained with the staining solution NBT/BCIP (Roche), 1:50 diluted in ALP buffer. Staining was performed at room temperature in the dark for 15 min. Then, the cells were washed with ALP buffer, covered with PBS, and imaged.

Calcium imaging

For calcium imaging, *mash1*-transfected MF-SSCs were washed with PBS, covered with a fresh medium containing 2 μM fura2 (Invitrogen), and incubated at room temperature for 50 min. Afterward, cells were washed 3 times with PBS and covered with fresh medium. Imaging was performed using an Olympus imaging system with an upright epifluorescent microscope equipped with an LD 20×water-immersion lens. *Mash1*-transfected cells were visualized by expression of cotransfected mOrange. Series of double frames were recorded with an air-cooled CCD camera (Hamamatsu Photonics) at a sampling rate of 4 Hz, with a total amount of 120 images/experiment. Stimulus was given at $t = 10$ s by addition of KCl in PBS to a final concentration of 70 mM. Images were analyzed using ratioplus ImageJ plugin (http://rsbweb.nih.gov/ij/plugins/ratio-plus.html) to calculate the ratios between calcium-bound and unbound fura2 (340/380 nm). $F(0)$ values were set as the average of 4 images taken immediately before stimulus.

Quantification of vasa::GFP expression upon master regulator transfection

Cells were transfected with mOrangeZeo, vasa::GFP, and either an empty vector (control) or the expression constructs for *mitf*, *mash1*, and *cbfa1*. Eight days posttransfection, widefield scans were taken and GFP- and mOrange-positive cells were determined in a total area of 0.6 mm². Data from 9 independent experiments were evaluated using Student's *t*-test.

Double-transgenic fish line

For generation of the double-transgenic fish, vasa::GFP stable transgenic fish were crossed with a dmrt1bY(9kb):: mCherry stable transgenic line. The vasa::GFP stable transgenic line is composed of an enhanced GFP open reading frame (eGFP; Clontech) flanked by the 5' region (5.1 kb) including exons 1 and 2 and the 3' region (0.64 kb) of medaka *vasa* gene [17]. For generation of the dmrt1bY(9kb)::mCherry stable transgenic line, a 9.107-kb fragment upstream of the Dmrt1bY ORF was isolated by restriction enzyme digestion (*XhoI*/*EcoRI*) from Medaka BAC clone Mn0113N21 and cloned into pBSII-ISceI plasmid (pBSII-ISceI:9Kb Dmrt1bY prom). Subsequently, the mCherry gene was inserted between *EcoRI* and *NotI* sites of pBSII-ISceI:9Kb Dmrt1bY prom plasmid (pBSII-ISceI:9Kb Dmrt1bY prom:mCherry). For generation of stable transgenic lines, the meganuclease protocol was used [20].

Adult double-transgenic fish were sacrificed and testes were isolated and mounted in PBS. Confocal microscopy was performed using a Zeiss LSM 710 confocal microscope. Images were analyzed using the image reconstruction software Volocity.

Results

To investigate the differentiation potential of medaka spermatogonia, we used a cell line (MF-SG) derived from testes of adult medaka fish. As the spermatogonial identity of this cell line has already been confirmed [8], we now compared these cells with a medaka ESC-like cell line (MF-ESCs) [21,22] with respect to basic molecular markers. These tests were performed to enable discrimination between the 2 cell lines in later experiments. Further, this characterization allowed us to exclude cross-contamination of the cell lines. First, cells were tested for alkaline phosphatase (AP) activity as this feature is known to be a typical marker for self-renewing cells. MF-ESCs were already known to be AP positive [21]. Both cell types, MF-SG and MF-ESC, reacted positively (Fig. 1A–D), whereas OLF, a medaka fibroblast cell line, did not show any AP activity (Supplementary Fig. S1). The fact that MF-SG and MF-ESCs show AP activity was not usable for discrimination of cell types. However, it suggested that differentiation of MF-SG was possible. RT–PCR revealed expression of the spermatogonia-specific gene *dazl* [23] in wild-type MF-SG, whereas no expression of this gonad-specific gene was detectable in MF-ESCs (Fig. 1E). Both MF-SG and MF-ESC cultures tested negative for the Sertoli cell marker *dmrt1bY* [24] (Fig. 1E), suggesting that the cell cultures are devoid of Sertoli cell contamination. Additionally, we identified 2 genes exclusively transcribed in MF-ESCs (Supplementary Fig. S2): *c3orf54*, an uncharacterized medaka gene, and *atf5*, which is known to be downregulated during several differentiation processes [25–27]. Although the function of these 2 genes in MF-ESCs is still unknown, the fact that their transcripts were detectable in MF-ESCs, but not in MF-SG, indicates that these cell lines are different and that no cross-contamination has occurred.

Additionally, a murine Stra8::GFP reporter plasmid [28] was used in cotransfection assays together with a plasmid encoding for a fusion protein, Histone2B-mCherry. *Stra8* is a spermatogonia-specific gene described for mammals [29], and the promoter has been used to derive murine spermatogonial cell cultures [6]. After cotransfection of both MF-ESCs and MF-SG, mCherry-positive nuclei were found in both cultures, whereas only MF-SG expressed GFP driven by the Stra8 promoter (Fig. 1F–M). This observation strongly suggests that MF-SG have retained their spermatogonial
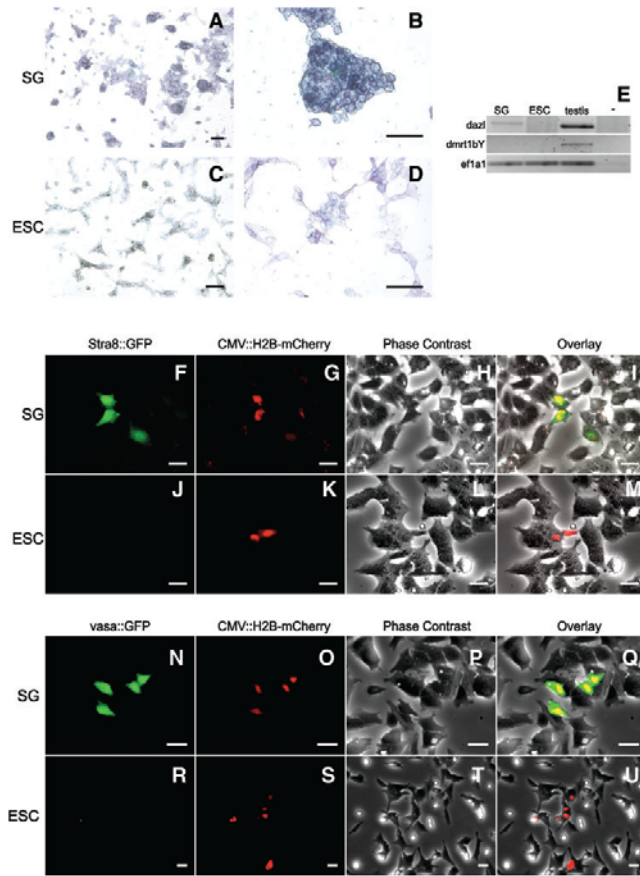
FIG. 1.   Characterization of medaka fish spermatogonial cell line (MF-SG) after long-term culture. (A–D) Alkaline phosphatase staining of MF-SG (A, B) and MF-embryonic stem cells (ESCs) (C, D; positive control). Both cell types show strong substrate turnover (blue precipitate). Scale bars: 50 μm. (E) RT–polymerase chain reaction (PCR) analysis revealing expression of spermatogonia-specific marker *dazl* in MF-SG but not in MF-ESCs and no expression of the Sertoli cell marker *dmrt1bY* in both cell lines. Testis cDNA was used as positive control. (F–M) Activation of the murine Stra8 promoter in MF-SG (F–I) but not in MF-ESCs (J–M) at 2 days posttransfection. Scale bars: 20 μm. (N–U) Remaining GFP signal upon transfection with medaka vasa::GFP-vasaUTR construct in MF-SG (N–Q) but not in MF-ESCs at 7 days posttransfection (R–U). Scale bars: 20 μm. Color images available online at www.liebertonline.com/scd.

identity. However, as a medaka homolog of Stra8 has not been identified, we wanted to strengthen this result using a medaka spermatogonia-specific promoter. Therefore, we performed a similar experiment using a *vasa* reporter construct, which had been previously proven to specifically label germ cells in medaka [17]. MF-ESCs exhibited only weak expression of the construct shortly after transfection and

barely above background, whereas MF-SG retained strong reporter gene expression even after 7 days (Fig. 1N–U). To be able to correlate the expression of used markers with the in vivo situation, we used double-transgenic medaka fish lines harboring the constructs vasa::GFP and dmrt1bY(9kb)::mCherry [20]. Confocal imaging of testes of adult transgenics confirmed the exclusive activation of both

DIRECTED DIFFERENTIATION OF SPERMATOGONIA   5

SF3 ▶ reporters (Supplementary Fig. S3) in germ cells and surrounding Sertoli cells, respectively. These results confirm that MF-SG retained their spermatogonial identity even after long-term culture of >30 passages and are clearly distinguishable from MF-ESCs.

To test the differentiation ability of medaka spermatogonia, MF-SGs were treated with RA, as RA is known to induce differentiation of mouse ESCs into various cell types, for example, adipocytes [30]. The majority of MF-SGs adopted
F2 ▶ clear adipocyte morphology within 12 days of culture (Fig. 2A). To test for an RA concentration dependency, a wide
SF4 ▶ range of concentrations were tested (Supplementary Fig. S4a) and the highest rate of differentiation (>237-fold increase vs. dimethyl sulfoxide treatment; Fig. 2C) was found to result from RA addition to a concentration of 10 μM. Adipocyte formation, albeit with lower efficiency, was also observed at an RA concentration of 1 μM, whereas a concentration of 100 μM led to no detectable adipocyte formation (Supplementary Fig. S4a). Therefore, detailed analyses of the observed cell type were performed with cells treated with 10 μM RA. First, cells were examined by electron microscopy at day 13 of RA treatment (Fig. 2B). Numerous lipid vesicles were clearly distinguishable, making up most of the cellular volume. To verify that the differentiation program for adipocytes was initiated, expression of the adipocyte marker *lipoprotein-lipase* (LPL) was analyzed by quantitative real-time PCR. This gene was chosen as it is not a direct target

gene of RA signaling [31]. After 7 days of RA treatment, MF-SG showed a 5.4-fold ($P = 0.012$) upregulation of LPL (Fig. 2D), strongly suggesting formation of adipocytes. As a biochemical test, thin-layer chromatography [32] was performed using lysates of untreated, mock (dimethyl sulfoxide), treated, and RA-treated MF-SGs (Fig. 2E). RA treatment clearly induced production of triglycerides as quantified by measurements of integrated density of triglyceride bands relative to lane background (Fig. 2F), again suggesting formation of fully differentiated adipocytes. Then, using time-lapse microscopy, it was possible to visualize serial fusion of these
vesicles (Fig. 3A–D). Quantification of vesicle fusion in 3 ◀ F3 independent positions showed an area increase of lipid vesicles of >1.8-fold within 12 h (Fig. 3E). These data demonstrate that cultured MF-SGs are able to differentiate across germ-layer borders by forming adipocytes. Importantly, their reaction to RA differentiation stimulation differs from that found in MF-ESCs, which did not form any adipocyte (Supplementary Fig. S4b) when exposed to RA in any of the tested concentrations for MF-SG (1–100 μM). This fact also rules out the possibility that the differentiating cells in MF-SG cultures are contaminating MF-ESCs.

To verify that adipocytes arose from cells with spermatogonial identity, RA was added to MF-SG transiently transfected with Stra8::GFP, the construct completely inactive in MF-ESCs. Some of the differentiating cells (clearly showing lipid vesicle formation) kept a GFP signal long
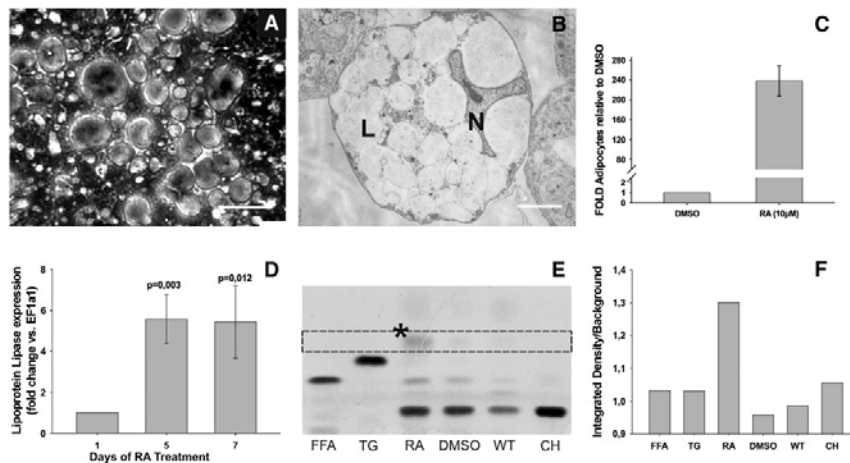

FIG. 2. Differentiation of MF-SG into adipocytes through retinoic acid (RA) treatment. (A) Phase-contrast picture of adipocytes at day 12 of RA treatment. Scale bar: 50 μm. (B) Transmission electron micrograph of an adipocyte at day 13 of RA treatment. L, lipid vesicle; N, nucleus. Scale bar: 1 μm. (C) Efficiency of RA-induced differentiation. Control (dimethyl sulfoxide, DMSO) treatment was set to a value of 1. (D) Quantitative RT-PCR showing significant upregulation of *lipoprotein-lipase* at days 5 and 7 of RA treatment. (E) Thin-layer chromatography demonstrating increased triglyceride content (*asterisk*) of RA-treated cells. RA-induced triglycerides ran farther because of their higher polarity than the used standard. FFA, free fatty acids; TG, triglycerides; RA, total lipids of MF-SG at day 12 of RA treatment; DMSO, total lipids of control MF-SG cells treated with DMSO; WT, total lipids of wild-type MF-SG; CH, cholesterol. (F) Quantification of thin-layer chromatography.
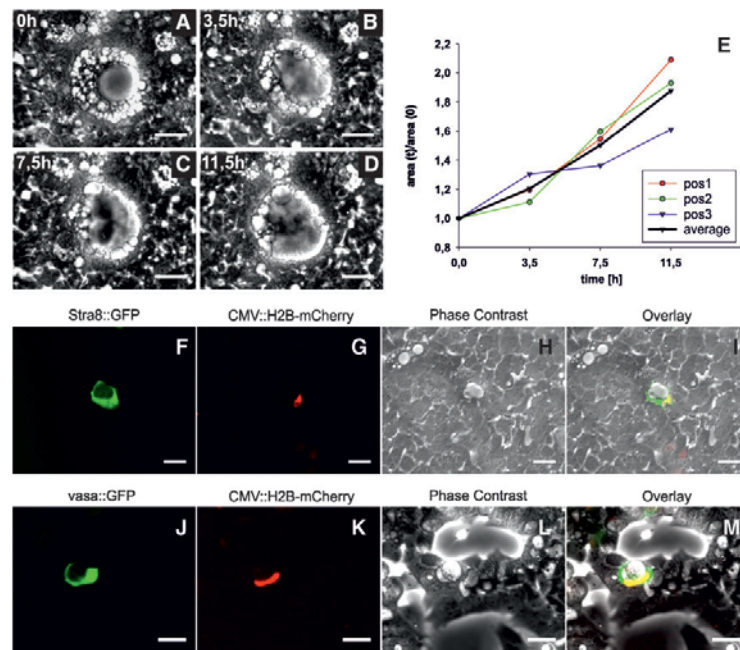
FIG. 3.   Differentiation of MF-SG into adipocytes through RA treatment. (A–D) Time-lapse microscopy analysis revealing fusion of lipid vesicles. Scale bars: 50 μm. (E) Relative increase of lipid vesicle size over time of 3 different adipocytes and average increase (*black line*). (F–I) Adipogenic differentiation of a Stra8::GFP-driving SG upon RA treatment. (F) Remaining GFP fluorescence confirms spermatogonial origin of developing adipocyte. (G) Expression of H2BmCherry as cotransfection control. Scale bars: 20 μm. (J–M) Adipogenic differentiation of a vasa::GFP-driving SG upon RA treatment. (J) Remaining GFP fluorescence confirms spermatogonial origin of developing adipocyte. (K) Expression of H2BmCherry as cotransfection control. Scale bars: 20 μm. Color images available online at www.liebertonline.com/scd.

enough (probably due to the long half-life of GFP), to definitively identify them as formerly Stra8::GFP-expressing cells (Fig. 3F–I). However, Stra8 expression is RA responsive in mammals [29,33]. Although Stra8 might be absent from teleost genomes, and additionally in zebrafish, spermatogenesis does not depend on RA [34], it might be possible that continued activation of Stra8 promoter is an effect of RA treatment. To unambiguously show that adipocytes arose from cells with spermatogonial identity, the same experiment was performed using the *vasa* reporter construct. Therefore, MF-SGs transfected with the medaka vasa::GFP reporter construct were treated with RA. Here, we also observed GFP-expressing adipocytes, confirming their spermatogonial origin (Fig. 3J–M). Thus, GFP expression clearly proves spermatogonial origin of differentiating cells and is not a side-effect of RA treatment.

Next, we wanted to establish a better defined and controllable differentiation assay. One possibility for tight control is the introduction of so-called master-regulator genes—factors that are sufficient for initiation of differentiation of stem cells into a single, defined cell type. The feasibility of this approach was demonstrated earlier through successful use of microphthalmia-associated transcription factor (Mitf-M) for terminal differentiation of MF-ESCs into melanocytes. Fibroblasts transiently transfected with *mitf-m*, however, were not able to form melanocytes [13], suggesting that this process requires a certain differentiation potential. Thus, this assay should allow a clear discrimination between differentiable and nondifferentiable cell types.

Eight days posttransfection of MF-SG with *mitf-m*, melanin-producing cells appeared in the culture (Fig. 4A–C). We found 13 times more melanocytes in *mitf-m*–transfected wells compared with mock transfections ($P = 0.006$; Fig. 4F). On the molecular level, induction of cell lineage marker genes *dct*, *tyr a/b*, *trp1b*, and *sox10* was readily detectable at 3 dpt (Fig. 4G). Many of these differentiation genes showed a wave-like expression pattern, disappearing upon terminal differentiation (7 dpt). Interestingly, we found expression of
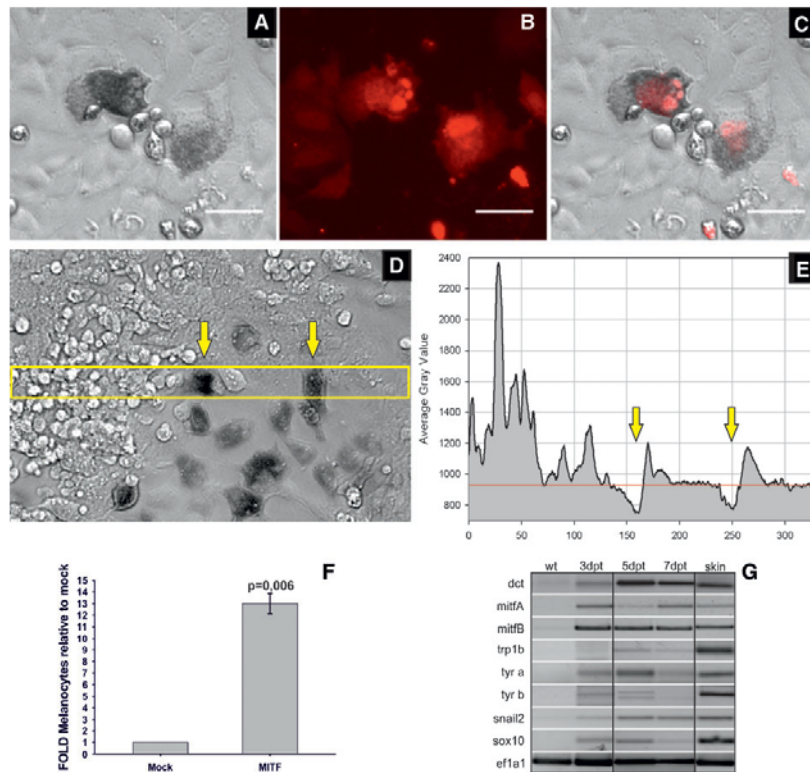
FIG. 4. Directed differentiation of MF-SG by ectopic expression of *mitf-m*. (A–C) Developing melanocytes at 8 dpt. (A) Bright-field view. (B) Dark-field view showing expression of cotransfected mOrange. (C) Overlay. Scale bars: 50 μm. (D) Developing melanocytes at 13 dpt with *mitf-m*. (E) Histogram of average fluorescence intensity values in the *box* in **D**. *Arrows* indicate melanin-mediated quenching of cotransfected mOrange fluorescence in pigmented cells. (F) Efficiency of Mitf-induced differentiation. When transfected with *mitf-m*, melanocytes appear >13 times as often as in mock-transfected MF-SG at 14 dpt. (G) RT-PCR of *mitf-m*–transfected MF-SG showing induction of melanocyte-specific genes. wt, wildtype; dpt, days post-transfection. Color images available online at www.liebertonline.com/scd.

the neural crest markers *snail2* [35] and *sox10*—a gene for upstream upregulation of *mitf* [36]. These findings suggest that the inherent differentiation program is initiated by Mitf. Mitf-transfected MF-SGs seem to progress through typical stages of melanocyte differentiation, including neural crest-like stages. In agreement with this concept, we observed upregulation of both variants of endogenous *mitf*. The molecular mechanism enabling Mitf, a downstream transcription factor in the genetic cascade of the neural crest lineage, to initiate early steps of differentiation remains elusive. On the functional level, *mitf-m*–transfected cells were able to absorb a broad wavelength spectrum of light (Fig. 4D, E), a vital function of terminally differentiated melanocytes. These

findings again demonstrate that MF-SGs are able to form cell types from other germ layers. Further, it is reported for the first time that their differentiation was inducible by ectopic expression of a single transcription factor.

As Mitf was the only thus far described factor able to specifically drive directed differentiation of MF-ESCs on its own, we tested the following other candidates in MF-SG: *cbfa1* [37], *mash1* [38,39], *runx1* [40], *scl* [41], and *sox10* [42]. For further analyses, we focused on the factors that displayed the most promising phenotypic changes, namely *cbfa1* and *mash1*.

To attempt differentiation into osteoblasts, we chose *core-binding factor alpha 1 subunit* (*cbfa1*, often referred to as *runx2*)

8

F5 ▶ as this gene was previously shown to be essential for osteoblastogenesis [37]. MF-SGs were thus transfected with an MF-*cbfa1* expression vector and expression of osteoblast marker genes was assayed (Fig. 5C). Entry into osteoblast differentiation was accompanied by expression of *distal-less homeobox 5* (MF-*dlx5*) expression, a transcription factor shown to regulate *cbfa1* expression, but its own expression was thus far not shown to be directly controlled by *cbfa1* [43]. RT-PCRs for *osteocalcin* (MF-*ocalcin*) and *osteoprotegerin* (MF-*opg*), late markers for osteoblastogenesis [44] and direct target genes of Cbfa1 [45], were positive as well. We also observed activation of osteoblast marker genes *gpnmb/osteoactivin* [46], *periostin* (*postn*) [47,48], and *nephronectin* (*npnt*) [49,50]. Hence, gene expression changes indicate both entry into and progression through the osteoblast differentiation program. Similar to differentiation mediated by *mitf*, upregulation of endogenous *cbfa1* was observed, indicating that differentiation—albeit induced by ectopic *cbfa1*—includes activation of the endogenous

pathway specific for the formation of the corresponding cell type.

A functional feature, and thus terminal differentiation of osteoblasts, can be determined by the cells' ability to form calcified matrix nodules. We therefore performed von Kossa staining to functionally test *cbfa1*-transfected MF-SG. Fourteen days posttransfection, MF-SG cultures stained positive for calcified matrix deposition, whereas mock-transfected controls showed weak or no staining (Fig. 5A, B).

As quantifiable and independent functional in vitro assay for matrix deposition by osteoblasts, the fluorescent Ca^{2+} indicator calcein was used as a live stain. Again, *cbfa1* as well as mock-transfected MF-SG cells were stained. Small patches of calcified matrix deposited adjacent to cells (Fig. 5D–F) became visible. Quantification of matrix depositions by 3-dimensional histograms revealed a significant difference between *cbfa1* and mock-transfected MF-SGs (Fig. 5H, I). To test if the ability to deposit calcified matrix is only mediated
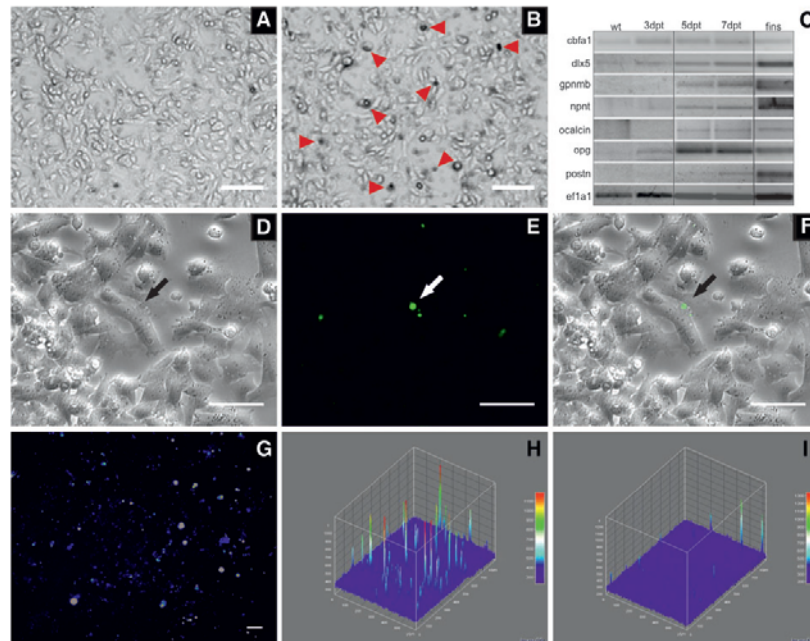

FIG. 5. Directed differentiation of MF-SG by ectopic expression of *cbfa1*. (A, B) von Kossa staining revealing calcium depositions (*arrowheads*) in *cbfa1*-transfected MF-SG (B) but not in mock-transfected MF-SG (A). Scale bars: 50 μm. (C) RT-PCR of *cbfa1*-transfected MF-SG showing induction of osteoblast-specific genes. (D–G) Calcein staining. (D) Bright-field view of osteoblast-like cell at 12 dpt with adjacent calcium deposition (*arrow*). (E) Dark-field view showing stained calcium (*arrow*). (F) Overlay. (G) Overview of calcein staining of *cbfa1*-transfected cells at 12 dpt; dark-field view showing numerous small calcium depositions. Fluorescence intensity is indicated by pseudocolours (RGB Rainbow LUT) ranging from black (lowest) to white (strongest). Scale bars: 50 μm. (H, I) Three-dimensional diagram showing fluorescence intensity of calcein staining of cbfa1- (H) and mock-transfected (I) cells at 12 dpt. Color images available online at www.liebertonline.com/scd.

◀ AU6

DIRECTED DIFFERENTIATION OF SPERMATOGONIA

by Cbfa1 and independent of the cell type used, we performed calcein staining with *cbfa1* and mock-transfected medaka fibroblasts (OLFs). Calcium depositions were observed in neither mock nor *cbfa1*-transfected fibroblasts (Supplementary Fig. S5). Together, these results demonstrate that *Cbfa1* is sufficient to induce and promote differentiation of MF-SG into functional osteoblasts. Further, this process appears to depend on the cell line used for transfection, as *cbfa1*-transfected fibroblasts do not gain functional features of osteoblasts (Supplementary Fig. S5).

Finally, to generate neuronal cell types, *mammalian achaete-scute homolog 1* (*mash1*) was chosen. Mash1 is a basic helix–loop–helix transcription factor that plays a critical role dur-

ing murine embryonic neurogenesis [38,39] and was shown to be able to drive differentiation of murine ES cells into neuronal lineages [16]. Six days posttransfection of MF-SG with *mash1*, cells with a neuron-like morphology became apparent (Fig. 6A, B). These cells were clearly identifiable by long, single protrusions and growth cone-like structures. Thirteen days posttransfection, these neuron-like cells were still detectable (Fig. 6D, E). It is important to note that the culture parameters were not altered to enhance neuronal cell differentiation or survival. RT-PCR analysis further revealed activation of several neuronal marker genes in *mash1*-transfected cells, namely *atonal homolog 3* (*ath3*) [51], *lim only protein 3* (*lmo3*) [52], *neuronal cell adhesion molecule*
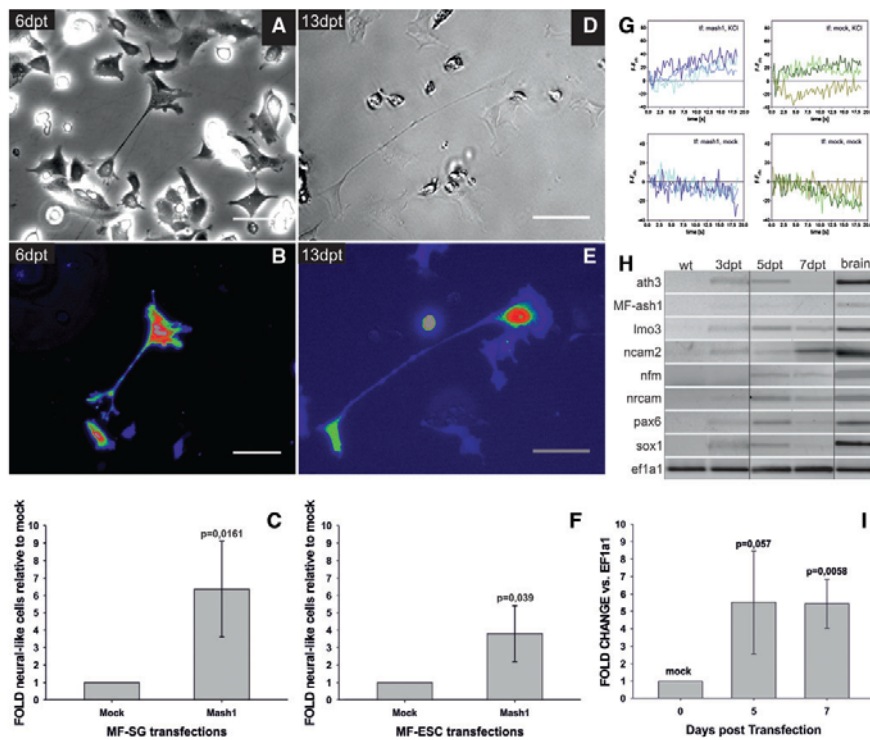
SF5 ►

◄ F6

FIG. 6. Directed differentiation of MF-SG by ectopic expression of *mash1*. (A, B, D, E) Examples of cells showing neuronal morphology at 6 dpt (A, B) and 13 dpt (D, E). Dark-field view (B, E) showing expression of cotransfected mOrange. Fluorescence intensity is indicated by pseudocolours (RGB Rainbow LUT) ranging from black (lowest) to white (strongest). Scale bars: 50 μm. (C, F) Efficiency of *mash1*-induced differentiation of MF-SG (C) and ESCs (F). Mock-transfected cells were set to a value of 1. (G) Calcium imaging of *mash1*- (left panels) and mock (right panels)-transfected MF-SG at 7 dpt. In each case, changes of fluorescence of fura2 to fluorescence $F(t=0)$ are shown for 3 representative cells after stimulation with KCl at $t=0$ (upper panels). Lower panels show changes of fluorescence of fura2 to fluorescence $F(t=0)$ for the same cells after mock stimulation. (H) RT-PCR showing induction of neuronal markers. (I) Quantitative RT-PCR analysis demonstrating significant upregulation of the neuronal marker *foxD3* at 5 and 7 dpt. Color images available online at www.liebertonline.com/scd.

(nrcam) [53,54], pax6 [55,56], and sox1 [57,58]. Further, expression of the late neuronal markers neurofilament-m (MF-nfm) and neural cell adhesion molecule 2 (ncam2) was detected (Fig. 6H). Quantitative real-time PCR revealed significant upregulation (5.43-fold, $P = 0.0058$) of the early neural-crest marker forkhead box protein D3 (foxD3) [59] 5 and 7 dpt in mash1 compared with mock-transfected cells (Fig. 6I). None of the assayed genes have been reported to be directly regulated by Mash1 on the transcriptional level. FoxD3 is even expressed at earlier stages during embryonic neurogenesis than mash1 [59,60]. Pax6 and sox1 are also known to belong to the earliest markers of neuroectoderm formation and at least the expression of sox1 precedes that of mash1 in vivo [58]. The upregulation of these genes therefore suggests initiation of a differentiation program running through developmental stages not directly controlled by Mash1 in vivo. These results are analogous to the findings described for the formation of melanocytes and osteoblasts. For endogenous MF-ash1, a very weak upregulation was detected at 3 and 5 dpt, indicating that differentiation is mediated only by the transfected murine version of ash1 (mash1). However, it has to be mentioned that until now there are no data about function and expression of medaka ash1, leaving open the possibility that cell fate conversion is mediated by an unknown endogenous factor.

The number of neuron-like cells found in mash1 versus mock-transfected MF-SG increased >6.3-fold ($P = 0.0161$; Fig. 6C). The same experimental procedure also led to the formation of neuron-like cells from MF-ESCs, but with a slightly lower efficiency (>3.7-fold increase vs. mock, $P = 0.039$; Fig. 6F).

As a functional test, calcium imaging was performed. After stimulation with KCl, no changes in intracellular calcium levels were observed in mock-transfected cells. Several mash1-transfected cells, however, showed an increase of intracellular Ca^{2+} (Fig. 6G), indicating the presence of voltage-dependent Ca^{2+} channels. Although this feature is not restricted to neuronal cells, this finding together with the results of gene expression pattern analyses and the clear neuronal morphology strongly suggest the formation of neuron-like cells upon mash1 transfection.

Next, we wanted to test whether MF-SGs not only adopt the properties of other cell types but also lose their spermatogonial features upon transfection with differentiation-inducing master regulators. Thus, MF-SGs were cotransfected with mOrangeZeo, the vasa::GFP reporter construct [17], and either mitf, mash1, or cbfa1, respectively. Eight days post-transfection, a significant decrease in vasa promoter activity was detected in master regulator-transfected cultures (Fig. 7I). The possibility that this was an effect of dilution of the vasa::GFP construct upon cell divisions can be excluded as vasa promoter activity was still high in mock-transfected cells. Further, only GFP-negative transfected MF-SG cultures clearly showed morphological changes, indicating formation of the corresponding cell types (Fig. 7A–H).

Discussion

Spermatogonia are to this point the only adult cell type capable of differentiating into cell types of all germ layers [5,61]. Isolation and culture of spermatogonial cells have been described for human [5], mouse [62], rat [7], and me-

daka [8], whereas pluripotency has only been demonstrated for mouse spermatogonia [6]. The derivation of differentiable spermatogonia from human testes has also been reported [5], but recent data indicate that these cells differ from truly pluripotent stem cells [9]. In this report, we show that an SG derived from adult medaka fish can differentiate across germ layer borders into at least 4 different cell types from 2 different somatic germ layer origins. These findings indicate that also in lower vertebrates spermatogonia have retained a certain differentiation potential, albeit pluripotency of MF-SG cannot be conclusively assumed. Further, the effects of long-term culture on the differentiation potential of the MF-SG cell line remain elusive. It cannot be excluded that their differentiation ability decreased during in vitro culture and that therefore primary spermatogonia are more differentiable. Similarly, it could be hypothesized that MF-SG dedifferentiate during long-term culture to a more differentiable state. However, our results demonstrate that the MF-SG still shows several features of germ cells such as high activity of spermatogonia-specific promoters and the expression of germ cell markers. It can thus be concluded that the cell line has largely retained its spermatogonial identity and clearly differs from medaka ESCs. Hence, medaka male germ cells obviously have a broad differentiation potential. Together with the data from mouse and human, this finding suggests that a certain differentiation ability of male germ cells that is not lost during long-term culture might be a conserved feature among vertebrates, albeit the grade of differentiation potential may differ from species to species.

In this study, we present 2 different approaches to induce differentiation of MF-SG, namely mediated by RA or by ectopic expression of key developmental genes. The effects of RA treatment were different in MF-SG and ESCs, whereas ectopic expression of the master regulator genes mitf-m and mash1 resulted in the formation of the same cell type in MF-SG and ESCs.

Various recent studies show that defined genes can dramatically influence cell fate determination. For example, it has been shown that a set of 3 neuron-specific genes can convert fibroblast to neurons [63]. Similarly, β-cells were generated from exocrine pancreatic cells using a combination of 3 pancreatic genes [64]. However, these studies report conversion of one somatic cell type into another using a combination of genes. Our study shows that a cell line with a certain differentiation potential can be induced to form one defined cell type solely by ectopic expression of a single gene and without the need for any other signal. Using this approach, we were able to obtain melanocytes, osteoblasts, and neuron-like cells. This path for directed differentiation has not been previously demonstrated for either mouse or human spermatogonia. As the efficiencies of terminal differentiation are thus far suboptimal, there is a lot of room for technical improvement. Importantly, it needs to be taken into consideration that nontransfected MF-SGs continued to proliferate and so the differentiating cells quickly exit the cell cycle and are thus overgrown. As differentiation was assessed after 7 or more dpt, nontransfected cells will have divided at least 5 times during this period. At the same time, harsh selection with antibiotics was found to have negative effects on differentiation. Finally, the transfected MF-SGs were kept in their standard growth medium throughout all differentiation assays to ensure comparability. This strategy

DIRECTED DIFFERENTIATION OF SPERMATOGONIA   11
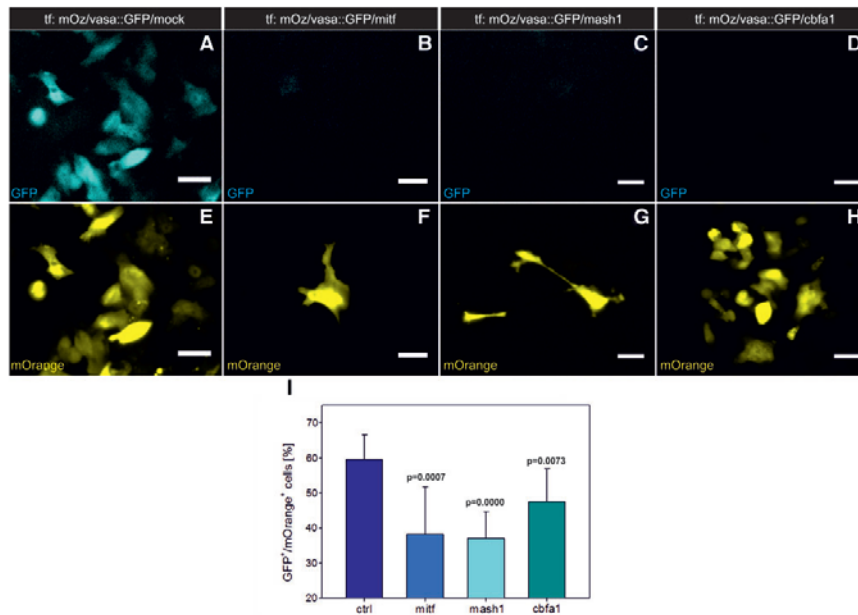

FIG. 7.   Loss of spermatogonial identity during differentiation of MF-SG. (A–H) Remaining GFP signal upon transfection with vasa::GFP construct in control transfected MF-SG (A) but not in master regulator-transfected MF-SG (B–D) at 8 dpt. (E–H) Cotransfected mOrange. *Mitf*-transfected cells display stellate cell shape characteristic for melanocytes (F). *Mash1*-transfected cells show neuron-like cell shape (G). (H) Developing osteoblasts upon *cbfa1* transfection. Note that cells appear in foci possibly because of division of transfected cells shortly after transfection. Scale bars: 20 μM. (I) Quantification of inactivation of vasa::GFP construct at 8 dpt. Color images available online at www.liebertonline.com/scd.

is likely to have negatively affected differentiation efficiency, but also demonstrates the inductive strength of the transfected genes: they enabled the cells to overcome external signals and the endogenous self-renewal program and also allowed them to become at least partially independent of external stimuli usually needed for terminal differentiation and survival.

However, the capacity of the transfected genes to induce the formation of a defined cell type obviously depends on the cell type used. As shown previously, fibroblasts are not able to form melanocytes upon *mitf-m* transfection [13]. Our results demonstrate that *cbfa1* transfection of fibroblasts also does not lead to the formation of osteoblasts as observed for MF-SGs. Thus, it can be assumed that a single-gene–mediated differentiation—at least with the factors tested in this study—does require a certain differentiation potential of the cell line used.

It will be interesting to see if other genes than the here reported *mitf*, *cbfa1*, and *mash1* also have the potential to induce directed differentiation of uncommitted cells without the need for additional signals. If so, this approach could be

used to generate many more cell types provided that the correct master regulators can be identified. Remarkably, all 3 analyzed master regulators apparently initiated a sequence of gene expression that resembled the cascades reported for the respective differentiation in vivo. In all cases, some marker genes were induced even though in vivo their expression precedes that of the transfected master regulators. Similarly, transfection of MF-ESCs with *mitf-m* [13] resulted in transient expression of *sox10*, a gene responsible for the activation of *mitf* in vivo [36]. Hence, this early marker activation was observed in 2 different cell lines and 3 independent differentiation processes. Therefore, it is likely that cascade reinitiation is not just an irrelevant side-effect, but a part of master regulator-mediated differentiation processes. Mitf-m was reported to be not able to induce differentiation of fibroblasts [13]. Hence, the cascade initiation mechanism might only be active in cells with broader differentiation capacity. The fact that this recapitulation of the physiological program is induced by all differentiation-inducing master regulators used here raises the question if an in vivo correlate of this phenomenon exists. Hypothetically, in vivo master

regulators irreversibly commit cells to a definitive lineage through their ability to reinitiate the respective genetic differentiation cascade. It has to be determined if the recapitulation of early differentiation stages always occurs during in vitro differentiation processes independent of the cell type formed and if it is an essential step to obtain terminally differentiated cells. The idea that the transfected master regulators initiate an endogenous gene expression cascade is also supported by the fact that at later stages of induced differentiation the genes were found to be expressed, which are not under direct control of the transfected factors.

Taken together, genetically induced terminal differentiation can be considered a powerful approach with high levels of control over the definitive cell type generated. This control is a very important prerequisite for obtaining fully differentiated cells, which are needed not only for medical purposes, but also for detailed biological analyses.

In summary, we first showed that a medaka SG is able to differentiate into somatic cell types from different germ layers, thus proving that spermatogonia of lower vertebrate have a broad differentiation potential in vitro. Second, we demonstrated that single genes can induce directed differentiation of spermatogonia. This approach represents a useful differentiation system with potential application in stem cell research as well as in regenerative medicine.

Acknowledgments

Author Disclosure Statement

All authors declare that they have no competing financial interests.

References

1. Nakagawa M, M Koyanagi, K Tanabe, et al. (2008). Generation of induced pluripotent stem cells without Myc from mouse and human fibroblasts. Nat Biotechnol 26:101–106.

2. Takahashi K and S Yamanaka. (2006). Induction of pluripotent stem cells from mouse embryonic and adult fibroblast cultures by defined factors. Cell 126:663–676.

3. Takahashi K, K Tanabe, M Ohnuki, et al. (2007). Induction of pluripotent stem cells from adult human fibroblasts by defined factors. Cell 131:861–872.

4. Wernig M, A Meissner, R Foreman, et al. (2007). In vitro reprogramming of fibroblasts into a pluripotent ES-cell-like state. Nature 448:318–324.

5. Conrad S, M Renninger, J Hennenlotter, et al. (2008). Generation of pluripotent stem cells from adult human testis. Nature 456:344–349.

6. Guan K, K Nayernia, LS Maier, et al. (2006). Pluripotency of spermatogonial stem cells from adult mouse testis. Nature 440:1199–1203.

7. Hamra FK, KM Chapman, DM Nguyen, et al. (2005). Self renewal, expansion, and transfection of rat spermatogonial stem cells in culture. Proc Natl Acad Sci U S A 102:17430–17435.

8. Hong Y, T Liu, H Zhao, et al. (2004). Establishment of a normal medakafish spermatogonial cell line capable of sperm production in vitro. Proc Natl Acad Sci U S A 101:8011–8016.

9. Ko K, MJ Araúzo-Bravo, N Tapia, et al. (2010). Human adult germline stem cells in question. Nature 465:E1; discussion E3.

10. Chadwick K, L Wang, L Li, et al. (2003). Cytokines and BMP-4 promote hematopoietic differentiation of human embryonic stem cells. Blood 102:906–915.

11. Maye P, S Becker, E Kasameyer, et al. (2000). Indian hedgehog signaling in extraembryonic endoderm and ectoderm differentiation in ES embryoid bodies. Mech Dev 94:117–132.

12. Nakano T, H Kodama and T Honjo. (1994). Generation of lymphohematopoietic cells from embryonic stem cells in culture. Science 265:1098–1101.

13. Béjar J, Y Hong and M Schartl. (2003). Mitf expression is sufficient to direct differentiation of medaka blastula derived stem cells to melanocytes. Development 130:6545–6553.

14. Bondue A, G Lapouge, C Paulissen, et al. (2008). Mesp1 acts as a master regulator of multipotent cardiovascular progenitor specification. Cell Stem Cell 3:69–84.

15. Gang EJ, D Bosnakovski, T Simsek, et al. (2008). Pax3 activation promotes the differentiation of mesenchymal stem cells toward the myogenic lineage. Exp Cell Res 314:1721–1733.

16. Ikeda R, MS Kurokawa, S Chiba, et al. (2004). Transplantation of motoneurons derived from MASH1-transfected mouse ES cells reconstitutes neural networks and improves motor function in hemiplegic mice. Exp Neurol 189:280–292.

17. Tanaka M, M Kinoshita, D Kobayashi, et al. (2001). Establishment of medaka (*Oryzias latipes*) transgenic lines with the expression of green fluorescent protein exclusively in germ cells: a useful model to monitor germ cells in a live vertebrate. Proc Natl Acad Sci U S A 98:2544–2549.

18. Cau E, G Gradwohl, C Fode, et al. (1997). Mash1 activates a cascade of bHLH regulators in olfactory neuron progenitors. Development 124:1611–1621.

19. Kasahara M, K Naruse, S Sasaki, et al. (2007). The medaka draft genome and insights into vertebrate genome evolution. Nature 447:714–719.

20. Herpin A, I Braasch, M Kraeussling, et al. (2010). Transcriptional rewiring of the sex determining dmrt1 gene duplicate by transposable elements. PLoS Genet 6:e1000844.

21. Hong Y, C Winkler and M Schartl. (1996). Pluripotency and differentiation of embryonic stem cell lines from the medakafish (*Oryzias latipes*). Mech Dev 60:33–44.

22. Hong Y, C Winkler, T Liu, et al. (2004). Activation of the mouse Oct4 promoter in medaka embryonic stem cells and

its use for ablation of spontaneous differentiation. Mech Dev 121:933–943.

23. Klüver N, M Kondo, A Herpin, et al. (2005). Divergent expression patterns of Sox9 duplicates in teleosts indicate a lineage specific subfunctionalization. Dev Genes Evol 215:297–305.

24. Nanda I, M Kondo, U Hornung, et al. (2002). A duplicated copy of DMRT1 in the sex-determining region of the Y chromosome of the medaka, *Oryzias latipes*. Proc Natl Acad Sci U S A 99:11778–11783.

25. Angelastro JM, TN Ignatova, VG Kukekov, et al. (2003). Regulated expression of ATF5 is required for the progression of neural progenitor cells to neurons. J Neurosci 23:4590–4600.

26. Angelastro JM, JL Mason, TN Ignatova, et al. (2005). Downregulation of activating transcription factor 5 is required for differentiation of neural progenitor cells into astrocytes. J Neurosci 25:3889–3899.

27. Mason JL, JM Angelastro, TN Ignatova, et al. (2005). ATF5 regulates the proliferation and differentiation of oligodendrocytes. Mol Cell Neurosci 29:372–380.

28. Nayernia K, M Li, L Jaroszynski, et al. (2004). Stem cell based therapeutical approach of male infertility by teratocarcinoma derived germ cells. Hum Mol Genet 13:1451–1460.

29. Oulad-Abdelghani M, P Bouillet, D Décimo, et al. (1996). Characterization of a premeiotic germ cell-specific cytoplasmic protein encoded by Stra8, a novel retinoic acid-responsive gene. J Cell Biol 135:469–477.

30. Dani C, AG Smith, S Dessolin, et al. (1997). Differentiation of embryonic stem cells into adipocytes in vitro. J Cell Sci 110 (Pt 1):1279–1285.

31. Oliver JD and MP Rogers. (1993). Effects of retinoic acid on lipoprotein lipase activity and mRNA level in vitro and in vivo. Biochem Pharmacol 45:579–583.

32. Michalec C, M Sulc and J Mestan. (1962). Analysis of cholesteryl esters and triglycerides by thin-layer chromatography. Nature 193:63–64.

33. Zhou Q, R Nie, Y Li, et al. (2008). Expression of stimulated by retinoic acid gene 8 (Stra8) in spermatogenic cells induced by retinoic acid: an in vivo study in vitamin A-sufficient postnatal murine testes. Biol Reprod 79:35–42.

34. Alsop D, J Matsumoto, S Brown, et al. (2008). Retinoid requirements in the reproduction of zebrafish. Gen Comp Endocrinol 156:51–62.

35. Thisse C, B Thisse and JH Postlethwait. (1995). Expression of snail2, a second member of the zebrafish snail family, in cephalic mesendoderm and presumptive neural crest of wild-type and spadetail mutant embryos. Dev Biol 172:86–99.

36. Elworthy S, JA Lister, TJ Carney, et al. (2003). Transcriptional regulation of mitfa accounts for the sox10 requirement in zebrafish melanophore development. Development 130:2809–2818.

37. Otto F, AP Thornell, T Crompton, et al. (1997). Cbfa1, a candidate gene for cleidocranial dysplasia syndrome, is essential for osteoblast differentiation and bone development. Cell 89:765–771.

38. Lo LC, JE Johnson, CW Wuenschell, et al. (1991). Mammalian achaete-scute homolog 1 is transiently expressed by spatially restricted subsets of early neuroepithelial and neural crest cells. Genes Dev 5:1524–1537.

39. Guillemot F, LC Lo, JE Johnson, et al. (1993). Mammalian achaete-scute homolog 1 is required for the early de-

velopment of olfactory and autonomic neurons. Cell 75: 463–476.

40. Kalev-Zylinska ML, JA Horsfield, MV Flores, et al. (2002). Runx1 is required for zebrafish blood and vessel development and expression of a human RUNX1-CBF2T1 transgene advances a model for studies of leukemogenesis. Development 129:2015–2030.

41. Dooley KA, AJ Davidson and LI Zon. (2005). Zebrafish scl functions independently in hematopoietic and endothelial development. Dev Biol 277:522–536.

42. Dutton KA, A Pauliny, SS Lopes, et al. (2001). Zebrafish colourless encodes sox10 and specifies non-ectomesenchymal neural crest fates. Development 128:4113–4125.

43. Shirakabe K, K Terasawa, K Miyama, et al. (2001). Regulation of the activity of the transcription factor Runx2 by two homeobox proteins, Msx2 and Dlx5. Genes Cells 6:851–856.

44. Simonet WS, DL Lacey, CR Dunstan, et al. (1997). Osteoprotegerin: a novel secreted protein involved in the regulation of bone density. Cell 89:309–319.

45. Thirunavukkarasu K, DL Halladay, RR Miles, et al. (2000). The osteoblast-specific transcription factor Cbfa1 contributes to the expression of osteoprotegerin, a potent inhibitor of osteoclast differentiation and function. J Biol Chem 275: 25163–25172.

46. Abdelmagid SM, MF Barbe, MC Rico, et al. (2008). Osteoactivin, an anabolic factor that regulates osteoblast differentiation and function. Exp Cell Res 314:2334–2351.

47. Takeshita S, R Kikuno, K Tezuka, et al. (1993). Osteoblast-specific factor 2: cloning of a putative bone adhesion protein with homology with the insect protein fasciclin I. Biochem J 294 (Pt 1):271–278.

48. Horiuchi K, N Amizuka, S Takeshita, et al. (1999). Identification and characterization of a novel protein, periostin, with restricted expression to periosteum and periodontal ligament and increased expression by transforming growth factor beta. J Bone Miner Res 14:1239–1249.

49. Hecht J, V Seitz, M Urban, et al. (2007). Detection of novel skeletogenesis target genes by comprehensive analysis of a Runx2(-/-) mouse model. Gene Expr Patterns 7:102–112.

50. Kahai S, S Lee, A Seth, et al. (2010). Nephronectin promotes osteoblast differentiation via the epidermal growth factor-like repeats. FEBS Lett 584:233–238.

51. Takebayashi K, S Takahashi, C Yokota, et al. (1997). Conversion of ectoderm into a neural fate by ATH-3, a vertebrate basic helix-loop-helix gene homologous to *Drosophila* proneural gene atonal. EMBO J 16:384–395.

52. Foroni L, T Boehm, L White, et al. (1992). The rhombotin gene family encode related LIM-domain proteins whose differing expression suggests multiple roles in mouse development. J Mol Biol 226:747–761.

53. Lustig M, L Erskine, CA Mason, et al. (2001). Nr-CAM expression in the developing mouse nervous system: ventral midline structures, specific fiber tracts, and neuropilar regions. J Comp Neurol 434:13–28.

54. Moscoso LM and JR Sanes. (1995). Expression of four immunoglobulin superfamily adhesion molecules (L1, Nr-CAM/Bravo, neurofascin/ABGP, and N-CAM) in the developing mouse spinal cord. J Comp Neurol 352:321–334.

55. Gruss P and C Walther. (1992). Pax in development. Cell 69:719–722.

56. Walther C and P Gruss. (1991). Pax-6, a murine paired box gene, is expressed in the developing CNS. Development 113:1435–1449.

57. Wood HB and V Episkopou. (1999). Comparative expression of the mouse Sox1, Sox2 and Sox3 genes from pregastrulation to early somite stages. Mech Dev 86:197–201.

58. Pevny LH, S Sockanathan, M Placzek, et al. (1998). A role for SOX1 in neural determination. Development 125:1967–1978.

59. Odenthal J and C Nüsslein-Volhard. (1998). Fork head domain genes in zebrafish. Dev Genes Evol 208:245–258.

60. Allende ML and ES Weinberg. (1994). The expression pattern of two zebrafish achaete-scute homolog (ash) genes is altered in the embryonic brain of the cyclops mutant. Dev Biol 166:509–530.

61. Guan K, S Wagner, B Unsöld, et al. (2007). Generation of functional cardiomyocytes from adult mouse spermatogonial stem cells. Circ Res 100:1615–1625.

62. Kanatsu-Shinohara M, N Ogonuki, K Inoue, et al. (2003). Long-term proliferation in culture and germline transmission of mouse male germline stem cells. Biol Reprod 69:612–616.

63. Vierbuchen T, A Ostermeier, ZP Pang, et al. (2010). Direct conversion of fibroblasts to functional neurons by defined factors. Nature 463:1035–1041.

64. Zhou Q, J Brown, A Kanarek, et al. (2008). In vivo reprogramming of adult pancreatic exocrine cells to beta-cells. Nature 455:627–632.

Address correspondence to:
Dr. Toni U. Wagner
Department of Physiological Chemistry I
University of Wuerzburg
Biozentrum am Hubland
Wuerzburg 97074
Germany

E-mail: toni.wagner@biozentrum.uni-wuerzburg.de

Supplementary Data
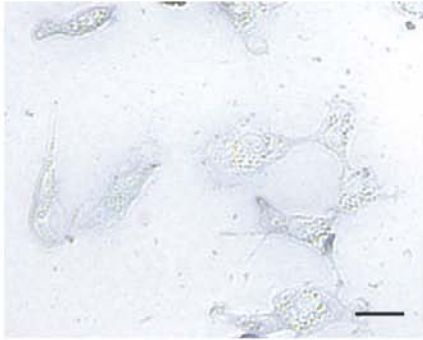
SUPPLEMENTARY FIG. S1. Alkaline phosphatase staining of medaka fibroblasts (OLFs). No alkaline phosphatase activity is detected. Slightly blue shape of cells is due to the contrast method used for image acquisition. Scale bar: 20 μm.
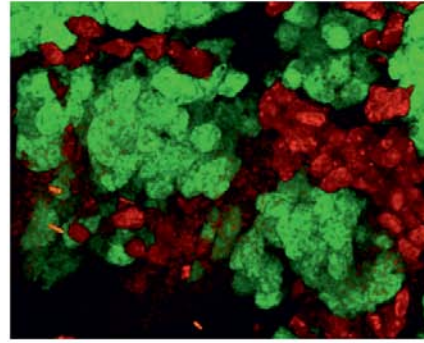
SUPPLEMENTARY FIG. S3. Confocal reconstruction of a sectioned testis of an adult medaka fish stably transgenic for vasa:GFP and *dmrt1bY*(9kb)::mCherry promoter reporter constructs. Clearly visible is the clustering of GFP-positive germ cells and the surrounding mCherry signal from Sertoli cells.
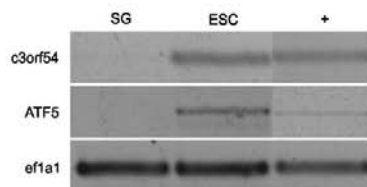
AU2 ► SUPPLEMENTARY FIG. S2. RT–polymerase chain reaction documenting expression of *atf5* and *c3orf54* only in medaka fish embryonic stem cells (MF-ESCs), but not in MF spermatogonial cell line (MF-SG).+, Positive control (cDNA from mixed medaka embryonic stages).
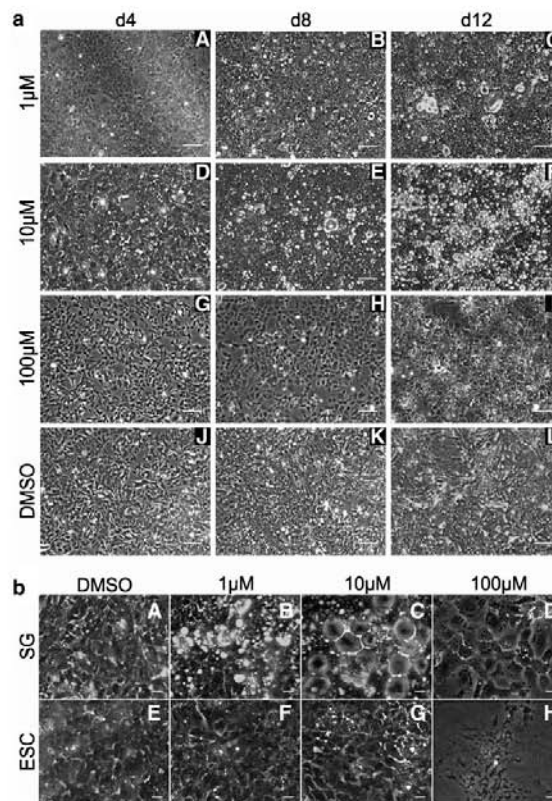
SUPPLEMENTARY FIG. S4. Effects of retinoic acid (RA) on medaka SG and ESCs. **(a)** MF-SGs form adipocytes with different efficiencies upon RA treatment. Upon addition of RA to their growth medium, MF-SGs form cells with clear adipocyte morphology (lipid vesicle formation). The effect is most pronounced at a final concentration of 10 μM **(D–F)**, whereas only a small number of adipocytes form at 1 μM **(A–C)** and no adipocytes were found at 100 μM **(G–I)**. Dimethyl sulfoxide (DMSO)-treated control cells **(J–L)** only show background levels of differentiation into various cell types, including isolated adipocyte-like cells. Scale bars: 100 μm. **(b)** Different reaction of MF-SGs **(A–D)** and MF-ESCs **(E–H)** to RA treatment. All images were taken at day 12 of RA treatment. MF-SGs form adipocytes at RA concentrations of 1 μM **(B)** and 10 μM **(C)**, whereas MF-ESCs treated in the same way **(F, G)** form no adipocytes. RA concentration of 100 μM induces nonadipocyte phenotypic changes in MF-SGs **(D)**, but is lethal to MF-ESCs **(H)**. Scale bars: 20 μm.
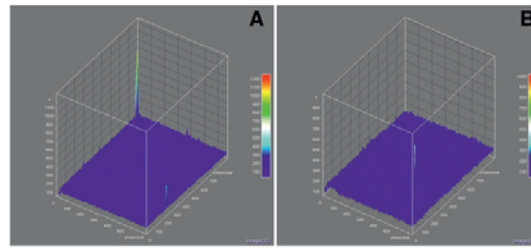
SUPPLEMENTARY FIG. S5. *Cbfa1*-transfected fibroblasts are not able to deposit calcium-containing matrix. Quantification of calcein staining of *cbfa1*-transfected **(A)** and mock-transfected **(B)** OLFs at 12 dpt. Fluorescence intensity is indicated by pseudocolours (RGB Rainbow LUT) ranging from black (lowest) to white (strongest).

SUPPLEMENTARY TABLE S1.   ◄AU7

Gene	T (°C)	Forward primer	Reverse primer
ef1a1	56	5′-GCCCCTGGACACAGAGACTTCATCA-3′	5′-AAGGGGGCTCGGTGGAGTCCAT-3′
dazl	56	5′-CTTTTTGTTGGAGGGATCGAC-3′	5′-CATCTGTGGAATCACTATCCC-3′
dmrt1bY	60	5′-CTGACATGAGCAAGGAGAAGCAG-3′	5′-CTGGTACTGCTGGTAGTTGTG-3′
ATF5	54	5′-CACCGCTACCACCACAACAA-3′	5′-AGGCAGGGCTCGTCCTTTAG-3′
C3orf54	54	5′-GAGCGGATTGATCTGTGATGG-3′	5′-CAGCTTTTCCGCAGTTGCTT-3′
Lpl	54	5′-TTCATCATTCCTGGCCAACC-3′	5′-CTGAGCCAAGCTGAGCCAGT-3′
Dct	59	5′-GACCAAACGGGACAGATCCA-3′	5′-CGTTCCAGGCTCAGAAGGTG-3′
mitf-a	54	5′-GTGCAGGCATAAGAAGCTGG-3′	5′-GCTGGTATATCTCTGGTGGG-3′
mitf-b	56	5′-GCGCCCCCAACAGCCCTATG-3′	5′-CGTTGATGTTGAACCTTCGTC-3′
trp1b	54	5′-GTTCAGAGAGCAGCCCCATC-3′	5′-CGCTGACAAACATTTCCGC-3′
tyr a	54	5′-ATATCGATTTTGCCCACGAG-3′	5′-TGCAGACTTCACAGGACTGG-3′
tyr b	59	5′-GGTTGGGTAGCAGTTCTCGTC-3′	5′-GAACAAATCCACCTCTCCAGC-3′
snail2	57	5′-TCACACGTTGCCTTGTGTTT-3′	5′-TTGGAGCAGTTCTTGCATTG-3′
sox10	54	5′-CCAAGGCTCAGATCAAAAGC-3′	5′-TGGTGCTCTCCGTAGTCAAA-3′
foxD3	60	5′-ATGCAGAAGCCCAAGAGCAG-3′	5′-CTCCCGGGGGATTTTTATGA-3′
ash1	57	5′-GCTGCAAACGCAGGCTAAAT-3′	5′-CAGCGTCTCCACTTTGCTCA-3′
ath3	54	5′-CCGAAAGGAACTTCACATCTCACT-3′	5′-TCCAAACAGCATGAATGCAAAC-3′
dat1	54	5′-CTGCAACCGGAAGATCAAGG-3′	5′-TGCCCTCATGACCATCTCAA-3′
ncam	64	5′-CAGCTCCCCTTCACCAACAG-3′	5′-GGGGCGAACGTTTACAATGA-3′
nfm	60	5′-AAGAAAGTTCAGTCGCTGCAGGACGA-3′	5′-CCTGGAGCCTGGCCAGTTCGCTA-3′
nrcam	54	5′-ACAGAATGGCGCTCCACAAT-3′	5′-ATCAGGTTCTTGGGGGCACT-3′
pax6	54	5′-TCTTTGCGTGGGAGATTCGT-3′	5′-TCCCCCAAGTTCCTGTCTGA-3′
sox1	54	5′-AGTTCATCTGGGGTCGGACA-3′	5′-CTGTACTGCAGGGCCGTCAT-3′
cbfa1	57	5′-GGCTCAGGGGTTTGTGTTTGAG-3′	5′-GAAGAAGTTCTGCTGACATGG-3′
dlx5	55	5′-CTGCGTCGCTGGGACTTACT-3′	5′-GGCTTTGTGGCTGAAGGTTG-3′
gpnmb	54	5′-CTCCCTGCCAGAAGGAGGAT-3′	5′-GTGCCTCCAGTCGTTGCTCT-3′
npnt	60	5′-ACCAAAAAGCGAGGGGATGT-3′	5′-GCGGGGTGAGAGGAAGAACT-3′
ocalcin	58	5′-TTGTGGAACCCGAGGTTATT-3′	5′-GTCCACAAGTGGATGCATGA-3′
opg	55	5′-TGTGGCGGGAGCAAAATAAG-3′	5′-CTGCAGGATGTGCTGTCTGG-3′
postn	52	5′-TTCTGTCAAAGTCCCAGAAG-3′	5′-TCAACATATCTTGTCCTAAA-3′

Manuscript 2: Transcriptional rewiring of the sex determining dmrt1 gene duplicate by transposable elements. PLOS Genetics, 2010

PLoS GENETICS

Transcriptional Rewiring of the Sex Determining *dmrt1* Gene Duplicate by Transposable Elements

Amaury Herpin[1,9]*, Ingo Braasch[1,9], Michael Kraeussling[1], Cornelia Schmidt[1], Eva C. Thoma[1], Shuhei Nakamura[2], Minoru Tanaka[2], Manfred Schartl[1,3]

1 University of Würzburg, Physiological Chemistry I, Biozentrum, Würzburg, Germany, 2 Laboratory of Molecular Genetics for Reproduction, National Institute for Basic Biology 5-1, Higashiyama, Okazaki, Japan, 3 University of Würzburg, Rudolf-Virchow-Center for Experimental Biomedicine (DFG research Center), Würzburg, Germany

Abstract

Control and coordination of eukaryotic gene expression rely on transcriptional and posttranscriptional regulatory networks. Evolutionary innovations and adaptations often require rapid changes of such networks. It has long been hypothesized that transposable elements (TE) might contribute to the rewiring of regulatory interactions. More recently it emerged that TEs might bring in ready-to-use transcription factor binding sites to create alterations to the promoters by which they were captured. A process where the gene regulatory architecture is of remarkable plasticity is sex determination. While the more downstream components of the sex determination cascades are evolutionary conserved, the master regulators can switch between groups of organisms even on the interspecies level or between populations. In the medaka fish (*Oryzias latipes*) a duplicated copy of *dmrt1*, designated *dmrt1bY* or *DMY*, on the Y chromosome was shown to be the master regulator of male development, similar to *Sry* in mammals. We found that the *dmrt1bY* gene has acquired a new feedback downregulation of its expression. Additionally, the autosomal *dmrt1a* gene is also able to regulate transcription of its duplicated paralog by binding to a unique target Dmrt1 site nested within the *dmrt1bY* proximal promoter region. We could trace back this novel regulatory element to a highly conserved sequence within a new type of TE that inserted into the upstream region of *dmrt1bY* shortly after the duplication event. Our data provide functional evidence for a role of TEs in transcriptional network rewiring for sub- and/or neo-functionalization of duplicated genes. In the particular case of *dmrt1bY*, this contributed to create new hierarchies of sex-determining genes.

Introduction

Control and coordination of eukaryotic gene expression rely on transcriptional and posttranscriptional regulatory networks. From an evolutionary point of view innovations and changes in given functional linkages of regulatory networks have to occur at the DNA level by alteration of the *cis*-regulatory sequence defining transcription factor binding sites. While such alterations may occur in any *cis*-regulatory module, they will have fundamentally different effects depending on where in the structure of the network they occur (see [1] for review). After the discovery of the ubiquitousness of repeated sequences, a long standing hypothesis proposed that repeated sequences were likely to be active in the 5′ regions of genes controlling transcription [2] and that they could move and supply evolutionary variations [3].

From an evolutionary perspective, transposable elements (TEs) have recently been attributed an important role in shaping the gene regulation landscape [4,5,6]. In spite of and, to some extent, because of their selfish and parasitic nature, the movement and accumulation of TEs have exerted a strong influence on the evolutionary trajectory of their host genome [7]. Many ways have

been illustrated through which TEs can directly influence the regulation of nearby gene expression, both at the transcriptional and post-transcriptional levels (for review see [5]). Genome-scale bioinformatic analyses have shown that many promoters and polyadenylation signals of human and mouse genes are derived from primate and rodent specific TEs respectively [8,9]. Hence, it is postulated that insertion of TEs harbouring "ready-to-use" *cis*-regulatory sequences probably contributed to the establishment of lineage-specific patterns of gene expression [10]. In addition to donating *cis*-elements and creating new regulatory networks, the movement and accumulation of TEs have recently been proposed to participate in the rewiring of pre-established regulatory networks (see [5] for review).

Such rewiring is especially important when rapid adaptation of existing regulatory networks or new networks become necessary. One system where fast changes obviously regularly occurred during evolution is the genetic control of sexual development [11,12]. It is well documented that different groups of organisms and sometimes even closely related species of different populations of the same species have fundamentally different modes of sex determination. Comparative evolutionary studies of the genetic

Author Summary

Evolutionary innovations and adaptations often require rapid changes in gene regulation. Transposable elements constitute the most dynamic part of eukaryotic genomes. Insertions of transposable elements can influence the expression of surrounding genes by donating new regulatory elements. A longstanding hypothesis postulates that the dispersal of transposable elements may rewire regulatory links between genes, thereby changing regulatory networks and shuffling regulatory cascades. A regulatory hierarchy of remarkable plasticity is the sex determination cascade. In the course of animal evolution, new master regulators frequently replace the sex determination gene on top of the hierarchy. In the medaka fish, a duplicate of the *dmrt1* transcription factor gene, *dmrt1bY*, has become the sex master regulator. Its ancestor *dmrt1a*, in contrast, has a downstream position in the sex determination cascade. We show that after the duplication of the *dmrt1* gene, the new hierarchy has been established by the insertion of a transposable element into the regulatory region of the *dmrt1bY* gene on the sex chromosome. This transposable element, harboring a Dmrt1 binding site, enables the self- and cross-regulation of *dmrt1bY* expression by Dmrt1 proteins. Our study therefore provides strong evidence for the important role of transposable elements in the rewiring of gene regulatory networks.

cascades controlling sex determination in different species revealed that the master genes at the top of the regulatory hierarchy can change dramatically as new species evolve, while the downstream genes at the bottom of the hierarchy remain the same, exerting essentially identical functions from one species to the next (see [12,13] for review).

The most conserved downstream component characterized to date, a gene with homology to both the *Drosophila doublesex* and *C. elegans mab-3* sex regulatory genes, is the *Dmrt1* (Doublesex and Mab-3 Related Transcription factor 1) gene of vertebrates [14]. All three genes encode proteins sharing a common DNA-binding domain and belong to the DM domain gene family, which has been shown to be involved in sex determination and differentiation in organisms as phylogenetically divergent as corals, worms, flies and all vertebrate groups ranging from fish to mammals. Of note, in humans, haploinsufficiency of the genomic region that includes *DMRT1* and its paralogs *DMRT2* and *DMRT3* leads to XY male to female sex reversal [15]. In chicken and other avian species *Dmrt1* is located on the Z chromosome, but absent from W, making it an excellent candidate for the male sex-determining gene of birds [16,17].

In the medaka fish (*Oryzias latipes*), which has XY-XX sex determination, a duplicated copy of *dmrt1*, designated *dmrt1bY* or *DMY*, on the Y-chromosome was shown to be the master regulator of male development [18,19], similar to *Sry* in mammals. Interestingly, also in *Xenopus laevis* a W-specific duplicate of *dmrt1* was shown to participate in primary gonad development [20]. Because medaka *dmrt1bY* acts, like *Sry*, as a dominant male determiner [21], it is believed that it is functionally equivalent to the mammalian gene and might share many molecular features [22,23]. Although many of the early cellular and morphological events downstream of *Sry* have been characterized, as well as a number of genes involved in these processes (for review see [24-26]), little is known about the mode of action and the biological targets of *Sry* [27]. Interestingly, *dmrt1*, the ancestor of *dmrt1bY*, is one of these downstream effectors of *Sry*. Contrary to

the situation with *Sry*, it is totally unknown how in medaka *dmrt1bY* expression is regulated. As a prerequisite to elucidate the function of *dmrt1bY*, information on its expression regulation at the transcriptional level is required. Here, we found a feed back down-regulation of the *dmrt1bY* promoter. Also *dmrt1a*, the autosomal ancestor of *dmrt1bY*, is able to down-regulate transcription of its paralog. Interestingly we found clear evidence that the major *cis*-regulatory element, pre-existing within a new medaka-specific TE at the time of its insertion, was co-opted in order to confer to Dmrt1bY its specific expression pattern after gene duplication. This is the first experimental evidence supporting a role of TEs for transcriptional network rewiring in sub- and/or neo-functionalization of duplicated genes. Additionally, in the particular case of *dmrt1bY*, this contributed to create new hierarchies of sex determining genes.

Results

Sequence evolution of the *dmrt1bY* promoter

To obtain insights into the sequence evolution of the *cis*-regulatory region of the *dmrt1bY* gene on the Y-chromosome, we first compared its genomic region and that of its autosomal progenitor, the *dmrt1a* gene from linkage group 9 (LG9), with those of the available *dmrt1* orthologs from other teleosts (stickleback, Tetraodon, Fugu, zebrafish), chicken and human. This phylogenetic footprinting approach should point to the conservation of regulatory elements being putatively essential for vertebrate *Dmrt1* gene expression (Figure S1). Furthermore, it could possibly indicate *cis*-regulatory subfunctionalization between the medaka *dmrt1* paralogs as observed for other pairs of duplicated genes with spatio-temporal expression divergence [28,29]. However, our VISTA plots (Figure S1) did not reveal sequence conservation in the promoter regions of neither *dmrt1bY* nor *dmrt1a* with other vertebrates except for stretches corresponding to the teleost *MHCL* gene, which are pseudogenes in both medaka *dmrt1* 5′ regions [30]. Conserved non-coding elements were also not found between the other vertebrate sequences suggesting that the regulatory regions of vertebrate *Dmrt1* orthologs diverged strongly despite their conserved position in the sex determination cascade. High turn-over of *cis*-regulatory regions in the face of conserved expression is commonly found for vertebrate genes [31].

However, longer stretches of conservation between promoter regions of *dmrt1bY* and *dmrt1a* in medaka were evident (Figure S1). Thus, we compared in more detail the promoter regions of the medaka *dmrt1* paralogs upstream of the transcriptional start site to the last exons of their upstream gene, *KIAA00172*, which is a pseudogene on the Y chromosome but functional on the autosomal LG9 [30] (Figure 1A). This region spans around 9 Kb on the Y chromosome but only around 6 Kb on autosomal LG9.

In the upstream sequence of *dmrt1* paralogs, five regions contribute to length divergence between autosome and Y chromosome (Table 1, Figure 1A, Figure S1 and Figure S2). Region I located 69 bp upstream of the transcriptional start site of *dmrt1bY* is over 2 Kb in length and absent from *dmrt1a*. Similarly, regions II-IV further upstream are only found on the Y chromosome but not on the autosome.

Region V, in contrast, is missing from the Y chromosome but present on the autosome. This region contains two exons of the *KIAA0172* gene and obviously has been lost during the pseudogenization of the Y chromosomal *KIAA0172* copy after the duplication of the *dmrt1* region [30].

Region III is directly adjacent to the *MHCL* pseudogenes [30,32] present in both *dmrt1* promoters and a stretch of sequence similarity with other teleost *MHCL* orthologs is found within

Figure 1. Comparative analysis of the *dmrt1bY* promoter and its transcription factor binding sites. (A) The analyzed promoter region of *dmrt1bY* in comparison to its *dmrt1a* paralog. Length differences between the promoters are based on regions I–IV, of which three (I, II, IV) have been added to the *dmrt1bY* promoter after duplication, while two others have been lost from the *dmrt1bY* promoter (*KIAA0172* region V) or from the *dmrt1a* promoter (*MHCLp* region III), respectively. Bold dashed lines indicate cutting sites for transcriptional regulation analyses. Region I contains a putative *Izanagi* DNA transposons (repeat 1), into which a *Rex1* element (repeat 2) was inserted secondarily. The upstream part of split repeat 1 (repeat 1b) in the *dmrt1bY* promoter contains multiple Sox5 and Pax2 binding sites as well as a Dmrt1 binding site. Dark green indicates coding sequence of genes and pseudogenes, light green indicates their untranslated regions. (B) Alignment of the Y chromosomal repeat 1b with 17 exemplary repeat copies in the medaka genome. Dots indicate conserved sites. The Dmrt1 binding site is perfectly conserved suggesting that it is an integral part of repeat 1 elements. All 28 copies of repeat 1b in medaka with the Dmrt1 binding sites are listed in Table S1.
doi:10.1371/journal.pgen.1000844.g001

region III on the Y chromosome (Figure S1). Furthermore, region III is present only once in the medaka genome and does not constitute a repetitive element according to RepeatMasker analysis. Thus, region III seems to have been lost from the autosomal *dmrt1a* region after duplication, but has been kept on the Y chromosome.

Next, we further characterized the additional regions I, II and IV for the presence of repetitive sequences. As each of these three regions is present in multiple copies in the medaka genome (Table 1), they constitute repetitive sequences that were rather added to the Y chromosomal region than lost from the autosome.

Each repeat element is only present once in the analyzed section of the *dmrt1bY* region and is often found in poorly assembled regions of the medaka genome emphasizing their repetitive character. BLAST searches in other teleost genomes failed to find the repeat elements identified here in other species suggesting that they are specific to the medaka lineage.

Particularly, region I is subdivided into three parts with a non-LTR retrotransposable *Rex1* element of the LINE family (class I transposable elements) as middle segment ("repeat 2") (Table 1).

The surrounding parts ("repeat 1a", "repeat 1b") also represent repetitive sequences with multiple copies in the medaka genome.

Table 1. Characterization of regions contributing to length differences between *dmrt1* upstream sequences.

Region	Absent from	Repeat/Gene	Length (bp)	TF binding sites	Genomic copies[b]
region I	*dmrt1a*		2,348		
		repeat 1 (*Izanagi*)[a]	1,316		13
		repeat 1a	440	Pax2, HMG-A	
		repeat 1b	876	Sox5 (7x), Pax2 (2x), **Dmrt1**	
		repeat 2 (*Rex 1*)[a]	1,024	Sox5, Pax2, Est Rec, Sox9 (2x), Prog Rec, And Rec	14
region II	*dmrt1a*	**repeat 3**	315	-	49
region III	*dmrt1a*	*MHCLp*	598	Sox9, HMG-P1, WT1	1
region IV	*dmrt1a*	**repeat 4**	496	And Rec (2x), SF1, Pax2	68
region V	*dmrt1bY*	*KIAA0172*	728	HGM-A, HGM-P1	1

Abbreviations: TF: transcription factor.
[a]Repeat 2 insertion splits repeat 1 into repeat 1a and repeat 1b.
[b]Copy numbers in the medaka genome assembly (version HdrR, Oct 2005) estimated by BLASTN searches with ≥85% sequence identity over ≥85% of query length.
doi:10.1371/journal.pgen.1000844.t001

These two repeat regions are found side by side in other regions of the genome. Thus, they together build a larger repeat element ("repeat 1") into which repeat 2 was inserted (see below). Repeat 1 has a length of 1316 bp and is characterized by 27 bp terminal inverted repeats (TIRs) (5′-CAATGAGTTATATCACTAGAG-GAGACA-3′) assigning it to DNA transposons (class II transposable elements). However, it does not contain a transposase gene or any other open reading frame and thus constitutes a non-autonomous class II element. Only few diagnostic motifs are available to classify such elements [33]. Repeat 1 in the *dmrt1bY* promoter has a 8 bp target site duplication (5′- GTGTGGCT-3′) and other copies of this element in the medaka genome have target site duplications of the same length. Repeat 1 is found in multiple copies in the medaka genome (Table 1 and Table S1), which generally have target site duplications. This points to an active state of repeat 1 in the medaka genome.

From the consensus sequence of the multiple repeat 1 elements in the medaka genome, a THAP protein domain composed of three putative exons was deduced (Figure S2 and Figure S3). In the repeat 1 element in the *dmrt1bY* promoter, the second putative exon of the THAP domain has been disrupted by the insertion of the repeat element (Figure S2 and Figure S3). The THAP domain is a DNA-binding zinc finger motif present in the *P* element transposases from *Drosophila* [34]. Furthermore, the terminal motif of repeat 1 is similar to the consensus sequence for the *P* element superfamily of DNA transposons (5′-YARNG-3′) [7]. Thus, we conclude that we have identified a new, medaka-specific non-autonomous *P* element element that we term *Izanagi* (named after an ancient Japanese deity, "*the male who invites*"; for etymology see Text S1).

Vertebrate mobile DNA transposons of the *P* element family have been only found so far in zebrafish [35,36]. However, the THAP domain has been recurrently recruited from domesticated *P* elements during chordate evolution [37]. In the *Izanagi* family, the THAP domain is degenerated and, in the case of repeat 1, has been additionally disrupted by the repeat 2 insertion.

Region II ("repeat 3") and region IV ("repeat 4") also have multiple copies in the medaka genome (Table 1). They do not contain open reading frames and, like repeat 1, they also lack similarity to known transposable elements. Furthermore, target site duplication or other diagnostic features could not be recognized preventing further classification as putative transposable elements.

Identification of putative transcription factor binding sites within *dmrt1bY* promoter and transcriptional activity in different cell lines

The sequence of the medaka *dmrt1bY* promoter region (9.107 Kb) was next analyzed for the presence of putative transcription factor binding sites using the MatInspector program (Figure 1A and Figure S4 and Table 1). Most interestingly, the *Izanagi* element is characterized by an overrepresentation of putative binding sites for Sox5 (Figure 1 and Figure S4). In this region seven Sox5 binding sites are present while random prediction would expect 15 times less (only 0.46 sites; MatInspector). This, together with the fact that Sox5 expression has been correlated with direct *dmrt1* promoter down-regulation in zebrafish [38] suggests that region to be of primary interest for medaka Dmrt1bY transcriptional regulation, but remains to be investigated for the proposed functional role of Sox5.

Additionally, the 9 Kb *dmrt1bY* promoter region contains several other putative transcription factor binding sites such as Pax2, HMG-box protein 1, HMG-A, Sox9, WT1 and SF1 binding sites that are reasonable candidates for gonadal-specific transcriptional regulation (Figure 1A and Figure S4 and Table 1). Several of them are conserved with the *dmrt1a* promoter (Figure S4) and might be essentially required for *dmrt1* expression.

To evaluate the mechanisms regulating *dmrt1bY* transcription, a portion of the medaka gene from +117 bp to −8990 bp of the transcriptional start site was cloned upstream of the *Gaussia* luciferase gene (pBSII-ISceI::9 Kb Dmrt1bY prom::GLuc) and the activity of the promoter was measured in a variety of cell types using transient transfection analysis. Sequential deletions of the 9 Kb promoter were generated from pBSII-ISceI::9 Kb Dmrt1bY prom::GLuc. In all three cell types basal promoter activity was detectable when using the 3 Kb proximal region (Figure S5). In fibroblast cell lines (*Xiphophorus* A2 and medaka HN2), but not in Sertoli TM4 cells, a dramatic drop in promoter activity was observed when the region from bp −2985 to −6207 was added (Figure S5). Similarly, the same decrease of promoter activity was apparent in Sertoli TM4 cells when the bp −6207 to −8996 region was additionally inserted (Figure S5). This indicates the possible presence of Sertoli cell specific transcriptional repressing sequence(s) within the most distal part of the *dmrt1bY* promoter. The most proximal part of the promoter always accounted for the basal activity in all the cell lines tested. Interestingly, two adjacent

binding sites for Steroidogenic factor 1 (Sf1) are located at positions −5933 and −5524 (Figure S4). Being specifically expressed in Sertoli -and Leydig- cells, it is tempting to assume that the presence of these two distinct SF-1 binding sites nested in this −3 to −6 Kb fragment is accounting for this difference. A similar situation has been shown for the porcine *Sry* promoter for which SF-1 transactivation occurs at two SF1 binding sites [39].

A unique Dmrt1 binding site is present in medaka *dmrt1bY* but not in *dmrt1* promoter

Using the vertebrate Dmrt1 binding site matrix [40], different *dmrt1* promoters -including medaka *dmrt1a* and *dmrt1bY*- (up to 9 KB upstream the ORF) were scanned for such target site sequences. A unique and robust Dmrt1 binding site of high prediction probability was found only in the medaka *dmrt1bY* promoter (CTGCAACAATGCATT; weight: 8.5, pValue: 1.0 e-05, lnPval:−11.492) (Figure 1A and Figures S2, S3, S4) but not in the *dmrt1a* promoter (lower threshold set to 0). Interestingly, this predicted Dmrt1 binding site is nested within the above newly described *Oryzias latipes Izanagi* element in the proximal active part of *dmrt1bY* promoter (Figure 1A and Figure S5). The medaka putative Dmrt1 binding site is present at position −2132 within repeat 1b in close proximity to the Sox5 binding site-rich region (Figure 1A and Figure S4). We first asked about the origin of this Dmrt1 binding site. It might have either evolved *de novo* from sequence provided by repeat 1b or been an integral part of such repeats and then was inserted into the *dmrt1bY* promoter after duplication. We therefore blasted the region approximately 300 bp up-and downstream of the Dmrt1 binding site to the medaka genome and aligned the obtained repeat sequences (Figure 1B). In total, we identified 28 elements that are highly similar to repeat 1b and that contain the same Dmrt1 binding site found in the *dmrt1bY* promoter (Table S1). Furthermore, the predicted Dmrt1 binding site is present in the derived *Izanagi* consensus sequence. Hence, this putative Dmrt1 binding site is a regular and conserved part of the *Izanagi* transposon family.

Timing of the *Izanagi* element insertion into the dmrt1bY promoter

Given that the Dmrt1 binding site donated to the *dmrt1bY* promoter by the *Izanagi* element has been important for the evolution of *dmrt1bY* function within the sex determining cascade, we asked about the timing of the *Izanagi* insertion in relation to the duplication of the medaka *dmrt1* genes. The *dmrt1* gene duplication occurred in a common ancestor of medaka (*O. latipes*), *O. curvinotus* and *O. luzonensis* around 10 million years ago [41].

First, we estimated the sequence divergence between repeat 1 from the *dmrt1bY* promoter and the *Izanagi* element consensus and mapped it onto a linearized neighbour joining (NJ) tree of *dmrt1* genes from the genus *Oryzias*, which was based on neutral sites only (third codon positions). This analysis showed that the repeat 1 insertion occurred after the split from *O. mekongensis* but before the divergence of medaka, *O. curvinotus* and *O. luzonensis* (Figure S6A). This is exactly the branch on which the *dmrt1* duplication occurred. We also estimated the *dmrt1* duplication by the same method. There has to be a note of caution with dating the age of the *dmrt1* duplication due to the enhanced rate of molecular evolution of *dmrt1bY* after duplication [41]. Nevertheless, based on sequence divergence data the insertion of repeat 1 is certainly estimated to be younger than the *dmrt1* duplication (Figure S6A). Using a different nuclear marker to date the divergence of the *Oryzias* species, the *tyrosinase a* gene, a similar result was obtained (Figure S6A). The analogous analysis for the secondary insertion of

repeat 2 into repeat 1, in contrast, revealed that this insertion is quite young and must have occurred in *Oryzias latipes*.

We conclude that our sequence divergence estimates are consistent with an insertion of repeat 1 and thereby of the Dmrt1 binding site shortly after the *dmrt1* duplication, supporting its importance for the evolution the Dmrt1bY sex determinator function.

Transcription of *dmrt1bY* is regulated by its own gene product and by that of its paralog

1-Dmrt1bY that down-regulates activity of its own promoter. Co-transfection analyses were used to examine the predicted interaction between medaka Dmrt1bY and its own promoter (Figure 2A). For this purpose, the proximal 2868 bp *dmrt1bY* promoter region containing the putative Dmrt1 binding site at position −2132 (see Figure 1 and Figure 2) fused to luciferase was used and co-transfected with different amounts of a plasmid expressing *dmrt1bY* (Figure 2A). In presence of *dmrt1bY* expressing plasmids *dmrt1bY* promoter activity was considerably reduced, up to 74%, in all cell types tested (*Mus musculus* Sertoli TM4, *Xiphophorus xiphidium* fibroblast A2 and *Oryzias latipes* spermatogonial (Sg3) and embryonic stem (MES1) cells) (Figure 2A). To confirm the possible direct interaction with the putative Dmrt1 target binding site, a *dmrt1bY* mutant promoter with a modified Dmrt1 target site was created (Figure 2B and Materials and Methods). When co-transfected with the *dmrt1bY* expressing plasmid, the activity of the mutant promoter was clearly increased (up to almost 5 fold) in comparison to the wild-type promoter (Figure 2B) whereas the mutant promoter did not reveal any significant regulation by Dmrt1bY (Figure S7).

2-Dmrt1a, the autosomal ancestor of Dmrt1bY, regulates the transcriptional activity of the *dmrt1bY* promoter. We next addressed the question of a possible cross-regulation of the Dmrt1a protein towards the *dmrt1bY* promoter. The above-described experiments employing Dmrt1bY were repeated, this time using the autosomal Dmrt1a. When the proximal 2868 bp *dmrt1bY* promoter region containing the putative Dmrt1 binding site fused to luciferase was co-transfected with a plasmid expressing Dmrt1a, *dmrt1bY* promoter activity was considerably reduced up to 92%- (Figure 3A and 3B). This reduction is higher than observed for *dmrt1bY* (ranging from −55% to 74%). Using the mutant *dmrt1bY* promoter revealed that removing the Dmrt1 target site was able to restore transcriptional activity (Figure 3C and 3D) in medaka MES1 and Sg3 cell lines.

3-Dmrt1bY and Dmrt1a both bind to the putative Dmrt1 response element within *dmrt1bY* promoter. Electrophoretic mobility shift assays (EMSAs) were performed to show the direct interaction of Dmrt1a and Dmrt1bY proteins within the target site in the *dmrt1bY* promoter (Figure 4). DNA binding assays using the *dmrt1bY* Dmrt1-target sequence and *in vitro* translated Dmrt1a or Dmrt1bY demonstrated that both proteins are indeed able to bind to the Dmrt1 target sequence (position −2132 bp) (Figure 4). Binding specificity was confirmed using a mutated Dmrt1 binding site as competitor (Figure 4).

Analysis of *dmrt1bY* expression *in vivo*

Thus far we could show feed back down-regulation of *dmrt1bY* and regulation by its paralog Dmrt1a *in vitro*. We next addressed whether this regulation indeed exists *in vivo*.

***In vivo* quantification of the 9Kb*dmrt1bY*promoter activity in transgenic fish indicates a strong Dmrt1a cross-regulation.** To get a first information of the *in vivo* *dmrt1bY* transcriptional regulation, a transgenic line where the *dmrt1bY* promoter drives dmrt1bY::GFP fusion protein expression
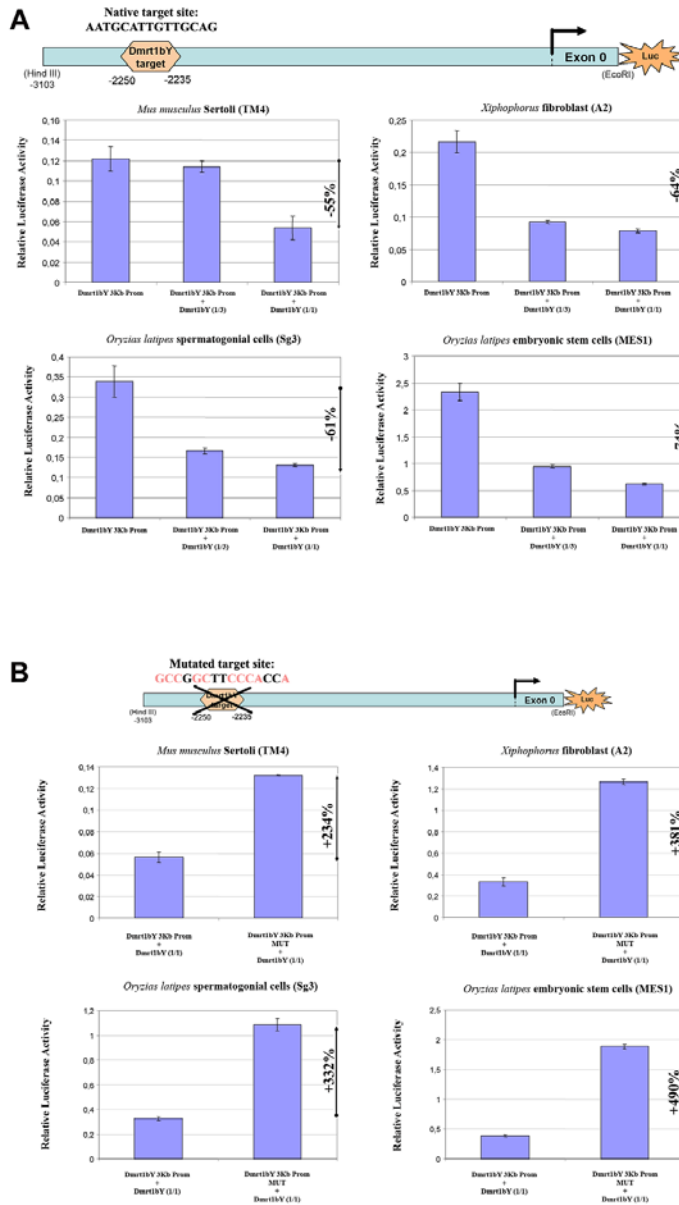
Figure 2. Transient-transfection analysis. (A) Transient-transfection analysis of proximal *dmrt1bY* promoter activity co-transfected in different ratios of a *dmrt1bY* expressing plasmid. The 3 Kb proximal *dmrt1bY* promoter construct was co-transfected with different amounts of *dmrt1bY*-expressing plasmid (1:3 and 1:1 ratios) in different cell lines. (B) Transient-transfection analysis of mutant proximal *dmrt1bY* promoter activity. In all the cell lines, when overexpressing Dmrt1bY, the 3 Kb mutant proximal *dmrt1bY* promoter construct (lacking the Dmrt1 binding site) shows higher activity compared to the "wild-type" construct containing the Dmrt1 target site. The data are presented as the firefly/Gaussia luciferase activity. Transfections were done three times; error bars represent the standard errors of the means.
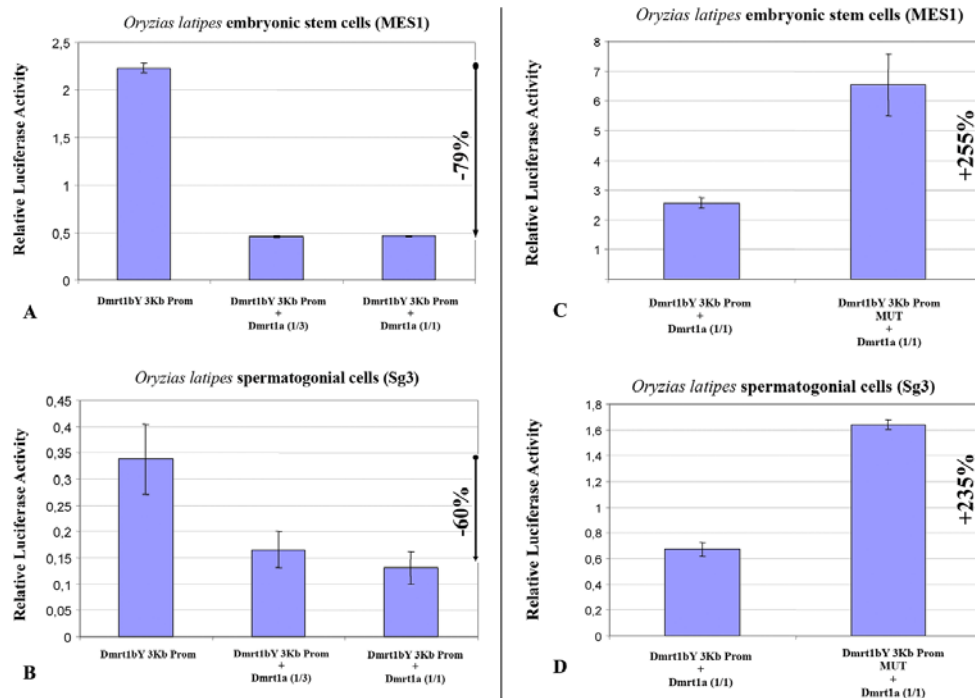doi:10.1371/journal.pgen.1000844.g002

Figure 3. Transient-transfection analysis of *dmrt1bY* promoter activity when co-transfected with different ratios of a Dmrt1a expressing plasmid. (A,B) The 3 Kb proximal *dmrt1bY* promoter construct was co-transfected with different amounts of *dmrt1a*-expressing plasmid (1:3 and 1:1 ratios). (C,D) The 3 Kb mutant proximal *dmrt1bY* promoter construct was co-transfected with different amounts of *dmrt1a*-expressing plasmid (1:3 and 1:1 ratios). The data are presented as the firefly/Gaussia luciferase activity. Transfections were done three times; error bars represent the standard errors of the means.
doi:10.1371/journal.pgen.1000844.g003

was established with the goal of quantifying gonadal *dmrt1bY* promoter activity in either Dmrt1a expressing or non-expressing tissues (Figure 5). These transgenic fish showed a strong correlation of higher gonadal *dmrt1bY* promoter activity (5.5 times more in average) in absence of *dmrt1a* expression (ovary) compared to the *dmrt1a* expressing (testes) background (Figure 5).

***In vivo* Dmrt1bY binding to the *Izanagi* Dmrt1 target site.** To assess *in vivo* Dmrt1bY interaction with its own promoter, two additional stable transgenic lines expressing either the full Dmrt1bY protein or a truncated form lacking the DNA binding domain, both fused to GFP, were created. The two lines were used for *in vivo* Tissue Chromatin ImmunoPrecipitation (Tissue-ChIP) on testis tissue using GFP antibody for immunoprecipitation. An up to 7-fold enrichment compared to the control confirmed the capacity of Dmrt1bY to bind not only to the Dmrt1 promoter-nested *Izanagi*-target site but also to the *Izanagi* Dmrt1bY-target site in general (Figure 6).

Expression domains of the two dmrt1 paralogs indicating cross-regulation during male gonad development *in vivo*. Stable transgenic lines expressing fluorescent reporter protein (GFP and/or mCherry) were established to monitor the expression dynamics of Dmrt1a or Dmrt1bY *in vivo*. Analysis of early

(10 to 30 35 dph) gonadal expression (Figure 7A) in two different (9KbDmrt1bYprom::GFP or 9KbDmrt1bYprom::mCherry) transgenic lines revealed identical fluorescent reporter protein expression in Sertoli cells (Figure 7C and 7D) as well as in interstitial tubule cells (Figure 7B). This exactly matches the protein expression pattern reported earlier from studies using a Dmrt1bY-specific antibody [42]. Later on, fluorescence declined in Sertoli cell (Figure 7E 7G to be compared to Figure 7H 7J). Noteworthy, corroborating the *in vitro* data, in double transgenic fish (9KbDmrt1bYprom::mCherry and BACdmrt1a::GFP) the decline of *dmrt1bY* promoter driven fluorescence was paralleled by a rise of *dmrt1a* promoter expression in Sertoli cells (Figure 7E 7G to be compared to Figure 7I and 7J). In fully mature testes (over 45 50 dph), *dmrt1bY* promoter expression remained only in few Sertoli cells scattered around the germ cells (Figure 7H) while the *dmrt1a* promoter was now predominantly expressed (Figure 7I and 7J).

Discussion

Sex determination involves a complex hierarchy of genes. Expression screen analyses have resulted in hundreds of candidate
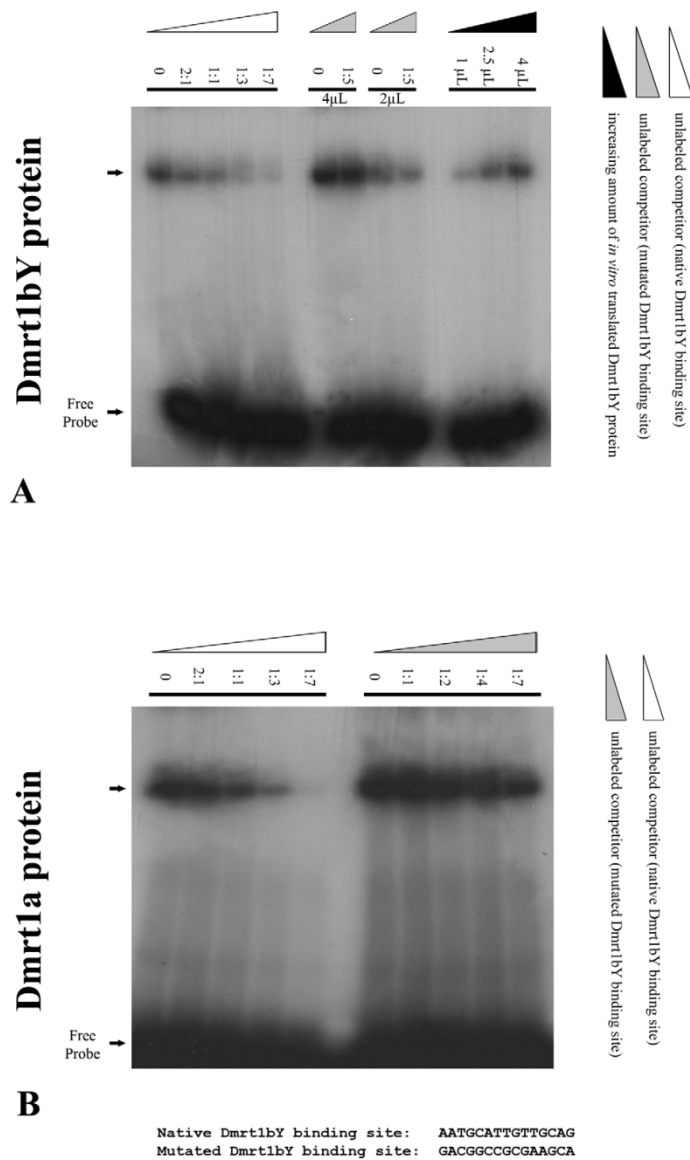
Transcriptional Rewiring of Duplicated Genes

Figure 4. Electrophoretic Mobility Shift Analysis (EMSA) of *in vitro* **translated Dmrt1bY protein interaction with the Dmrt1 binding target derived from its own promoter.** Gel mobility shift using increasing amounts of either *in vitro* translated Dmrt1bY or Dmrt1a proteins to shift a constant amount of radiolabelled *dmrt1* probe. Binding reactions were resolved on a 5% polyacrylamide gel. (A) *In vitro* translated Dmrt1bY protein was incubated with radiolabelled Dmrt1bY target sequence as a probe, and non-radiolabelled probe was used as a competitor. (B) *In vitro* translated Dmrt1a protein was incubated with radiolabelled Dmrt1bY target sequence as a probe, and non-radiolabelled control (non-specific) probe was used as a competitor.
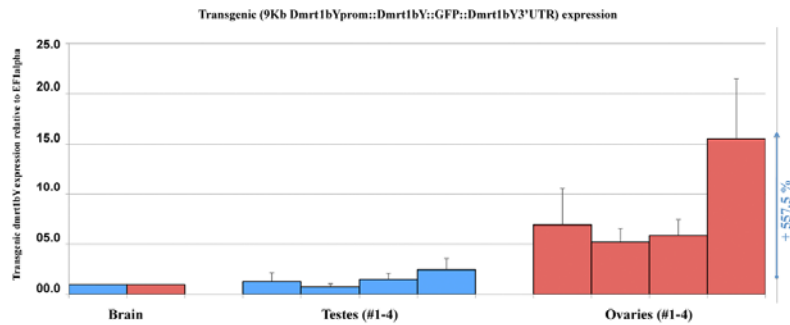
doi:10.1371/journal.pgen.1000844.g004

Figure 5. _In vivo_ quantification of the 9KbDmrt1bYpromoter activity in transgenic fish. Real-time PCR quantification of the 9KbDmrt1bYpromoter activity in two different gonadal backgrounds either expressing dmrt1a (testes, #1–4) or not (ovaries, #1–4) reveals higher activity (+557.5% expression) in absence of _dmrt1a_ expression. _Dmrt1bY_ expression is relative to elongation factor 1 alpha (ef1 alpha) and normalised to brain background expression (set to 1).
doi:10.1371/journal.pgen.1000844.g005

genes that show sex-specific expression pattern. However it has been difficult to place these genes into a network of gene regulation and function. Nevertheless, several genes encoding for transcription factors, with specific temporal and spatial expression patterns during early gonad induction, have been suggested to participate in this process. Among them, from _C. elegans_ to mammals, genetic evidence has suggested that the _dmrt1_ gene is an important regulator of male development at a downstream position of the regulatory network. In medaka, a duplicated copy of _dmrt1_ has acquired the upstream position of the sex-determining cascade. The analysis presented here provides evidences that this evolutionary novelty, which is predicted to require a rewiring of the regulatory network is brought about by co-option of "ready-to-use" pre-existing _cis_-regulatory elements carried by transposing elements. We could show that the master sex determining gene of medaka, _dmrt1bY_, is able to bind to one of these elements in its own promoter. This binding leads to a significant repression of its own transcription.

During early stages when the primordial gonad is formed, _dmrt1bY_ is exclusively expressed and exerts its sex determining function [18]. The _dmrt1a_ gene, with its proposed specification and maintenance function for the Sertoli cells, is expressed only when the testes are in the process of differentiation. Notably, the master sex determinator gene _dmrt1bY_, continues to be expressed. In adult testes, where both paralogs have been shown to be expressed, the predominant expression of _dmrt1a_ compared to _dmrt1bY_ (50 fold higher; [43]) argues for a downregulation of _dmrt1bY_. Although additional post-transcriptional mechanisms accounting for _dmrt1bY_ expression regulation, involving the 3′ UTR [44], have been shown to be essential for spatial expression pattern in the embryo and restricted expression to the gonad in adult fish, the data presented here indicate that a feed back auto-regulation of _dmrt1bY_ promoter activity and trans-regulation by its paralog Dmrt1a is a key mechanism of _dmrt1bY_ transcriptional tuning (Figure 8).

With respect to the evolutionary history of the two _dmrt1_ genes in medaka, it is of note that the newly generated paralog _dmrt1bY_, independently of any functional considerations, is kept back under tight transcriptional regulation of the ancestral _dmrt1a_ gene. Consequently this avoids any kind of expression pattern redundancy in testes after their development is initiated and could then be a reasonable way of preserving both genes from any purification/degeneration processes after duplication, thus favouring a subsequent sub-neo-functionalization.

So far no putative Dmrt1 binding site could be observed within the more than 10 Kb upstream medaka _dmrt1a_ sequence inspected. Similarly such Dmrt1 target sites are absent from the zebrafish, fugu, stickleback, mouse or human 10 kB upstream _dmrt1_ promoter regions. This together with the apparent loss of Dmrt1 canonical _cis_-regulatory sequences (such as Gata4) indicates a particular transcriptional context acquired by _dmrt1bY_ during its evolution towards becoming a novel master sex determination gene.

It was previously reported that multiple TEs inserted into the Y-specific region on medaka LG1 [30]. Interestingly, our study revealed that the _cis_-regulatory element containing the Dmrt1 binding site, pre-existing within the _Izanagi_ element at the time of its insertion, was co-opted in order to confer _dmrt1bY_ its specific expression pattern after gene duplication around 10 million years ago [19,41]. This fact has interesting evolutionary implications, since TEs are probably the most dynamic part of the genome. Dmrt1 possibly also regulates other genes in the proximity of _Izanagi_ elements via the Dmrt1 binding site (Table S1).

In the context of gene duplication and its correlated process of sub-/neo- functionalization (see [45 47] for review), the contribution of TEs to the remodelling of the sex determination cascade (see [12,48] for review) is of prime interest. The case reported here for the medaka-specific _Izanagi_ element bringing in a novel regulatory element into the _dmrt1bY_ promoter is -at least to our knowledge- the first example showing that TEs not only change/rewire the expression of existing genes but surely lead to the creation of new regulatory hierarchies within recently duplicated genes. The present case is even more interesting since this new TE-derived TFBS confers transcriptional control from the ancestral gene against the duplicate and allows the _dmrt1bY_ gene to take an upstream position in the sex determination cascade without excluding its _dmrt1_ ancestor from a role in sexual development.

This supports a role of TEs for transcriptional network rewiring in sub- and/or neo- functionalization of duplicated genes in creating new hierarchies of sex determining genes.
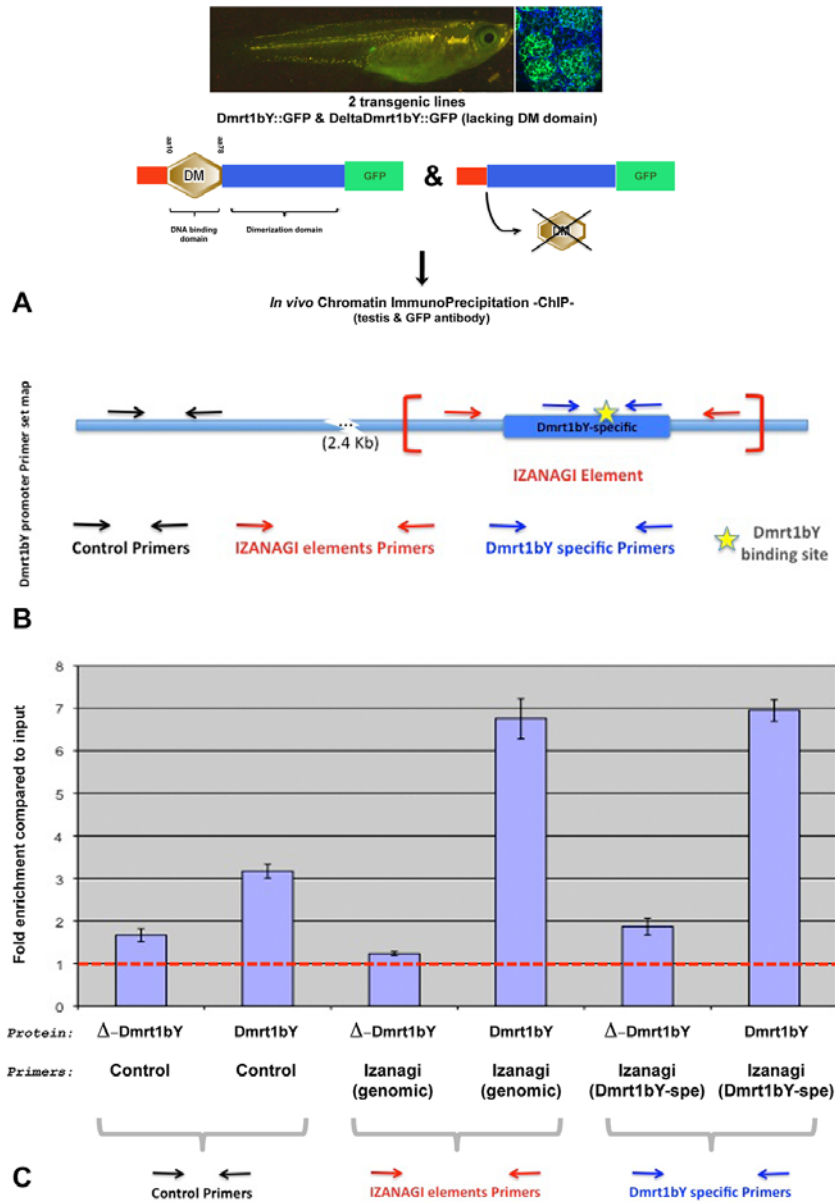
Figure 6. Tissue Chromatin immunoprecipitation (Tissue–ChIP) of Dmrt1bY binding to the *Izanagi*-nested Dmrt1 target site. Chromatin immunoprecipitation using both Dmrt1bY::GFP and deltaDmrt1bY::GFP transgenic lines respectively expressing either Dmrt1bY or a control truncated Dmrt1bY (delta DM form lacking the DNA binding domain) fused to GFP revealed specific *in vivo* Dmrt1bY protein affinity to the *Izanagi*-nested *dmrt1* target site, including the one described within *dmrt1bY* promoter. (A) Transgenic lines established for *in vivo* tissue–ChIP. (B) *Dmrt1bY* promoter primer sets map. (C) Specific enrichment of *Izanagi*-nested Dmrt1 binding sites subsequent to *in vivo* Dmrt1bY immunoprecipitation.
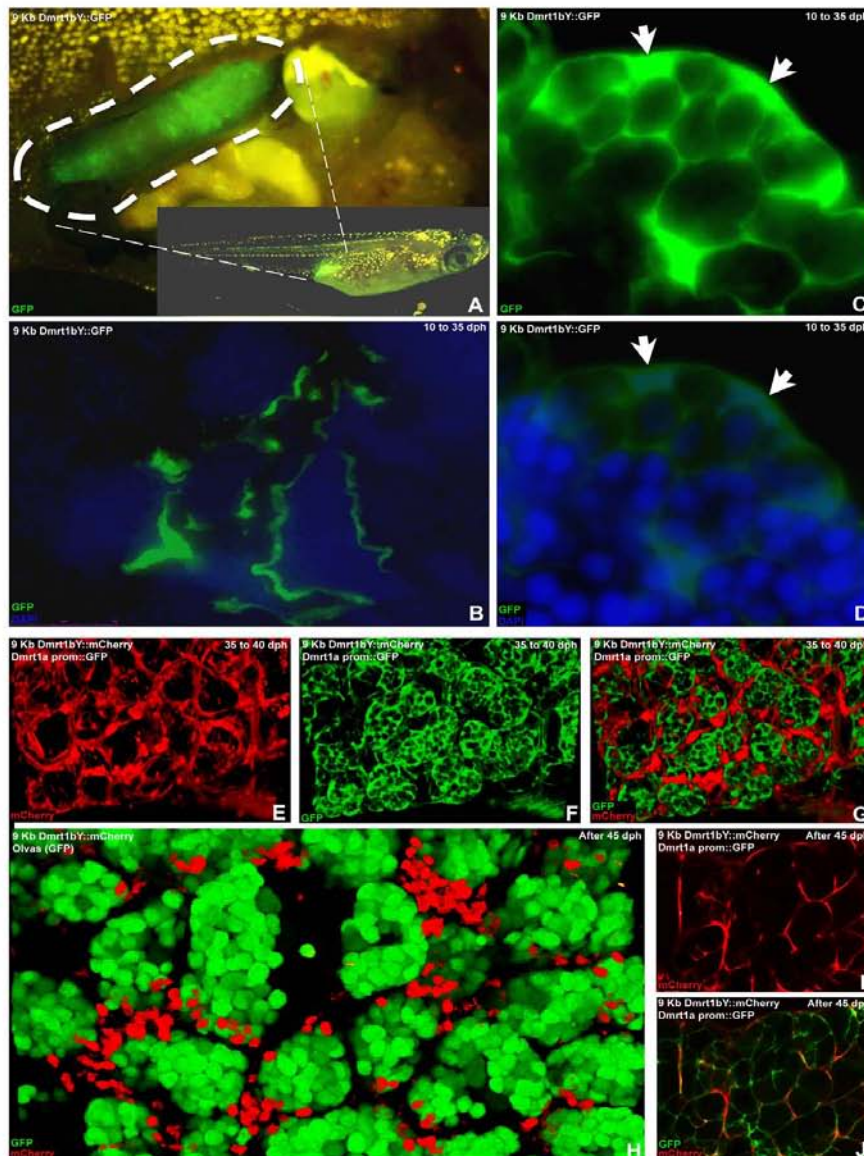doi:10.1371/journal.pgen.1000844.g006

Figure 7. *In vivo* **visualization of expression of the two medaka Dmrt1 paralogs.** (A) Testis-specific GFP expression in 9KbDmrt1bYprom::GFP transgenic fish. (B) From testis formation (10 dph) up to adulthood, in 9KbDmrt1bYprom::GFP transgenic fish, robust testicular GFP expression is persistently noticeable in the epithelial cells of the intratesticular efferent duct. (C,D) Concomitantly, in agreement with the endogenous *dmrt1bY* expression, from 10 dph up to 30–35 dph strong specific GFP fluorescence is also detected in Sertoli cells. (E–G,I,J) By 35 dph, Sertoli cell-specific decline in fluorescence (mCherry) could be observed (E,I,H). In double transgenic fish (9KbDmrt1bYprom::mCherry and BACdmrt1a::GFP) this 9KbDmrt1bYprom-driven mCherry decline in expression is balanced by the rise of *dmrt1a* expression in Sertoli and germ cells (GFP in F,G,J). (H–J) In fully mature testes (after 45–50 dph), 9KbDmrt1bYprom-driven mCherry expression remains in scattered Sertoli cells around the germ cells (GFP in N) while Dmrt1a is now predominantly expressed in Sertoli cells (J).
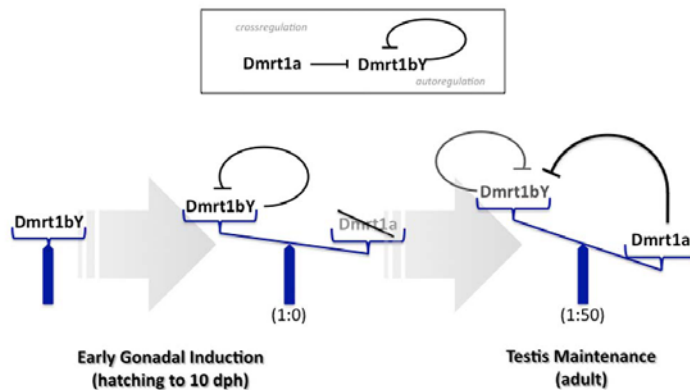doi:10.1371/journal.pgen.1000844.g007

Figure 8. Model for feedback and cross-regulation of the medaka dmrt1 paralogs. During sex determination stages only *dmrt1bY* is expressed and *dmrt1a* is off. Hence, the sex determining function of *dmrt1bY* is exerted. In adult testes, both paralogs are expressed notably in Sertoli cells, but the autorepression of the *dmrt1bY* promoter by its own gene product and the cross-regulation by Dmrt1a lead to a predominant expression of *dmrt1a* compared to *dmrt1bY* (appox. 50 fold).
doi:10.1371/journal.pgen.1000844.g008

Materials and Methods

Bioinformatic analyses

Comparative analysis of vertebrate *Dmrt1* genomic regions were performed with mVISTA at http://genome.lbl.gov/vista [49] using the Shuffle-LAGAN alignment program [50]. Medaka *dmrt1a* (LG9) and *dmrt1bY* (LG1) region sequences were obtained from [30], all other regions from the Ensembl Genome Browser (http://www.ensembl.org/; release 49, March 2008): stickleback groupXIII, scaf57; Fugu scaf4; Tetraodon chr12, scaf14966; zebrafish chr5, scaf463; chicken chrZ, supercontig194; human chr9, supercontig NT_008413.

Screens for repetitive elements were performed with Repeat-Masker (http://www.repeatmasker.org/). Additional copies of repeat elements and their genomic environment in the medaka genome (version HdrR, Oct 2005) were identified with BLASTN with >85% sequence identity over >85% of query length (Table 1). Alignments of repeat elements were obtained with CLUSTALW as implemented in BioEdit [51] followed by manual improvement. 50% threshold frequency was used for inclusion in repeat consensus sequences. The putative THAP domain found in the *Izanagi* consensus was identified by comparison to the PFAM database (http://pfam.sanger.ac.uk/).

Transcription factor binding sites were determined using MatInspector of the Genomatix portal (http://www.genomatix.de/). Binding sites for Dmrt1 in different genomes were identified using the matrix provided by [40] together with the Regulatory Sequence Analysis Tools portal; RSat (http://rsat.ulb.ac.be/rsat/). MEGA4 [52] was used to estimate sequence divergence between repeat 1 and the *Izanagi* element consensus (0.034 +− 0.005) as well as between repeat 2 and the *Rex1* element consensus (0.010 +− 0.003) using the Kimura-2-parameter model. Linearized neighbor-joining trees of *dmrt1* and *tyrosinase a* gene were obtained as described in ref. [41], with the only exception that they were based on third codon positions only. Other models of sequence evolution gave similar results. Accession numbers are given in Figure S6.

Cloning of the 9.107 Kb 5′ flanking sequence of medaka Dmrt1bY and plasmid constructs

For promoter analysis, a 9107 bp fragment upstream of the Dmrt1bY open reading frame (ORF) was isolated by restriction enzyme digestion (*XhoI/EcoRI*) from BAC clone Mn0113N21 [30], was cloned into pBSII-ISceI plasmid (pBSII-ISceI::9 Kb Dmrt1bY prom. plasmid). Subsequently, *Gaussia* luciferase gene from pGLuc-basic (New England Biolabs) plasmid was inserted between *EcoRI* and *NotI* sites of pBSII-ISceI::9 Kb Dmrt1bY prom (pBSII-ISceI::9 Kb Dmrt1bY prom::GLuc plasmid). pBSII-ISceI::3 Kb Dmrt1bY prom::GLuc and pBSII-ISceI::6 Kb Dmrt1bY prom::-GLuc plasmids were constructed the same way removing 5′ fragments of the 9107 bp Dmrt1bY promoter region using *Eco47III* and *HindIII* restriction enzyme digestion respectively and re-ligation.

Mutation of the Dmrt1bY binding site was performed by PCR in the context of pBSII-ISceI::3 Kb Dmrt1bY prom::GLuc plasmid (native form: AATGCATTGTTGCAG; mutated form: GCCGGCTTCCCACCA). All PCR-obtained fragments were sequenced.

To generate plasmids for *in vitro* transcription, full-length cDNAs encoding medaka *dmrt1a* or *dmrt1bY* were subcloned into *EcoRI/NotI* digested pRN3 plasmid [53].

For establishment of transgenic lines, either GFP or mCherry open reading frames were inserted between *EcoRI* and *NotI* sites of pBSII-ISceI::9 Kb Dmrt1bY prom (pBSII-ISceI::9 Kb Dmrt1bY prom::GFP or mCherry plasmids respectively). GFP fusion protein vector (dmrt1bY::GFP and deltadmrt1bY::GFP) were constructed as described in [43].

Cell lines, cell transfection, and Luciferase assay

Mouse TM4 Sertoli cells, *Xiphophorus* embryonic epithelial A2 cells, and medaka spermatogonial (Sg3) and fibroblast like (HN2) cells were cultured as described [54,55,56,57]. Cells were grown to 80% confluency in 6-well plates and transfected with 5 µg expression vector using FuGene (Roche) or Lipofectamine (Invitrogen) reagents as described by the manufacturers.

Gaussia luciferase activity was quantified using the Luciferase Reporter Assay System from Promega and normalized against co-tranfected firefly luciferase expressing plasmid (ptkLUC+; [58]). When DNA amounts transfected are expressed as a ratio, the total amount of expression vector remained constant (5 µg) by filling in the reaction with empty vector. Experiments for which error bars are shown result from at least three replicates and error bars represent the standard error of the mean.

Electrophoretic Mobility Shift Assays (EMSA)

(Dmrt1bY-Trgt) 5′-AGCTTAATGCATTGTTGCAGAGCT-3′, (Competitor) 5′-AGCTGACGGCCGCGAAGCAAGCT and respective complements were annealed by heating to 90°C for five minutes in 1X T4 PolyNucleotide Kinase (PNK) buffer (70 mM Tris-HCl (pH 7.6), 10 mM MgCl$_2$, 5 mM dithiothreitol); slow-cooled to 50°C; held at that temperature for 5 minutes and then cooled to room temperature. For radioactive labelling 50 pmol of the duplex 5′ termini were used together with 50 pmol of gamma-[^{32}P]-ATP and 20 units of T4 PNK in 1X adjusted T4 PNK buffer and incubated for 20 minutes at 37°C. Unincorporated nucleo-tides were removed through a Sephadex G-50 spin column.

For producing Dmrt1a and Dmrt1bY proteins, pRN3::Dmrt1a or pRN3::Dmrt1bY plasmids were linearized using *KpnI* and then *in vitro* transcribed using mMessage mMachine kit (Ambion). Finally, Dmrt1a or Dmrt1bY proteins were *in vitro* translated using Ambion's Retic Lysate Kit from the previously *in vitro* transcribed capped *Dmrt1a* or *Dmrt1bY* RNAs.

DNA binding reaction contained 10 mMTris-HCl (pH 7.9), 100 mM KCl, 10% glycerol, 5 mM MgCl$_2$, 1 µg torula rRNA, 0.075% Triton X-100, 1 mM DTT, 1 µg BSA, 0.5 ng radiola-beled duplex probe and 2 or 4 µL *in vitro* translation mix in a total volume of 20 µL. 1/10 volume heparin (50 mg/mL) was added just before loading the binding reaction. For control reticulocyte lysate alone together with radiolabeled duplex probe was used and did not result in any shift (data not shown). Binding reactions were performed on ice for ten minutes and complexes were resolved on a 5% native acrylamide (37.5:1) gel in 0.5 X TBE and then directly subjected to autoradiography.

Expression analyses

Total RNA was extracted from 9KbDmrt1bYprom::Dmrt1-bY::GFP::Dmrt1bY3′UTR transgenic fish (Carbio genetic back-ground) using the TRIZOL reagent (Invitrogen) according to the supplier's recommendation. After DNase treatment, reverse transcription was done with 2 micrograms total RNA using RevertAid First Strand Synthesis kit (Fermentas) and random primers. Real-time quantitative PCR was carried out with SYBR Green reagents and amplifications were detected with an i-Cycler (Biorad). All results are averages of at least two independent RT reactions and 2 5 PCR reactions from each RT reaction using each time third set of primer combination (DMTYk: 5′-CC-TTCTTCCCCAGCAGCCT-3′/eGFP3: 5′-AGTCGTGCTGC-TTCATGTGGTC-3′; DMTYa2: 5′-CGACTCCATGAGCAG-TGAAA-3′/eGFP3: 5′-AGTCGTGCTGCTTCATGTGGTC-3′; DMTYa2: 5′-CGACTCCATGAGCAGTGAAA-3′/eGFP5: 5′-GAACTTCAGGGTCAGCTTGC-3′. Error bars represent the standard deviation of the mean. Relative expression levels (according to the equation 2 DeltaCT) were calculated after correction of expression of elongation factor 1 alpha (*elf1alpha*) and brain expression was set to 1 as a reference.

In vivo Chromatin Immunoprecipitation

For *in vivo* chromatin immunoprecipitation, the EpiQuik Tissue Chromatin Immunoprecipitation kit (Epigentek) was utilized according to the manufacturers instructions, using testis tissue samples either from dmrt1bY::GFP or deltadmrt1bY::GFP transgenic fish (20 testes for each) and GFP antibody (Upstate) for immunoprecipitation. After immunoprecipitation [(*Izanagi* element Dmrt1bYspeF003) 5′-TCCGGTCTCTCCGGCGTGT-GG-3′/(*Izanagi* element *Dmrt1bYspeR00*) 5′-TTGTAAGAGGA-CCTGCAACAATG-3′; (*Izanagi* element F01) 5′-CTATCTTG-GTGAGGTCGACGATGCC-3′/(*Izanagi* element R01) 5′-AAT-TTAAATTACATGTCAAAGAGGTC-3′; (Dmrt1bYCtrF04) 5′-GTTCTGACTTTCAGCGTCTCACCTG-3′/(Dmrt1bYCtrR04) 5′-GGTTCTGGTCCAAATCTGTCAGAAG-3′] primer sets were used for enrichment quantification by real-time PCR.

Transgenic fish lines

For the generation of stable transgenic lines the meganuclease protocol [59] was used. Briefly, approximately 15 20 pg of total vector DNA in a volume of 500 pl injection solution containing I-*Sce*I meganuclease was injected into the cytoplasm of one cell stage medaka embryos (Carbio strain). Adult F0 fish were mated to each other and the offspring was tested for the presence of the transgene by PCR from pooled hatchlings. Siblings from positive F1 fish were raised to adulthood and tested by PCR from dorsal fin clips as described [60].

Identically to the transgenic line expressing the Dmrt1bY protein fused to GFP [61] a second line lacking the Dmrt1bY DNA binding domain (DM-domain between aminoacids 10 and 78) was established. These two lines were used for *in vivo* Chromatin Immunoprecipitation. Similarly, for *in vivo* Dmrt1bY promoter activity quantification another transgenic line expressing a 9Kbdmrt1bYprom driven dmrt1bY::GFP fusion protein was created. Dmrt1a prom::GFP transgenic medaka was generated following the BAC transgenic method [62]. The BAC clone including dmrt1a genomic region, ola1-171C06 (NCBI accession numbers; DE071574 and DE071575) was obtained from NBRP. The followings were the primers to amplify EGFP fragments for homologous recombination into the BAC clone; Forward: 5′-tctgacatgagcaaggagaagcagggcaggccggttccggagggcccggcTCAACC-GGTCGCCACCATGG-3′ Reverse:5′-ttcagcgggagacacgaagccg-tggttccggcagcgggagcacttgggcatcGTCGACCAGTTGGTGATTT-TG-3′.

Supporting Information

Figure S1 mVISTA plots of vertebrate *Dmrt1* upstream regions. Medaka Y chromosomal *dmrt1bY* region (upper part) and autosomal *dmrt1a* region (LG9; lower part) are used as references. Regions I IV contribute to length differences between the medaka *dmrt1* upstream regions. Dark blue and green indicate exons of genes and pseudogenes, respectively, light blue and green untranslated regions. Red indicates conserved non-coding se-quences. Conservation of medaka *dmrt1* promoters with other vertebrates is restricted to the *MHCL* pseudogene regions.

Found at: doi:10.1371/journal.pgen.1000844.s001 (3.97 MB PDF)

Figure S2 Annotation of the *dmrt1bY* promoter. *KIAA0172p* and *MHCLbp* regions are green shaded, regions IV III and repeat 2 are grey shaded. The *Izanagi* element (repeat 1) is red shaded, its terminal inverted repeats are black shaded and the 8 bp target site duplication is underlined. The three identified putative THAP domain-encoding exons are pink shaded. The dmrt1bY exon 0 is blue shaded. Red lines mark border segments for the transcriptional regulation analysis ("3 Kb", "6 Kb", "9 Kb" promoter). See also Figure 1 and Figure S4.

Found at: doi:10.1371/journal.pgen.1000844.s002 (0.02 MB PDF)

Figure S3 Putative THAP domain in the *Izanagi* element. (A) Structure of the *Izanagi* element. Pink boxes indicate the three putative exons constituting the THAP domain are. The insertion of repeat 2 in the *dmrt1bY* promoter splitting repeat 1 into repeat 1b is indicated by the arrow. Note that the *Izanagi* element is shown here in reverse complement compared to the *dmrt1bY* promoter. (B) Alignment of the putative THAP protein domain from the *Izanagi* element consensus sequence with the THAP domain from the PFAM database. Identical essential residues are yellow shaded; other identical residues are blue shaded. + indicates similar residues.
Found at: doi:10.1371/journal.pgen.1000844.s003 (1.01 MB PDF)

Figure S4 Repeat elements and transcription factor binding sites in the *dmrt1bY* promoter. The three segments correspond to the regions used for transcriptional regulation analysis. Transcription factor binding sites conserved with the *dmrt1a* promoter are boxed. Of particular importance for transcriptional regulation of *dmrt1bY* might be the repeat 1b area (beige box) with multiple Sox5 and Pax2 binding sites, as well as a Dmrt1 binding site (red). Further upstream, two SF1 binding sites are located (red). For further characterization see Figure 1A and Table 1. Prog Rec: progesterone receptor; Est Rec: estrogen receptor; And Rec: androgen receptor binding sites.
Found at: doi:10.1371/journal.pgen.1000844.s004 (2.37 MB PDF)

Figure S5 Activity of *dmrt1bY* promoter deletion constructs in different cell lines. (A C) Various 5′-deletions mutants (3 Kb and 6 Kb) from pBSII-ISceI::9 Kb *dmrt1bY* prom::GLuc plasmid were transfected either into Mouse TM4 Sertoli, *Xiphophorus* embryonic epithelial A2 or medaka HN2 fibroblast like cells. Transfections were repeated three times; error bars represent the standard errors of the means.
Found at: doi:10.1371/journal.pgen.1000844.s005 (0.62 MB PDF)

Figure S6 Timing of repeat insertions into the *dmrt1bY* promoter. Linearized NJ trees for *dmrt1* (A) and *tyra* (B) genes based on third codon positions using the Kimura-2-parameter model are shown. The split between fugu and *Oryzias* species was set to 95 million years ago (MYA) [41]. The sequence divergence between repeats 1 and 2 and their consensus sequence, respectively, is indicated. The repeat 1 origin falls onto the branch, at which the *dmrt1* gene duplication has occurred [41] and is younger than the inferred *dmrt1* duplication period (blue). The repeat 2 insertion is very recent. Other models of sequence evolution gave similar results.
Found at: doi:10.1371/journal.pgen.1000844.s006 (2.49 MB PDF)

Figure S7 Transient transfection analysis of the Dmrt1bY promoter nested Dmrt1 binding site. Transcriptional activity of the mutant 3 Kb proximal Dmrt1bY promoter (mutated Dmrt1 binding site) was not significantly impaired while overexpressing dmrt1bY or not.
Found at: doi:10.1371/journal.pgen.1000844.s007 (1.78 MB PDF)

Table S1 Location and adjacent genes of repeat 1 elements containing Dmrt1 binding sites in the medaka genome.
Found at: doi:10.1371/journal.pgen.1000844.s008 (0.06 MB DOC)

Text S1 Izanagi and Izanami: Creators of Japan.
Found at: doi:10.1371/journal.pgen.1000844.s009 (6.88 MB PDF)

Author Contributions

Conceived and designed the experiments: AH IB MS. Performed the experiments: AH IB MK CS ET. Analyzed the data: AH IB SN MT MS. Contributed reagents/materials/analysis tools: AH IB SN MT. Wrote the paper: AH IB MS.

References

1. Davidson, ed (2006) The regulatory genome. Gene regulatory networks in development and evolution. Burlington: Elsevier. 289 p.
2. Britten RJ, Davidson EH (1969) Gene regulation for higher cells: a theory. Science 165: 349 357.
3. Britten RJ, Davidson EH (1971) Repetitive and non-repetitive DNA sequences and a speculation on the origins of evolutionary novelty. Q Rev Biol 46: 111 138.
4. Bejerano G, Lowe CB, Ahituv N, King B, Siepel A, et al. (2006) A distal enhancer and an ultraconserved exon are derived from a novel retroposon. Nature 441: 87 90.
5. Feschotte C (2008) Transposable elements and the evolution of regulatory networks. Nat Rev Genet 9: 397 405.
6. Lowe CE, Cooper JD, Brusko T, Walker NM, Smyth DJ, et al. (2007) Large-scale genetic fine mapping and genotype-phenotype associations implicate polymorphism in the IL2RA region in type 1 diabetes. Nat Genet 39: 1074 1082.
7. Feschotte C, Pritham EJ (2007) DNA transposons and the evolution of eukaryotic genomes. Annu Rev Genet 41: 331 368.
8. Marino-Ramirez L, Lewis KC, Landsman D, Jordan IK (2005) Transposable elements donate lineage-specific regulatory sequences to host genomes. Cytogenet Genome Res 110: 333 341.
9. van de Lagemaat LN, Landry JR, Mager DL, Medstrand P (2003) Transposable elements in mammals promote regulatory variation and diversification of genes with specialized functions. Trends Genet 19: 530 536.
10. Marino-Ramirez L, Jordan IK (2006) Transposable element derived DNaseI-hypersensitive sites in the human genome. Biol Direct 1: 20.
11. Charlesworth D, Charlesworth B (2005) Sex chromosomes: evolution of the weird and wonderful. Curr Biol 15: R129 131.
12. Herpin A, Schartl M (2008) Regulatory putsches create new ways of determining sexual development. EMBO Rep.
13. Graham P, Penn JK, Schedl P (2003) Masters change, slaves remain. Bioessays 25: 1 4.
14. Raymond CS, Shamu CE, Shen MM, Seifert KJ, Hirsch B, et al. (1998) Evidence for evolutionary conservation of sex-determining genes. Nature 391: 691 695.
15. Raymond CS, Parker ED, Kettlewell JR, Brown LG, Page DC, et al. (1999) A region of human chromosome 9p required for testis development contains two genes related to known sexual regulators. Hum Mol Genet 8: 989 996.
16. Nanda I, Shan Z, Schartl M, Burt DW, Koehler M, et al. (1999) 300 million years of conserved synteny between chicken Z and human chromosome 9. Nat Genet 21: 258 259.
17. Shetty S, Kirby P, Zarkower D, Graves JA (2002) DMRT1 in a ratite bird: evidence for a role in sex determination and discovery of a putative regulatory element. Cytogenet Genome Res 99: 245 251.
18. Matsuda M, Nagahama Y, Shinomiya A, Sato T, Matsuda C, et al. (2002) DMY is a Y-specific DM-domain gene required for male development in the medaka fish. Nature 417: 559 563.
19. Nanda I, Kondo M, Hornung U, Asakawa S, Winkler C, et al. (2002) A duplicated copy of DMRT1 in the sex-determining region of the Y chromosome of the medaka, Oryzias latipes. Proc Natl Acad Sci U S A 99: 11778 11783.
20. Yoshimoto S, Okada E, Umemoto H, Tamura K, Uno Y, et al. (2008) A W-linked DM-domain gene, DM-W, participates in primary ovary development in Xenopus laevis. Proc Natl Acad Sci U S A 105: 2469 2474.
21. Matsuda M, Shinomiya A, Kinoshita M, Suzuki A, Kobayashi T, et al. (2007) DMY gene induces male development in genetically female (XX) medaka fish. Proc Natl Acad Sci U S A 104: 3865 3870.
22. Matsuda M (2005) Sex determination in the teleost medaka, Oryzias latipes. Annu Rev Genet 39: 293 307.
23. Swain A (2002) Vertebrate sex determination: a new player in the field. Curr Biol 12: R602 603.
24. Ross AJ, Capel B (2005) Signaling at the crossroads of gonad development. Trends Endocrinol Metab 16: 19 25.
25. Sekido R, Lovell-Badge R (2009) Sex determination and SRY: down to a wink and a nudge? Trends Genet 25: 19 29.
26. Wilhelm D, Palmer S, Koopman P (2007) Sex determination and gonadal development in mammals. Physiol Rev 87: 1 28.
27. Sekido R, Lovell-Badge R (2008) Sex determination involves synergistic action of SRY and SF1 on a specific Sox9 enhancer. Nature 453: 930 934.
28. Kleinjan DA, Bancewicz RM, Gautier P, Dahm R, Schonthaler HB, et al. (2008) Subfunctionalization of duplicated zebrafish pax6 genes by cis-regulatory divergence. PLoS Genet 4: e29. doi:10.1371/journal.pgen.0040029.
29. Woolfe A, Elgar G (2007) Comparative genomics using Fugu reveals insights into regulatory subfunctionalization. Genome Biol 8: R53.
30. Kondo M, Hornung U, Nanda I, Imai S, Sasaki T, et al. (2006) Genomic organization of the sex-determining and adjacent regions of the sex chromosomes of medaka. Genome Res 16: 815 826.

Transcriptional Rewiring of Duplicated Genes

31. Chan TM, Longabaugh W, Bolouri H, Chen HL, Tseng WF, et al. (2009) Developmental gene regulatory networks in the zebrafish embryo. Biochim Biophys Acta 1789: 279 298.

32. Brunner B, Hornung U, Shan Z, Nanda I, Kondo M, et al. (2001) Genomic organization and expression of the doublesex-related gene cluster in vertebrates and detection of putative regulatory regions for DMRT1. Genomics 77: 8 17.

33. Wicker T, Sabot F, Hua-Van A, Bennetzen JL, Capy P, et al. (2007) A unified classification system for eukaryotic transposable elements. Nat Rev Genet 8: 973 982.

34. Roussigne M, Kossida S, Lavigne AC, Clouaire T, Ecochard V, et al. (2003) The THAP domain: a novel protein motif with similarity to the DNA-binding domain of P element transposase. Trends Biochem Sci 28: 66 69.

35. Hagemann S, Hammer SE (2006) The implications of DNA transposons in the evolution of P elements in zebrafish (Danio rerio). Genomics 88: 572 579.

36. Hammer SE, Strehl S, Hagemann S (2005) Homologs of Drosophila P transposons were mobile in zebrafish but have been domesticated in a common ancestor of chicken and human. Mol Biol Evol 22: 833 844.

37. Quesneville H, Nouaud D, Anxolabehere D (2005) Recurrent recruitment of the THAP DNA-binding domain and molecular domestication of the P-transposable element. Mol Biol Evol 22: 741 746.

38. Gao S, Zhang T, Zhou X, Zhao Y, Li Q, et al. (2005) Molecular cloning, expression of Sox5 and its down-regulation of Dmrt1 transcription in zebrafish. J Exp Zoolog B Mol Dev Evol 304: 476 483.

39. Pilon N, Daneau I, Paradis V, Hamel F, Lussier JG, et al. (2003) Porcine SRY promoter is a target for steroidogenic factor 1. Biol Reprod 68: 1098 1106.

40. Murphy MW, Zarkower D, Bardwell VJ (2007) Vertebrate DM domain proteins bind similar DNA sequences and can heterodimerize on DNA. BMC Mol Biol 8: 58.

41. Kondo M, Nanda I, Hornung U, Schmid M, Schartl M (2004) Evolutionary origin of the medaka Y chromosome. Curr Biol 14: 1664 1669.

42. Kobayashi T, Matsuda M, Kajiura-Kobayashi H, Suzuki A, Saito N, et al. (2004) Two DM domain genes, DMY and DMRT1, involved in testicular differentiation and development in the medaka, Oryzias latipes. Dev Dyn 231: 518 526.

43. Hornung U, Herpin A, Schartl M (2007) Expression of the male determining gene dmrt1bY and its autosomal coorthologue dmrt1a in medaka. Sex Dev 1: 197 206.

44. Herpin A, Nakamura S, Wagner TU, Tanaka M, Schartl M (2009) A highly conserved cis-regulatory motif directs differential gonadal synexpression of Dmrt1 transcripts during gonad development. Nucleic Acids Res 37: 1510 1520.

45. Meyer A, Schartl M (1999) Gene and genome duplications in vertebrates: the one-to-four (-to-eight in fish) rule and the evolution of novel gene functions. Curr Opin Cell Biol 11: 699 704.

46. Meyer A, Van de Peer Y (2005) From 2R to 3R: evidence for a fish-specific genome duplication (FSGD). Bioessays 27: 937 945.

47. Postlethwait J, Amores A, Cresko W, Singer A, Yan YL (2004) Subfunction partitioning, the teleost radiation and the annotation of the human genome. Trends Genet 20: 481 490.

48. Wright S, Finnegan D (2001) Genome evolution: sex and the transposable element. Curr Biol 11: R296 299.

49. Frazer KA, Pachter L, Poliakov A, Rubin EM, Dubchak I (2004) VISTA: computational tools for comparative genomics. Nucleic Acids Res 32: W273 279.

50. Brudno M, Malde S, Poliakov A, Do CB, Couronne O, et al. (2003) Glocal alignment: finding rearrangements during alignment. Bioinformatics 19 Suppl 1: i54 62.

51. Hall TA (1999) BioEdit: a user-friendly biological sequence alignment editor and analysis program for Windows 95/98/NT. Nucl Acids Symp 41: 95 98.

52. Tamura K, Dudley J, Nei M, Kumar S (2007) MEGA4: Molecular Evolutionary Genetics Analysis (MEGA) software version 4.0. Mol Biol Evol 24: 1596 1599.

53. Lemaire P, Garrett N, Gurdon JB (1995) Expression cloning of Siamois, a Xenopus homeobox gene expressed in dorsal-vegetal cells of blastulae and able to induce a complete secondary axis. Cell 81: 85 94.

54. Beverdam A, Wilhelm D, Koopman P (2003) Molecular characterization of three gonad cell lines. Cytogenet Genome Res 101: 242 249.

55. Hong Y, Liu T, Zhao H, Xu H, Wang W, et al. (2004) Establishment of a normal medakafish spermatogonial cell line capable of sperm production in vitro. Proc Natl Acad Sci U S A 101: 8011 8016.

56. Komura J, Mitani H, Shima A (1988) Fish cell culture: Establishment of two fibroblast-like cell lines (OL-17 and OL-32) from fins of the medaka, Oryzias latipes. In Vitro Cellular & Developmental Biology 24: 294 298.

57. Kuhn C, Vielkind U, Anders F (1979) Cell cultures derived from embryos and melanoma of poeciliid fish. In Vitro 15: 537 544.

58. Altschmied J, Duschl J (1997) Set of optimized luciferase reporter gene plasmids compatible with widely used CAT vectors. Biotechniques 23: 436 438.

59. Thermes V, Grabher C, Ristoratore F, Bourrat F, Choulika A, et al. (2002) I-SceI meganuclease mediates highly efficient transgenesis in fish. Mech Dev 118: 91 98.

60. Altschmied J, Hornung U, Schlupp I, Gadau J, Kolb R, et al. (1997) Isolation of DNA suitable for PCR for field and laboratory work. Biotechniques 23: 228 229.

61. Herpin A, Schindler D, Kraiss A, Hornung U, Winkler C, et al. (2007) Inhibition of primordial germ cell proliferation by the medaka male determining gene Dmrt I bY. BMC Dev Biol 7: 99.

62. Nakamura S, Saito D, Tanaka M (2008) Generation of transgenic medaka using modified bacterial artificial chromosome. Dev Growth Differ 50: 415 419.

Manuscript 3: A single transcription factor is sufficient to induce differentiation of embryonic stem cells into mature neurons. *Draft.*

A single transcription factor is sufficient to induce differentiation of embryonic stem

cells into mature neurons

Eva Christina Thoma[1], Erhard Wischmeyer[2], Nils Offen[3], Katja Maurus[1], Anna-Leena Sirén[3], Manfred Schartl[1], and Toni Ulrich Wagner[1+]

+corresponding author: toni.wagner@biozentrum.uni-wuerzburg.de

1: Physiological Chemistry I, University of Wuerzburg

Biozentrum am Hubland

97074 Wuerzburg, Germany

Fon +49 931 31 84165

Fax +49 931 31 84150

2: Physiologisches Institut, University of Wuerzburg

Röntgenring 9

97070 Wuerzburg

3: Department of Neurosurgery, University of Wuerzburg

Josef-Schneider Str. 11

97080 Wuerzburg

Short title: Single gene mediated neural differentiation

Abstract

Recent work showed that combinations of transcription-factors (TFs) can reprogram somatic cells to a pluripotent state or convert them to other cells. This raises the question if single TFs can determine cell fate of stem cells. We show that the neural TF *neurogenin2* (*ngn2*) is sufficient to induce rapid neuronal differentiation of embryonic stem cells without the need for any additional signals and even in the presence of pluripotency-promoting signals. Differentiated cells displayed neuron-specific gene and protein expression, and functional features. These findings show that a single TF is able to determine the cell fate of totally uncommitted stem cells.

Keywords: Pluripotent Stem Cells, Cell Differentiation, Neurogenesis

Introduction

During embryogenesis, all cells of the body arise from a few stem cells by differentiation. Transcription factors (TFs) play an important role during this process by regulating the gene expression program of the various differentiation stages or by triggering the transition to the next step. It has been shown that the ability of such key developmental genes to influence cell fates can also be operative outside of normal physiological development and alter the identity of already committed cells: Somatic cells are reprogrammed to a pluripotent state (Takahashi and Yamanaka, 2006) or converted into another cell type by specific combinations of defined TFs (Vierbuchen et al., 2010; Zhou et al., 2008).

In these studies, cell conversion or reprogramming was performed with differentiated cells and required combinations of genes to alter a cell's identity. Moreover, protocols included the use of specific culture media components to allow and enhance formation and survival of the desired cell types. Similarly, in reports describing directed differentiation of pluripotent stem cells by single TFs, differentiation itself was induced and promoted by external parameters like embryoid body formation and the addition of specific differentiation media (Chung et al., 2002; Reyes et al., 2008).

Thus, until now, cell fate determination by key developmental TFs always included additional factors, making it difficult to evaluate the direct effects and the cell fate defining potential of such genes.

We wanted to test if a single TF can define the cell fate of pluripotent stem cells without the need for any other differentiation-inducing or lineage-promoting signals. We focused on the formation of neuronal cells as this differentiation pathway is of great interest for both potential stem cell therapy and research. We show that ectopic expression of the neural TF *neurogenin2* (*ngn2*) is sufficient to induce and promote neuronal differentiation of mouse embryonic stem cells (mESCs) towards the appearance of mature, functional neurons.

Results

Murine ESCs were transiently co-transfected with a *ngn2* expression construct and GFPzeo. Leukemia inhibitory factor (LIF) which prevents differentiation of mESCs was withdrawn from the medium. Five days post transfection (dpt), *ngn2*-transfected cells displayed neuron-like morphology and expressed pan-neuronal proteins Tuj1 and Map2ab (Suppl. Fig. 1A-D).

On the molecular level, early (*math3*, *olig2*, *pax6*, and *sox1* (Pevny et al., 1998; Takebayashi et al., 1997; Walther and Gruss, 1991; Zhou et al., 2000)) and late (*dcx* (Francis et al., 1999; Gleeson et al., 1999), *NeuN* (Mullen et al., 1992)) neural marker genes as well as endogenous *ngn2* were upregulated in *ngn2*-transfected cells 5 and 7dpt (Suppl. Fig. 1K). This confirms induction and progression of neural differentiation upon *ngn2* transfection. We found a significantly higher number of Tuj1 positive cells in *ngn2*-transfected versus mock-transfected cells (Suppl. Fig. 1L) excluding the possibility of neurons arising due to LIF withdrawal.

A typical step during differentiation of stem cells is the loss of stem cell markers like Nanog (Chambers et al., 2003). Immunofluorescence staining revealed a loss of Nanog expression specifically in *ngn2*-transfected cells 3dpt (Suppl. Fig. 1E-J) indicating that the *ngn2*-induced differentiation process included the loss of stem cell markers.

Next, to determine the inductive strength of *ngn2*, mESCs were transfected with *ngn2* and, for the full duration of the following experiments, were kept in adherent culture in complete ESC medium containing LIF. Surprisingly, even under these pluripotency-supporting conditions, *ngn2*-transfected cells adopted neuronal morphology within 5dpt and expressed Tuj1 and Map2ab (Fig. 1A-F) while mock-transfected cells did not show any Tuj1-specific staining (Fig. 1B,N). Analyses of the gene expression pattern of *ngn2*-transfected cells in LIF-containing medium led to similar results compared to cells differentiated in the absence of LIF: Early and late neural marker genes were upregulated 7dpt (Fig. 1M). Furthermore, even in the presence of LIF, loss of Nanog expression was detected specifically in *ngn2*-transfected cells (Fig. 1G-L).

To confirm active LIF signaling, ESCs treated with conditioned medium from *ngn2*-transfected cells were stained for STAT3, a known effector of LIF signaling (Niwa et al., 1998). The staining showed clear activation of STAT3 visualized by its location in the cells' nuclei (Suppl. Fig. 2).

Thus, one can conclude that the differentiation process induced by *ngn2* is not influenced by pluripotency-promoting signals regarding time-course, gene expression, and loss of stem cell markers.

To avoid the problems linked with transient transfection systems, we generated two ES cell lines (E14-P2Angn2 and E14-CreP2Angn2) transgenic for constructs that allow induction of *ngn2* and subsequent selection of *ngn2*-expressing cells. Expression of *ngn2* and the puromycin resistance gene is switched on after deletion of a

GFPzeo open reading frame by Cre recombinase. Cre recombinase was added as purified protein or transgenic CreERT was activated by tamoxifen treatment (Fig. 2A, Suppl. Fig. 3A). Successful recombination (Fig. 2B-E, Suppl. Fig. 3B-D) and subsequent *ngn2*-induced differentiation (Suppl. Fig. 3E, Fig. 2F,G) were confirmed for both cell lines. For further experiments, E14-CreP2Angn2 line was used.

As *ngn2*-expressing cells can be selected with puromycin, it was possible to determine the percentage of *ngn2*-expressing cells differentiating into neurons. 7dpr, Tuj1 positive cells were about 40 percent in the absence of LIF and about 16 percent in the presence of LIF (Fig. 2H). The lower percentage observed in the presence of LIF resulted from a higher number of total cells - likely due to a higher proliferation rate of cells that did not respond to *ngn2* expression by neuronal differentiation. This idea is also supported by the fact that in the presence of LIF differentiating cultures still contained stem cell like colonies (Fig. 2F). However, quantification of Nanog positive cells showed that induction of *ngn2* led to significant decrease of Nanog-expressing cells both in the absence and in the presence of LIF (Fig. 2I, Suppl. Fig. 4).

Gene expression pattern of E14-CreP2Angn2 derived neurons was highly similar to that observed in transient transfection experiments with upregulation of early and late neuronal marker genes (Fig. 3A). Interestingly, expression levels of transgenic *ngn2* were similar in transient transfection experiments and E14-CreP2Angn2 cell line at day 3 of differentiation. At day 7, however, *ngn2* levels had dramatically decreased in transient transfection assays, possibly due to dilution of transfected plasmid or silencing of the CMV promoter (Fig. 3B). This decrease however, did obviously not affect the *ngn2*-induced differentiation process in respect to time course, gene and protein expression, and loss of Nanog expression.

Ngn2-derived neurons expressed vesicular glutamate receptors *vGLUT1* and *vGLUT2* on mRNA level. On protein level, cells were positive for vGLUT1 and NMDA receptor 1 (NR1) (Fig. 3C-J) indicating the formation of glutamatergic neurons. Both, vGLUT1 and NR1 protein were also expressed in *ngn2*-derived neurons grown in the presence of LIF (Suppl. Fig. 5).

Functionally, *ngn2*-derived neurons showed voltage-gated currents typical for terminally differentiated neurons in the voltage-clamp mode of whole-cell patch-clamp recordings. Depolarizing pulses from a holding potential of -70 mV elicited fast-activating transient inward currents typical for voltage-activated Na^+-currents (Na_v channels) followed by a delayed outward current indicative of voltage-activated potassium currents (K_v channels). In the current-clamp mode injection of depolarizing current elicited an action potential with a duration of 5 ms and an amplitude of 105 mV (Fig. 4A,B).

In co-culture with primary mouse hippocampal neurons, the E14-CreP2Angn2 cells expressed the presynaptic marker synapsin-1 and formed morphologically tight contacts with the hippocampal neurons (Fig. 4C-H).

5

Discussion

Exact cell fate determination is of crucial importance for correct embryogenesis. Although numerous studies indicate that certain genes are essential for this process, it is still not clear if such genes can determine cell fate on their own, or if their cell fate defining potential depends on the presence of a specific environment or auxiliary factors.

Here, we demonstrate that the TF *ngn2* alone is sufficient to induce rapid formation of functional neurons from pluripotent stem cells. These results indicate that certain genes have the potential to determine the cell fate choice of totally uncommitted stem cells outside the normal process of development. In contrast to earlier studies, our findings also prove that this cell fate defining potential is totally independent of additional external or internal signals like media components, embryoid body formation, or ectopic expression of other genes.

The formation of neurons was confirmed by morphology, gene and protein expression, and electrophysiological activity. Furthermore, *ngn2*-derived neurons formed contacts with hippocampal neurons in co-culture signifying their ability to interconnect with physiological neuronal networks.

Interestingly, *math3* and *olig2* were upregulated during *ngn2*-differentiation process. It has been shown that in vivo *ngn2* expression precedes that of *math3* (Fode et al., 1998) and that Math3 augments Ngn2 activity (Mattar et al., 2008). Similarly, *ngn2* and *olig2* have combinatorial roles in the generation of motor neurons (Mizuguchi et al., 2001; Novitch et al., 2001). Thus, in our in-vitro assay Ngn2 did not induce unspecific neuronal differentiation, but apparently activated the corresponding physiological genetic cascade including induction of its interaction partners.

Importantly, *olig2* also regulates *ngn2* expression in motor neurons (Zhou and Anderson, 2002) in-vivo. Likewise, *pax6* was shown to directly regulate *ngn2* (Scardigli et al., 2001; Scardigli, 2003) and expression of *sox1* precedes that of *ngn2* (Pevny et al., 1998). Nevertheless, these genes, *sox1, pax6,* and *olig2,* were activated during *ngn2*-induced in vitro differentiation although during physiological differentiation, *ngn2* is located genetically downstream in the cascade. One hypothesis explaining this phenomenon would be that differentiating cells recapitulate the sequence of steps documented for neurogenesis in-vivo, including stages that precede activation of *ngn2*. Further detailed experimental studies will have to be performed to gain insights into the underlying mechanism.

A similar observation is reported in another study describing cell conversion of medakafish spermatogonia into various somatic cell types by ectopic expression of lineage-specific TFs(Thoma et al., 2010). In that study, the activation of genes that are in-vivo located upstream of the inducing factors was also detected for three different processes of cell fate conversion. This finding supports the idea that the here reported upregulation of *sox1,*

pax6, and *olig2* during *ngn2*-mediated differentiation might be a conserved part of the in-vitro differentiation process, as a similar phenomenon was observed in a similar process in another species.

Another important finding of this study is that *ngn2* is able to induce and promote differentiation under conditions normally enhancing pluripotency. Thus, cells were grown in the presence of LIF (Smith et al., 1988; Williams et al., 1988) and serum that is normally omitted during in vitro neuronal differentiation protocols (Tropepe et al., 2001; Wiles and Johansson, 1999). However, our results prove that even under this conditions *ngn2* expression led to the loss of characteristic pluripotency markers like Nanog suggesting that the network maintaining pluripotency can be overcome by single defined signals albeit the mechanism of this process remains elusive.

Altogether, our data prove that ectopic expression *ngn2* is sufficient to induce the formation of mature neurons from stem cells. This is, to our knowledge, the first study reporting that a single TF determines the fate of totally uncommitted stem cells without the need for additional signals and independent of culture conditions.

TF-induced differentiation therefore suggests a promising differentiation method for stem cell research and the potential application of stem cells in regenerative medicine. Furthermore, the here presented system provides a valuable tool for studies of neural development, the loss of pluripotency, and basic mechanisms of differentiation.

Ultimately, our findings are a proof of concept for the feasibility of single gene mediated differentiation. We suggest that this approach can be extended to generate other cell types if the appropriate TFs are identified.

Methods

See Supplementary information for cell culture, plasmids, quantification experiments, and electrophysiology.

PCR

Total RNAs were isolated using the Total RNA Isolation Reagent (AB Gene). Samples were digested with DNAseI (Fermentas) followed by cDNA synthesis (Fermentas).

Primers are shown in Supplementary Table 1. qRT-PCR was performed using a Biorad-iCycler. Ef1a1 primers were used for template normalization. All PCRs were performed in triplicate and data from three independent experiments were analysed.

Immunofluorescence

Immunofluorescence staining was performed as described (Wagner et al., 2008) using anti-Tuj1 antibody (Novus Biologicals), anti MAP2ab antibody (Acris Antibodies GmbH), anti-Nanog-antibody (antikoerper-online), anti-Stat3 antibody (Santa Cruz), anti-vGlut1 antibody (Synapticsystems), anti-tau antibody (Synapticsystems), anti-NR1 antibody (Sigma), anti-Synapsin 1 (SynapticSystems), anti-MAP2 (Chemicon), Hoechst 33258 (Molecular probes), and DAPI (Sigma). For coculture experiments, 10%NHS instead of 5% BSA was used for blocking.

Microscopy

Light microscopy was performed using a Leica DMI6000B inverted microscope. For confocal microscopy was performed using either a Nikon C1 confocal microscope or a SP5 Confocal Microscope (Leica). All images were analysed using ImageJ software.

Acknowledgements

Supplementary information is available at EMBO reports online.

References

Chambers, I., Colby, D., Robertson, M., Nichols, J., Lee, S., Tweedie, S., Smith, A. (2003). Functional expression cloning of Nanog, a pluripotency sustaining factor in embryonic stem cells.*Cell* **113**, 643-55.

Chung, S., Sonntag, K.-C., Andersson, T., Bjorklund, L. M., Park, J.-J., Kim, D.-W., Kang, U. J., Isacson, O., Kim, K.-S. (2002). Genetic engineering of mouse embryonic stem cells by Nurr1 enhances differentiation and maturation into dopaminergic neurons.*European Journal of Neuroscience* **16**, 1829-1838.

Fode, C., Gradwohl, G., Morin, X., Dierich, a, LeMeur, M., Goridis, C., Guillemot, F. (1998). The bHLH protein NEUROGENIN 2 is a determination factor for epibranchial placode-derived sensory neurons.*Neuron* **20**, 483-94.

Francis, F., Koulakoff, a, Boucher, D., Chafey, P., Schaar, B., Vinet, M. C., Friocourt, G., McDonnell, N., Reiner, O., Kahn, a, et al. (1999). Doublecortin is a developmentally regulated, microtubule-associated protein expressed in migrating and differentiating neurons.*Neuron* **23**, 247-56.

Gleeson, J. G., Lin, P. T., Flanagan, L. a, Walsh, C. a (1999). Doublecortin is a microtubule-associated protein and is expressed widely by migrating neurons.*Neuron* **23**, 257-71.

Mattar, P., Langevin, L. M., Markham, K., Klenin, N., Shivji, S., Zinyk, D., Schuurmans, C. (2008). Basic helix-loop-helix transcription factors cooperate to specify a cortical projection neuron identity.*Molecular and cellular biology* **28**, 1456-69.

Mizuguchi, R., Sugimori, M., Takebayashi, H., Kosako, H., Nagao, M., Yoshida, S., Nabeshima, Y., Shimamura, K., Nakafuku, M. (2001). Combinatorial roles of olig2 and neurogenin2 in the coordinated induction of pan-neuronal and subtype-specific properties of motoneurons.*Neuron* **31**, 757-71.

Mullen, R. J., Buck, C. R., Smith, a M. (1992). NeuN, a neuronal specific nuclear protein in vertebrates.*Development (Cambridge, England)* **116**, 201-11.

Niwa, H., Burdon, T., Chambers, I., Smith, a (1998). Self-renewal of pluripotent embryonic stem cells is mediated via activation of STAT3.*Genes & development* **12**, 2048-60.

Novitch, B. G., Chen, a I., Jessell, T. M. (2001). Coordinate regulation of motor neuron subtype identity and pan-neuronal properties by the bHLH repressor Olig2.*Neuron* **31**, 773-89.

Pevny, L. H., Sockanathan, S., Placzek, M., Lovell-Badge, R. (1998). A role for SOX1 in neural determination.*Development (Cambridge, England)* **125**, 1967-78.

Reyes, J. H., O'Shea, K. S., Wys, N. L., Velkey, J. M., Prieskorn, D. M., Wesolowski, K., Miller, J. M., Altschuler, R. a (2008). Glutamatergic neuronal differentiation of mouse embryonic stem cells after transient expression of neurogenin 1 and treatment with BDNF and

GDNF: in vitro and in vivo studies.*The Journal of neuroscience : the official journal of the Society for Neuroscience* **28**, 12622-31.

Scardigli, R., Schuurmans, C., Gradwohl, G., Guillemot, F. (2001). Crossregulation between Neurogenin2 and pathways specifying neuronal identity in the spinal cord.*Neuron* **31**, 203-17.

Scardigli, R. (2003). Direct and concentration-dependent regulation of the proneural gene Neurogenin2 by Pax6.*Development* **130**, 3269-3281.

Smith, A. G., Heath, J. K., Donaldson, D. D., Wong, G. G., Moreau, J., Stahl, M., Rogers, D. (1988). Inhibition of pluripotential embryonic stem cell differentiation by purified polypeptides.*Nature* **336**, 688-90.

Takahashi, K., Yamanaka, S. (2006). Induction of pluripotent stem cells from mouse embryonic and adult fibroblast cultures by defined factors.*Cell* **126**, 663-76.

Takebayashi, K., Takahashi, S., Yokota, C., Tsuda, H., Nakanishi, S., Asashima, M., Kageyama, R. (1997). Conversion of ectoderm into a neural fate by ATH-3, a vertebrate basic helix-loop-helix gene homologous to Drosophila proneural gene atonal.*The EMBO journal* **16**, 384-95.

Thoma, E. C., Wagner, T. U., Weber, I. P., Herpin, A., Fischer, A., Schartl, M. (2010). Ectopic expression of single transcription factors directs differentiation of a Medaka spermatogonial cell line.*Stem cells and development* .

Tropepe, V., Hitoshi, S., Sirard, C., Mak, T. W., Rossant, J., Kooy, D. van der (2001). Direct neural fate specification from embryonic stem cells: a primitive mammalian neural stem cell stage acquired through a default mechanism.*Neuron* **30**, 65-78.

Vierbuchen, T., Ostermeier, A., Pang, Z. P., Kokubu, Y., Südhof, T. C., Wernig, M. (2010). Direct conversion of fibroblasts to functional neurons by defined factors.*Nature* **463**, 1035-41.

Wagner, T. U., Kraeussling, M., Fedorov, L. M., Reiss, C., Kneitz, B., Schartl, M. (2008). STAT3 and SMAD1 signalling in Medaka embryonic stem-like cells and blastula embryos.*Stem cells and development* .

Walther, C., Gruss, P. (1991). Pax-6, a murine paired box gene, is expressed in the developing CNS.*Development (Cambridge, England)* **113**, 1435-49.

Wiles, M. V., Johansson, B. M. (1999). Embryonic stem cell development in a chemically defined medium.*Experimental cell research* **247**, 241-8.

Williams, R. L., Hilton, D. J., Pease, S., Willson, T. A., Stewart, C. L., Gearing, D. P., Wagner, E. F., Metcalf, D., Nicola, N. A., Gough, N. M. (1988). Myeloid leukaemia inhibitory factor maintains the developmental potential of embryonic stem cells.*Nature* **336**, 684-7.

Zhou, Q., Wang, S., Anderson, D. J. (2000). Identification of a novel family of oligodendrocyte lineage-specific basic helix-loop-helix transcription factors.*Neuron* **25**, 331-43.

Zhou, Q., Anderson, D. J. (2002). The bHLH transcription factors OLIG2 and OLIG1 couple neuronal and glial subtype specification.*Cell* **109**, 61-73.

Zhou, Q., Brown, J., Kanarek, A., Rajagopal, J., Melton, D. A. (2008). In vivo reprogramming of adult pancreatic exocrine cells to beta-cells.*Nature* **455**, 627-32.

Legends to Figures:

Figure 1: Induction of neuronal differentiation by transient transfection with *ngn2* in complete stem cell growth medium with LIF. (A,B) Wide field scan of Tuj1 staining 5 days post transfection (dpt). (A) *Ngn2*-transfected cells. (B) mock-transfected cells. Scale bars: 200μm. (C-F) Neuronal marker expression 5dpt. (C,D) Tuj1. (E,F) Map2ab. Scale bars: 20μm. (G-L) Loss of Nanog expression (arrowheads) in *ngn2*-transfected (G,I,K), but not in mock-transfected cells (H,J,L). Transfected cells are visualized by expression of cotransfected GFP (G,H). Scale bars: 20μm. (M) Gene expression pattern of untreated (ut), *ngn2*-transfected (d5+,d7+), and mock-transfected (d5-,d7-) mESCs 5 and 7dpt. b: Brain cDNA. (N) Tuj1 positive cells in *ngn2*-transfected and mock-transfected cells 5 and 7dpt. N=3.

Figure 2: Directed neuronal differentiation using E14-CreP2Angn2 cell line. (A) Induction construct of E14-CreP2Angn2 cell line and method of induction. (B,C) Loss of GFP signal in 4OHT treated cells 1 day post recombination (dpr) (D,E) Mock treated cells 1dpr. Scale bars: 20μm. (F,G) Tuj1 staining 7dpr of cells grown in the presence (F) or absence (G) of LIF. Nuclei are visualized by Hoechst staining. Scale bars: 50μm. (H) Numbers of total and Tuj1 positive cells 7dpr in the presence and absence of LIF. N=3. (I) Nanog positive cells in mock and 4OHT treated cells 3dpr in the presence and absence of LIF.

Figure 3: Characterization of differentiation process of E14-CreP2Angn2 cell line in the absence of LIF. (A) Gene expression pattern of untreated (ut), 4OHT-treated (d3+,d7+), and mock-treated (d3-,d7-) mESCs 3 and 7dpr. b: Brain cDNA. (B) Expression levels of ectopic *ngn2* after transient transfection and in E14-CreP2Angn2 cell line. (C) Expression of neuronal protein tau. Scale bar: 20μm. (D-J) Expression of vGLUT1/2 mRNA (G), vGLUT1 protein (D-F), and NMDA receptor 1 (NR1) (H-J) indicating formation of glutamatergic neurons. Scale bars: 20μm (C-F), 10μm (H-J).

Figure 4: Functionality of ngn2-derived neurons. (A,B) Whole-cell patch clamp recordings of neurons 10dpr. (A) Voltage-clamp recording upon application of depolarizing pulses ranging from -80 mV to +40 mV from a holding potential of -70 mV. Transient Na^+ inward current (also: inset at -20 mV) were followed by sustained K+ outward current (inset: at +40 mV). (B) Current-clamp recording upon injection of a depolarizing pulse elicits a fast and high-amplitude action potential. (C-H) Contacts of *ngn2*-induced neurons with primary hippocampal neurons. (C) CellTracker™ Green CMFDA (CT) labeled *ngn2*-mESC derived neurons (magenta). (D) Nuclei visualized by DAPI staining (blue). (E) MAP2 staining (cyan). (F) Synapsin-1 staining (yellow). (G)

Overlay of CT, DAPI, and synapsin-1 staining. (H) Overlay of C, D, E, F. Arrowheads mark the position of CT labeled *ngn2*-mESC derived neurons. Scale bars: 20μm.

Supplementary Figure 1: Induction of neuronal differentiation by transient transfection with *ngn2* in the absence of LIF. (A-D) 5dpt, *ngn2*-transfected cells display neuronal morphology and express neuronal marker proteins like Tuj1 (A,B) and Map2ab (C,D). (B,D) Overlays of immunofluorescence staining and Hoechst staining. Scale bars: 20μm. (E-J) Loss of Nanog expression (arrowheads) in *ngn2*-transfected (E,G,I), but not in mock-transfected cells (F,H,J). Transfected cells are visualized by expression of cotransfected GFP (E,F). Scale bars: 20μm. (K) Gene expression pattern of untreated (ut), *ngn2*-transfected (d5+, d7+), and mock-transfected (d5-, d7-) mESCs 5 and 7dpt. b: Brain cDNA. (L) Tuj1 positive cells in *ngn2*-transfected and mock-transfected cells 5 and 7dpt. N=3.

Supplementary Figure 2: STAT3 immunofluorescence staining proving active LIF signaling. (A) mESC colony treated with conditioned medium from *ngn2*-transfected cells. (B) STAT3 staining. (C) Nuclei visualized by Hoechst staining. (D) Overlay of B and C showing nuclear localization of STAT3. Scale bars: 20μm.

Supplementary Figure 3: Directed neuronal differentiation using E14-P2Angn2 cell line and transduction of TATCre protein. (A) Induction construct of E14-P2Angn2 cell line and method of induction. (B) PCR using GFP-specific primers confirming successful recombination on gDNA and cDNA level. (C,D) Loss of GFP expression (arrowheads) verifying successful recombination 2dpr. (C) Dark field view. (D) Overlay. Scale bars: 20μm. (E) Developing neurons five days post recombination. Scale bar: 20μm. OR: Tuj1 staining of E14-P2Angn2 cells 7dpr. Scale bar: 200μm.

Supplementary Figure 4: Loss of Nanog protein expression upon induction of *ngn2* expression by 4OHT treatment. (A-F) 4OHT (D-F) and mock treated cells (A-C) 3dpr in the presence of LIF. (G-L) 4OHT (J-L) and mock treated cells (G-I) 3dpr in the absence of LIF. Scale bars: 20μm.

Supplementary Figure 5: Neuronal differentiation of E14-CreP2Angn2 cell line in the presence of LIF. Expression of vGLUT1 (A-C) and NR1 (D-F) indicating the formation of glutamatergic neurons. Scale bars: 10μm.
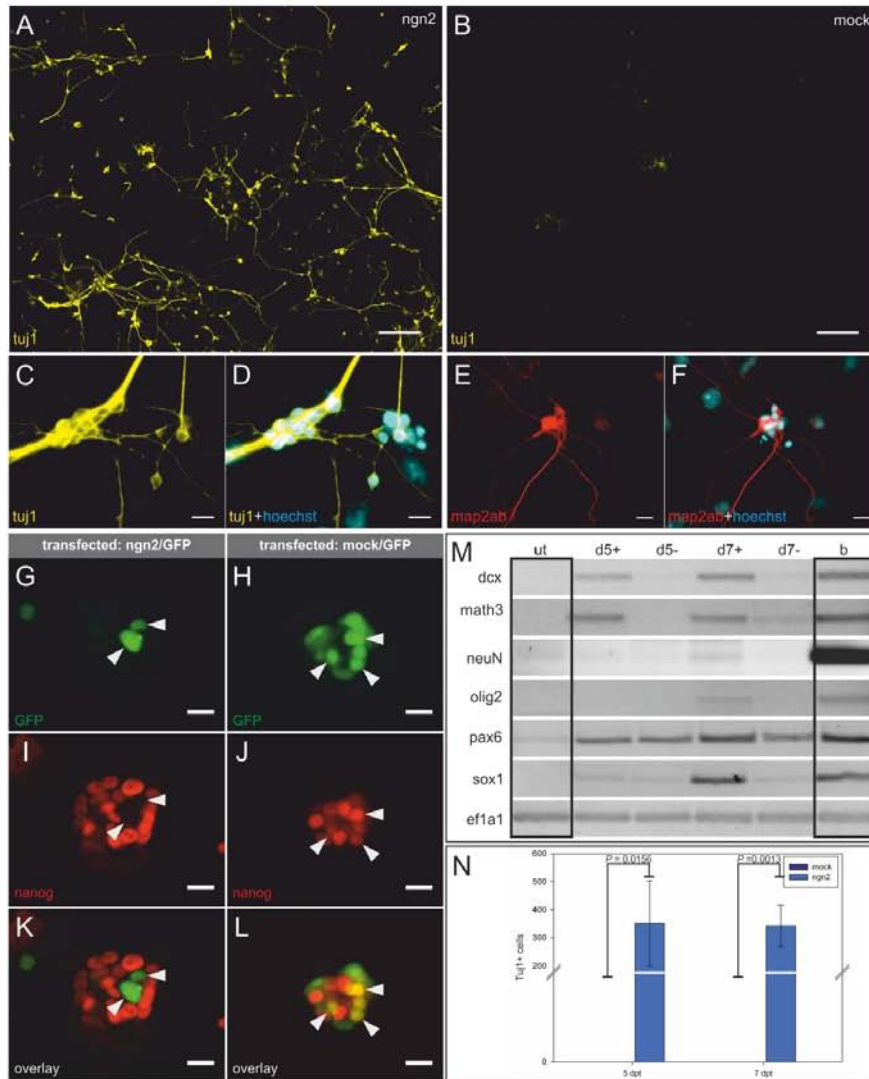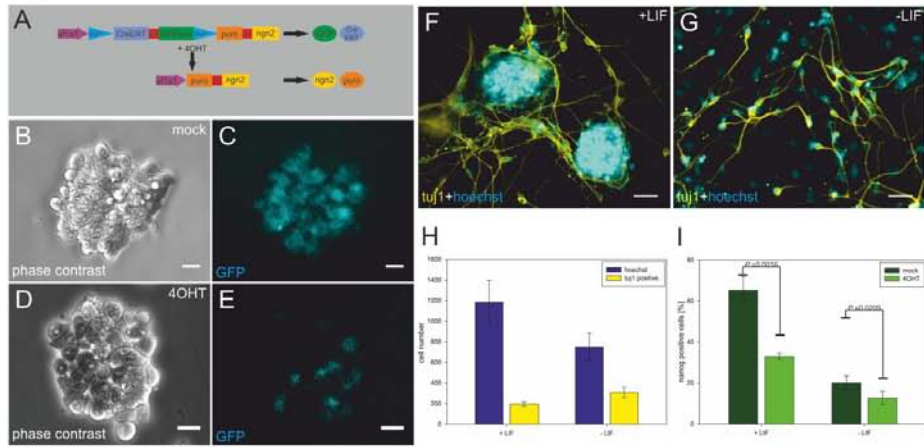
Figure 1

Figure 2

Figure 3
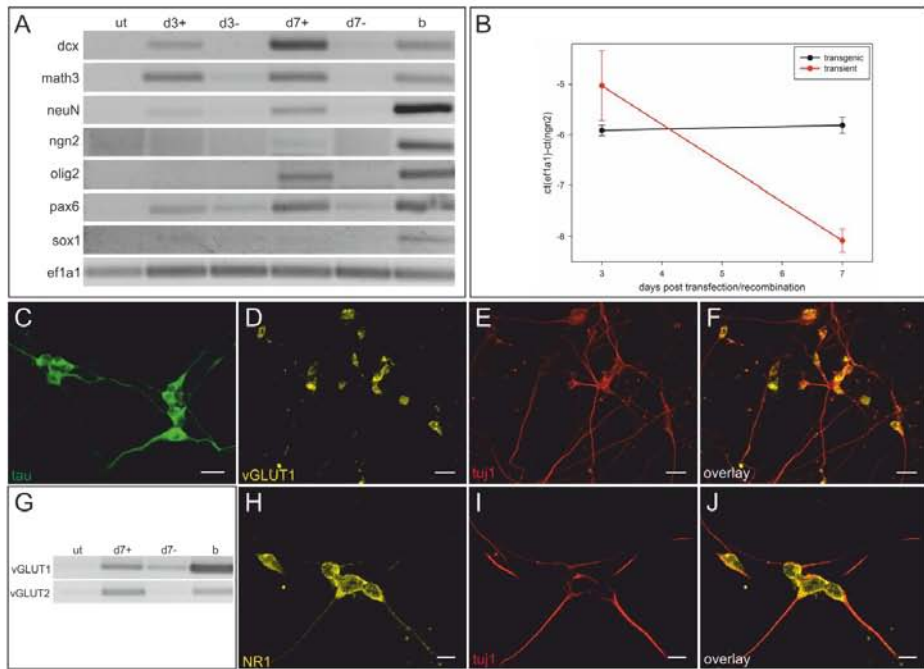
Figure 4
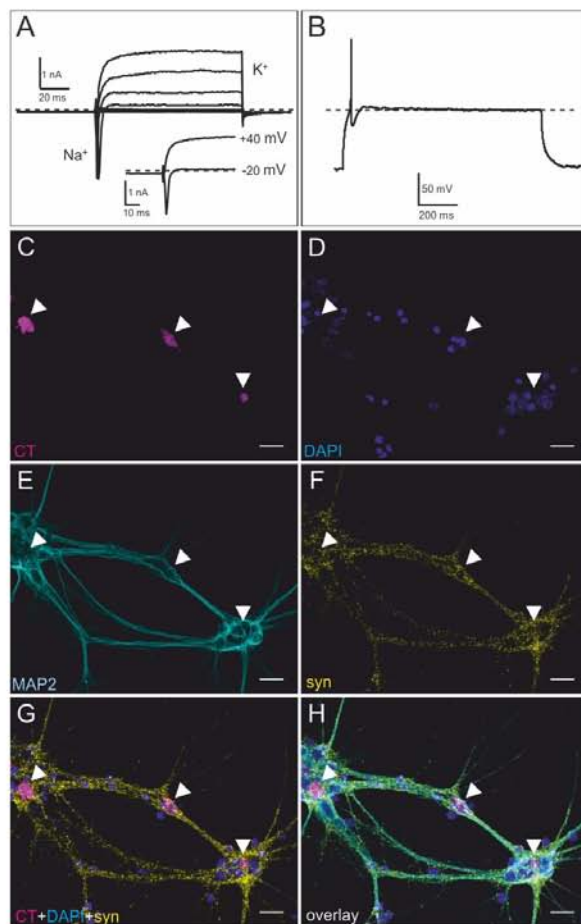
Suppl. Figure 1

Suppl. Figure 2

A phase contrast
B STAT3
C hoechst
D overlay

Suppl. Figure 3

A
B gDNA cDNA
   mock Cre   mock Cre
   GFP
   ef1a1
C GFP
D GFP+phase contrast
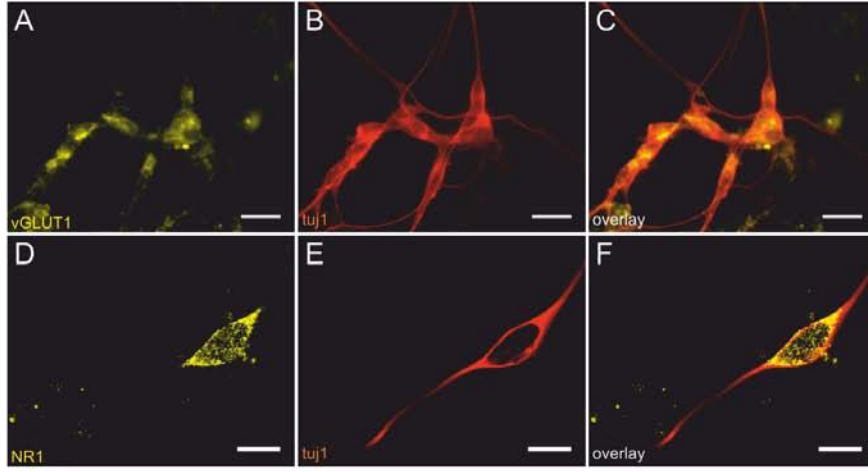E tuj1
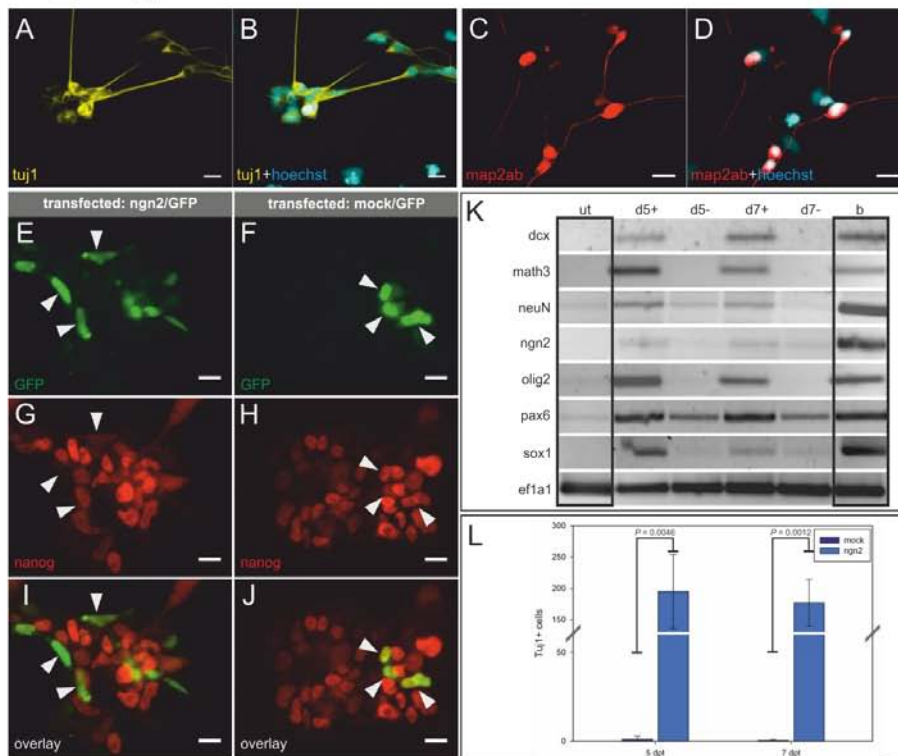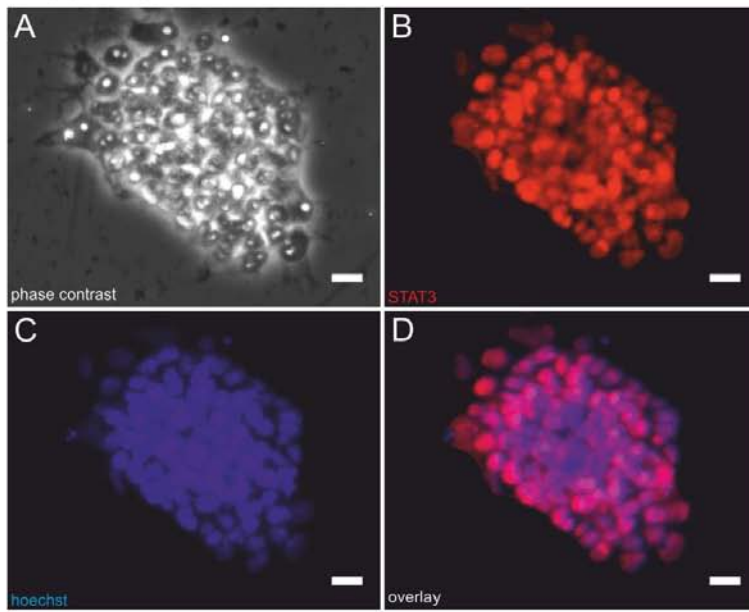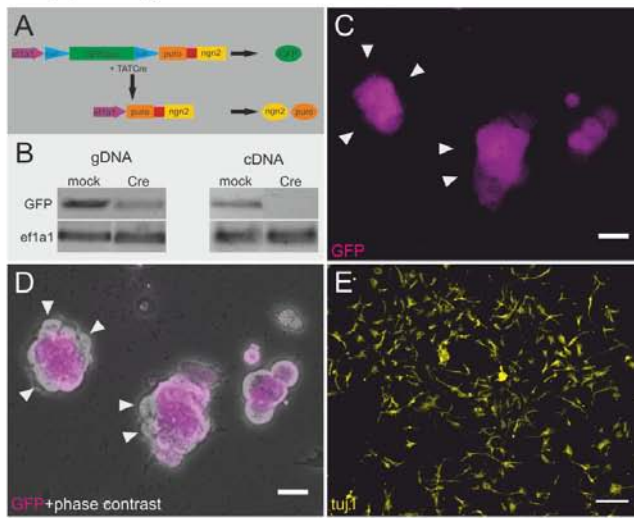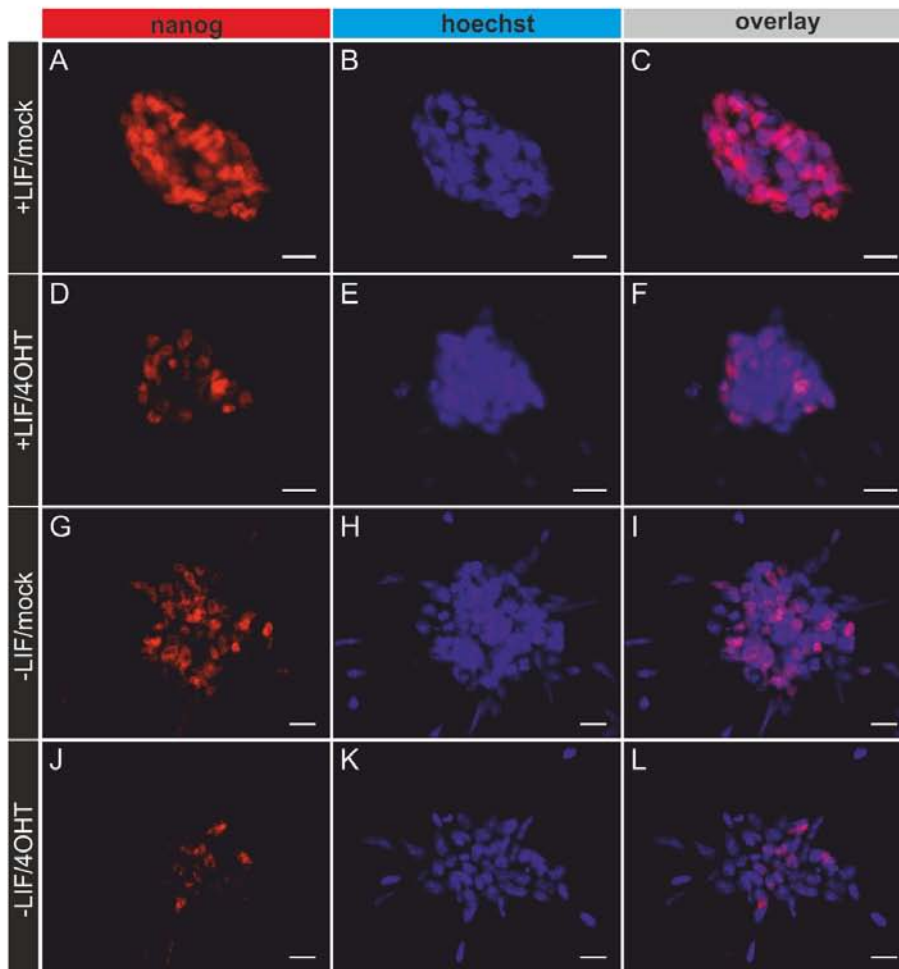
Suppl. Figure 4

Suppl. Figure 5

Supplementary Information

Methods

Cell culture

E14 mouse ES cells were grown at 37°C, 5% CO_2 on gelatin coated wells in DMEM with 10% FCS, sodium pyruvate (1mM), non-essential amino acids (0.1mM), penicillin/streptomycin (1mM), ß-mercaptoethanol (0.1mM), and LIF (1000U/ml). Transfections were performed using the Fugene HD transfection reagent (Roche) following the manufacturer's instructions.

During transient transfection experiments, cells were selected with Zeocin (100µg/ml). During all experiments, medium was changed every day.

For generation of E14-P2Angn2 and E14-CreP2Angn2 cell line, the tol2 transposase system (Kawakami and Noda, 2004) was used. Cells were transfected with a construct containing the coding sequence of the tol2 transposase under control of the CMV promoter and the P2Angn2 construct or the CreP2Angn2 construct, respectively, at ratio of 2:1 and subsequently selected with Zeocin (100µg/ml) for 10 days. Single colonies were picked, expanded, and checked for correct function of the induction constructs. For each cell line, one clone was chosen for further analysis.

For protein transduction, E14-P2Angn2 cells were seeded as single cell suspension on gelatin coated wells. After cell adhesion, cells were treated with serum-free stem cell medium containing 2.5µM TATCre recombinase (Peitz et al., 2007) (kind gift from F. Edenhofer) for 4 hours. Then, cells were kept in LIF-free, serum-containing medium.

For CreERT induction (Feil et al., 1996) of E14-CreP2Angn2 cell line, 4-hydroxytestosterone (4OHT, 1µM) was added to the medium for 24 hours. Puromycin selection was started 2 days after 4OHT addition at a concentration of 1µg/ml and was raised to 2µg/ml at day 5.

For both E14-P2Angn2 and E14-CreP2Angn2 cell line, Puromycin selection was started 2dpr at a concentration of 1µg/ml and raised to 2µg/ml 5dpr

For, coculture experiments, E14-CreP2Angn2 cells were seeded on poly-D-lysine coated coverslips and *ngn2* expression was induced by addition of 4OHT. Differentiating cells were cultured in stem cell medium without LIF and selected with Puromycin. Medium was changed every day. 8dpr, cells were labeled with CellTracker™ Green CMFDA (Invitrogen) according to the manufacturer's instructions and cultured together with hippocampal neurons from C57Bl/6 mouse fetuses at E18 (breeding pairs from Harlan-Winkelmann, Borchen, Germany) in MEM with 2% B27, 0.22% sodium bicarbonate, 1mM sodium pyruvate, 2mM L-glutamine, 1%

Penicillin/Streptomycin, and 0.6% glucose. Cultures were incubated at 37°C under 5% CO2/ 95% air and 90% humidity for 12 days. Medium was changed every second day.

Plasmids

The *ngn2* expression construct was a kind gift from F. Guillemot and contains the coding sequence of *ngn2* under control of the CMV promoter. As a transfection control, cells were co-transfected with pEGFP(C1)-Zeo, a vector coding for a fusion protein of the fluorescent protein EGFP and the Zeocin resistance under control of the CMV promoter allowing both visualization and selection of transfected cells. Ratios were 1,5µg expression vector + 0,5µg pEGFP(C1)-Zeo. Control cells were transfected with EBFP-N1 (kind gift of R. Campbell, P. Daugherty, and M. Davidson) instead of *ngn2*.

The P2Angn2 construct was generated by amplyfing the EGFP-Zeo coding sequence with primers containing flanking lox sites. PCR product was inserted in pMTCpA. The pMTCpA vector contains a CMV promoter, tol2 recognition sites, and polyA tail. CMV promoter was replaced by ef1a1 promoter resulting in pMTE-EGFP-Zeo. Subsequently, the coding sequence of ngn2 was amplified by PCR and inserted in pMTE-EGFP-Zeo resulting in pMTE-EGFP-Zeo-ngn2. Puromycin resistance gene and 2A sequence were amplified by PCR and cloned into pMTE-EGFP-Zeo-ngn2.

For generation of the CreP2Angn2 construct the coding sequence of CreERT2 linked to a 2A sequence was amplified by PCR and cloned into pMTE-EGFP-Zeo-P2Angn2.

Quantification experiments

To determine efficiency of neural differentiation after transient transfection, Tuj1 positive cells were counted in an area of 15.04 mm^2. Data from three independent experiments were evaluated using Student's t-test.

To determine efficiency of neural differentiation in E14-CreP2Angn2 cells, total cells and Tuj1 positive cells were counted in an area of 3 mm^2. Data from three independent experiments were evaluated using Student's t-test.

For quantification of Nanog expression 3dpr, total cells and Nanog positive cells were counted in six to eight representative stem cell colonies for mock and 4OHT treated cells. Data from three independent experiments were evaluated using Student's t-test.

Electrophysiology

Whole-cell recordings (Hamill et al., 1981) were performed at RT in a bath solution consisting of 125mM NaCl, 2.5mM KCl, 2mM CaCl$_2$, 1mM MgCl$_2$, 10mM HEPES, pH 7.4. Patch pipettes were pulled from borosilicate glass capillaries (Kimble Products, England), and heat-polished to give input resistances of 3-7 MΩ (whole-cell). The pipette recording solution contained 140mM KCl, 2mM MgCl$_2$, 0.01mM CaCl$_2$ mM ethylene-

bis(oxyethylenenitrilo) tetraacetate (EGTA), 1mM Na_2ATP, 0.1mM cyclic AMP, 0.1mM ATP and 5mM HEPES

(pH 7.3). Currents were recorded with an EPC9 (Heka) patch clamp amplifier and low pass-filtered at 1-2 kHz.

Stimulation and data acquisition were controlled by the PULSE/PULSEFIT software package (Heka) on a

Macintosh computer, and data analysis was performed with IGOR software (WaveMetrics, Lake Oswego, USA).

Feil, R., Brocard, J., Mascrez, B., LeMeur, M., Metzger, D., Chambon, P. (1996). Ligand-activated site-specific recombination in mice.*Proceedings of the National Academy of Sciences of the United States of America* **93**, 10887-90.

Hamill, O. P., Marty, A., Neher, E., Sakmann, B., Sigworth, F. J. (1981). Improved patch-clamp techniques for high-resolution current recording from cells and cell-free membrane patches.*Pflügers Archiv : European journal of physiology* **391**, 85-100.

Kawakami, K., Noda, T. (2004). Transposition of the Tol2 element, an Ac-like element from the Japanese medaka fish Oryzias latipes, in mouse embryonic stem cells.*Genetics* **166**, 895-9.

Peitz, M., Jäger, R., Patsch, C., Jäger, A., Egert, A., Schorle, H., Edenhofer, F. (2007). Enhanced purification of cell-permeant Cre and germline transmission after transduction into mouse embryonic stem cells.*Genesis (New York, N.Y. : 2000)* **45**, 508-17.

Supplementary Table 1

Gene	Primer forward	Primer reverse
ef1a1	5'-GGTGACAACATGCTGGAGCCAAGTG-3'	5'-CCCACAGGGACAGTGCCAATGC-3'
dcx	5'-CCATTGACGGATCCAGGAAG-3'	5'-TCTGGCTTGAGCACTGTTGC-3'
math3	5'-GCCCAGAGACTGTGGTACTGA-3'	5'-AGAGCCCGGTCTTCTCTCTT-3'
neuN	5'-AGGACTACTCCGGCCAGACC-3'	5'-TAGTCGTTTGGGCTGCTGCT-3'
endongn2	5'-GACATTCCCGGACACACACC-3'	5'-CTCCTCGTCCTCCTCCTCGT-3'
olig2	5'-ACAGACCGAGCCAACACCAG-3'	5'-CGGGCAGAAAAAGATCATCG-3'
pax6	5'-GAAGCGGAAGCTGCAAAGAA-3'	5'-GGAGTGTTGCTGGCCTGTCT-3'
sox1	5'-GCTGCAGTACAGCCCCATCT-3'	5'-GGCTCCGACTTGACCAGAGA-3'
vGLUT1	5'-CGCTTGTTTCTGCCTGTGTG-3'	5'-TGGTTAGGCGAGCCTTGAAA-3'
vGLUT2	5'-CAATTTAAATCTGGTAAGGCTGG	5'- CCTTCTTCTCAGGCACCTC-3'
GFP	5'-ACGTAAACGGCCACAAGTTC-3'	5'-GAACTCCAGCAGGACCATGT-3'
transient ngn2	5'-TCGCCCGCTAGCCCCGGGTC-3'	5'-CAAGCGGCTTCGGCCAGTAACGTTA-3'
inducible ngn2	5'-GTGCATGACCCGCAAGCCCG-3'	5'-CTCCTCGTCCTCCTCCTCGT-3'

Acknowledgements

Appendix

Eidesstattliche Erklärung

Gemäß §4, Abs. 3, Ziff. 3, 5 und 8

der Promotionsordnung der

Fakultät für Biologie der

Bayerischen Julius-Maximilians-Universität Würzburg

Hiermit erkläre ich ehrenwörtlich, dass ich die vorliegende Dissertation selbständig angefertigt und keine anderen als die angegebenen Quellen und Hilfsmittel verwendet habe.

Ich erkläre weiterhin, dass die vorliegende Dissertation weder in gleicher, noch in ähnlicher Form bereits in einem anderen Prüfungsverfahren vorgelegen hat.

Weiterhin erkläre ich, dass ich außer den mit Zulassungsantrag urkundlich vorgelegten Graden keine weiteren akademischen Grade erworben oder zu erwerben versucht habe.

Würzburg, Januar 2011

_____

Eva Thoma

Erklärungen zum Eigenanteil

Geleisteter Anteil von Eva Christina Thoma an der Veröffentlichung:

Ectopic expression of single transcription factors directs differentiation of a Medaka spermatogonial cell line. Stem Cells Dev. 2010 Nov 19.

Hiermit wird bestätigt, dass Eva Christina Thoma an der oben genannten Veröffentlichung selbstständig folgenden Anteil geleistet hat:

EC Thoma führte alle Zellkulturexperimente und einen Teil der PCR Analysen durch. Weiterhin war sie für die Mikroskopie zuständig, wertete die Ergebnisse aus und schrieb die erste Version des Manuskripts.

Unterschriften der Autoren:

Dr. Toni U. Wagner:

Ort, Datum: Würzburg, 27.01.11   Unterschrift:

Isabell P. Weber:

Ort, Datum: Dresden, 18.01.2011   Unterschrift:

Dr. Amaury Herpin:

Ort, Datum: Würzburg, 26.01.11   Unterschrift:

Dr. Andreas Fischer:

Ort, Datum: 19. 1. 2011   Unterschrift:

Prof. Dr. Dr. Manfred Schartl:

Ort, Datum: Würzburg, 27.01.11   Unterschrift:

Erklärungen zum Eigenanteil

Geleisteter Anteil von Eva Christina Thoma an der Veröffentlichung:

Transcriptional rewiring of the sex determining dmrt1 gene duplicate by transposable elements. PLoS Genet. 2010 Feb 12;6(2):e1000844

Hiermit wird bestätigt, dass Eva Christina Thoma an der oben genannten Veröffentlichung selbstständig folgenden Anteil geleistet hat:

EC Thoma war für die Kultivierung der Zelllinien Mes1 und SG3 zuständig und führte die Transfektionsexperimente mit diesen Zelllinien durch.

Unterschriften der Autoren:

Dr. Amaury Herpin:

Ort, Datum: Würzburg, 26.01.11   Unterschrift:

Dr. Ingo Braasch:

Ort, Datum: Eugene, 12.1.2011   Unterschrift:

Michael Kraeussling:

Ort, Datum: Würzburg, 26.01.11   Unterschrift:

Cornelia Schmidt:

Ort, Datum: Würzburg, 11.01.11   Unterschrift:

Prof. Dr. Dr. Manfred Schartl (stellvertretend für Dr. Shuhei Nakamura und Prof. Minoru Tanaka):

Ort, Datum: Würzburg, 27.01.11   Unterschrift:

Geleisteter Anteil von Eva Christina Thoma an der Veröffentlichung:

A single transcription factor is sufficient to induce differentiation of embryonic stem cells into mature neurons. *Draft.*

Hiermit wird bestätigt, dass Eva Christina Thoma an der oben genannten Veröffentlichung selbstständig folgenden Anteil geleistet hat:

EC Thoma führte alle Zellkulturexperimente, PCR Analysen und Immunfloreszenzfärbungen durch mit Ausnahme der Kokulturexperimente und der Differenzierungsansätze bei transienter ngn2-Transfektion mit LIF. Weiterhin war sie für die Mikroskopie zuständig, wertete die Ergebnisse aus und schrieb die erste Version des Manuskripts.

Unterschriften der Autoren:

Prof. Dr. Erhard Wischmeyer:

Ort, Datum: _Würzburg, 25.01.11_ Unterschrift: _____
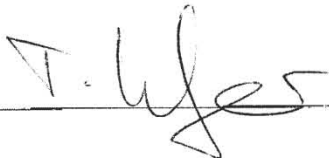
Dr. Nils Offen:

Ort, Datum: _Würzburg 25.01.11_ Unterschrift: _____

Katja Maurus:

Ort, Datum: _Würzburg, 26.01.11_ Unterschrift: _____

Prof. Dr. Anna-Leena Sirén:

Ort, Datum: _Würzburg 25.01.11_ Unterschrift: _____

Dr. Toni U. Wagner:

Ort, Datum: _Würzburg, 27.01.11_ Unterschrift: _____

Prof. Dr. Dr. Manfred Schartl:

Ort, Datum: _Würzburg, 27.01.11_ Unterschrift: _____